Zahara Saoud Faria Eltayari

Bachelor of Science Degree in Chemical and Biochemical Engineering

Engineering a 3D Novel *in vitro* Perfusion System for Pancreatic Cancer Research

Dissertation to obtain the Master of Science Degree in
Chemical and Biochemical Engineering

Supervisor: Eirini Velliou

Associate Professor, Faculty of Engineering and Physical Sciences from the University of Surrey

Jury

Chairperson: Isabel Maria Rôla Coelhoso

Associate Professor with Aggregation, Faculdade de Ciências e Tecnologia from Universidade Nova de Lisboa

Examiner: Frederico Castelo Ferreira

Associate Professor, Instituto Superior Técnico from Universidade de Lisboa

September, 2019

FACULDADE DE
CIÊNCIAS E TECNOLOGIA
UNIVERSIDADE NOVA DE LISBOA

Zahara Saoud Faria Eltayari

Bachelor of Science Degree in Chemical and Biochemical Engineering

Engineering a 3D Novel *in vitro* Perfusion System for Pancreatic Cancer Research

Dissertation to obtain the Master of Science Degree in
Chemical and Biochemical Engineering

Supervisor: Eirini Velliou

Associate Professor, Faculty of Engineering and Physical Sciences from the University of Surrey

Jury

Chairperson: Isabel Maria Rôla Coelhoso

Associate Professor with Aggregation, Faculdade de Ciências e Tecnologia from Universidade Nova de Lisboa

Examiner: Frederico Castelo Ferreira

Associate Professor, Instituto Superior Técnico from Universidade de Lisboa

September, 2019

FCt FACULDADE DE
CIÊNCIAS E TECNOLOGIA
UNIVERSIDADE NOVA DE LISBOA

Segue o teu destino,
Rega as tuas plantas,
Ama as tuas rosas.
O resto é sombra
De árvores alheias.

Fernando Pessoa

Acknowledgments

Making this thesis represented a fresh new start for me since one of my biggest wishes was able to come true. I did my master thesis abroad, in one of the places that I most like to be in the world, the United Kingdom. All the process before traveling was not easy and there were times that I thought my desire of choosing a place and a theme that I thought to be the most suitable for me, would never be possible. Fortunately, my guardian angel listened to my prayers and I can say now that I experienced one the best adventures of my yet short life.

First, I would like to thank to Professor Eirini Velliou for giving me the fantastic opportunity to work in her research group and for showing me her availability for all my enquiries and insecurities every time I needed. Secondly, I would like to show my acknowledgements to Doctor Priyanka Gupta, for teaching me everything I know, for always helping me when I asked the most absurd questions and for always being so patient to me. Without you this work would have never been possible. To all my office's and BioProChem Group's colleagues I would like to thank to Christina, Gaby, Katie, Stella, Tim, Marv and many others who went back home during this period, for their amazing personalities, for the funny moments spent together and for making me feel so comfortable in my working area. Obviously, I cannot end these acknowledgments without thanking to my landlord Birinder Arora for being such a good friend since the first day I landed in Guildford. I was very lucky to find someone who helped me a lot outside the university while I was alone in a foreign country.

Ao pilar de toda a minha vida, à minha família. À minha mamã por me atender sempre o telefone a qualquer hora do dia mesmo quando são quase 3 da manhã, por me ouvir e contar-me todas as histórias que perdi enquanto estive fora e por ser a primeira pessoa a quem recorro quando tudo parece estar mal. Ao meu papá que apesar de longe está sempre a pensar na minha segurança e conforto e me ligar de Abu Dhabi a perguntar como estão as coisas. Obrigada a vocês pais pois sem dúvida que sem vocês nada disto teria acontecido. Obrigada por todas a oportunidades que me deram ao longo da vida e que pensaram ser as melhores para mim. Amo-vos do fundo do meu coração e espero que um dia possa retribuir tudo aquilo que fizeram por mim! À minha mana mais velha, Muna, por sempre se preocupar comigo e por me fazer ver que o importante na vida é seguir aquilo que mais gostamos mesmo que o caminho para lá chegar não tenha sido o mais fácil ou o mais óbvio. Obrigada por todos os conselhos e conversas secretas! Aos meus tios e primos por o apoio sempre dado ao longo de todo o meu percurso académico e por ser relembrada constantemente como "o orgulho" da prima Joana!

A ti João, por seres aquele com mais paciência para mim e para os meus eternos dilemas, por falares comigo quase 24 horas por dia e por teres ido visitar-me a Inglaterra todas as vezes que conseguiste. À poucas pessoas como tu e tenho a certeza que o destino (apesar de não acreditares nele) quis reservar algo de muito bom para mim desde o dia em que te conheci!

Aos meus amigos de infância, adolescência e faculdade, Sofia Afonso, Carolina Angelino, Sara Vieira, Gonçalo Policarpo, Rita Carlota, um grande obrigada pelos momentos passados e por terem dado à minha vida, eternos momentos de pura felicidade, companheirismo, risada e muita maluqueira! Muito obrigada também a ti, Andreia Anjos, a minha mais recente amiga, por teres sido a maior surpresa destes 6 meses! Obrigada por seres uma pessoa que traz alegria e sorrisos a qualquer lugar! É irónico pensar como durante mais de 4 anos de curso quase não

tínhamos tido contacto uma com a outra e de repente tu tornares-te em alguém que faz parte do meu dia a dia! Coisas boas vêm por alguma razão e tu sem dúvida foste uma delas!

Por fim, quero agradecer à grandiosa FCT por ter sido a minha segunda casa ao longo destes 5 anos de curso. Cresci muito, moldei-me a uma nova vida e desafios e sinto que tudo aquilo que passei teve um propósito. Quando olho para trás e me lembro daquela menina ainda com 17 anos a chegar à porta da faculdade no carro da sua mãe para um dos dias de inscrição, leva-me a recordar tudo o que passei na faculdade e um grande sorriso surge na minha cara pois já não sou de todo aquela rapariga que não sabia para onde ia. Aprendi muito, trabalhei muito, sacrifiquei muito, mas também evolui muito e sinto que não podia ter escolhido um melhor local que me ensinasse a ser a melhor profissional que neste momento acredito que poderei vir a ser. Terei sempre orgulho em dizer que fiz parte do curso de MIEQB na FCT-UNL entre os anos de 2014 a 2019.

Abstract

The Pancreatic Ductal Adenocarcinoma is a malignant aggressive disease corresponding to a low survival rate of 5 years, only between 5 to 7%. This is mainly due to the high complexity and density of the malignant tumour microenvironment which difficult the efficiency of potential treatments and furthermore, to the disease's progression and inhibition of apoptotic pathways.

Over the last years, Tissue Engineering has been gaining an even more prominent role regarding the construction of tri-dimensional (3D) *in vitro* culture systems that enable a better comprehension of the physicochemical properties and a more realistic recapitulation of the structure of tumoural tissues.

In this study, it is described for the first time, the use of a perfusion bioreactor for the culture of pancreatic cancer cells in 3D porous polyurethane scaffolds previously coated with one of the most abundant proteins in the extracellular matrix, the fibronectin. This dynamic culture system allowed a higher proliferation of the tumoural cells as well as a greater cell viability when compared to static culture systems. The addition of a chemotherapy agent also showed a higher resistance by the cells cultured in the bioreactor in addition to a lower percentage of cells in apoptosis.

The results obtained suggest the great potentiality of perfusion bioreactors in high throughput studies regarding the *in vitro* culture of cancer cells for the vascularization mimicry of *in vivo* systems, including drug and treatment screening for patients detected with pancreatic cancer.

Keywords: Pancreatic Ductal Adenocarcinoma; Tissue Engineering; 3D *in vitro* Culture; Perfusion Bioreactor; 3D Porous Polyurethane Scaffolds

x

Resumo

O Adenocarcinoma Ductal Pancreático é uma doença maligna agressiva que corresponde a uma baixa taxa de sobrevência de 5 anos, apenas entre 5 a 7%. Isto deve-se principalmente à elevada complexidade e densidade do microambiente característico do tumor maligno que dificultam a penetração de potenciais tratamentos e posteriormente à progressão da doença e inibição de vias apoptóticas.

Nos últimos anos, a Engenharia de Tecidos tem ganho um papel cada vez mais proeminente no que diz respeito à construção de sistemas de cultura tri-dimensional (3D) *in vitro* que permitem uma melhor compreensão das propriedades físico-químicas e biológicas e uma recapitulação mais realista da estrutura dos tecidos tumorais.

Neste estudo, é retratado pela primeira vez, o uso de um bioreactor de perfusão para a cultura de células pancreáticas cancerígenas em matrizes de suporte porosas 3D de poliuretano previamente revestidas com uma das proteínas mais abundantes da matriz extracelular, a fibronectina. Este sistema de cultura dinâmica permitiu uma maior proliferação das células tumorais assim como uma maior viabilidade celular quando comparado com sistemas de cultura estática. A adição de um agente quimioterapêutico mostrou também uma maior resistência por parte das células cultivadas no bioreactor assim como uma menor percentagem de células em apoptose.

Os resultados obtidos sugerem a grande potencialidade de bioreactores de perfusão em estudos de elevada produtividade no que diz respeito à cultura de células cancerígenas *in vitro* para mimetismo da vascularização de sistemas *in vivo*, incluindo a triagem de medicamentos e tratamentos para pacientes detectados com cancro do pâncreas.

Palavras-chave: Adenocarcinoma Ductal Pancreático; Engenharia de Tecidos; Cultura 3D *in vitro*; Bioreactor de Perfusão; Matrizes de Suporte Porosas 3D de Poliuretano

List of Contents

List of Figures

List of Tables

List of Abbreviations

α-SMA	α-Smooth Muscle Actin
ANM	Athymic Nude Mouse
CAFs	Cancer-associated Fibroblasts
CBD	Cannabidiol
CLG	Collagen
CSCs	Cancer Stem Cells
CS-HA	Hyaluronan grafted Chitosan
DMEM	Dulbecco's Modified Eagle Medium
DMSO	Dimethyl Sulfoxide
DR	Desmoplastic Reaction
ECM	Extracellular Matrix
EGFR	Epidermal Growth Factor Receptor
FBS	Fetal Bovine Serum
FN	Fibronectin
GAGs	Glycosaminoglycan Chains
GEM	Gemcitabine
GFAP	Glial Fibrillary Acidic Protein
HA	Hyaluronic Acid
HIF1	Hypoxia-Inducible Factor-1
hiPSCs	Human-induced Pluripotent Stem Cells

HUVEC	Human Umbilical Vein Endothelial Cells
MMPs	Metalloproteinases
mOECs	Mouse Oesophageal Epithelial Cells
NFC	Nanofibrillar Cellulose
NK	Natural Killer Cell
NOD/SCID	Non-Obese Diabetic Mouse with SCID Mutation
PancNet	Pancreatic Neuroendocrine Tumour
PBS	Phosphate-buffered Saline
PDAC	Pancreatic Ductal Adenocarcinoma
PDMS	Polydimethylsiloxane
PEG	Poly (ethylene glycol)
Pen Strep	Penicillin - Streptomycin Solution
PGA	Polyglycolic Acid
PGTC/G	Poly (glycolide-co-trimethylene carbonate)/Gelatin
PHEMA	Poly (2-hydroxyethyl methacrylate)
PLLA	Polylactic Acid
POT/PBT	Poly (ethylene oxide terephthalate)/Poly (butylene terephthalate)
PSCs	Pancreatic Stellate Cells
PU	Polyurethane
PVA/G	Poly (vinyl alcohol)/Gelatin
PVOH	Poly (vinyl alcohol)
rOSFs	Rat Oesophageal Stromal Fibroblasts
SCID	Severely Compromised Immunodeficient Mouse
TE	Tissue Engineering
TME	Tumour Microenvironment
2D	Two-Dimensional
3D	Three-Dimensional
5-FU	5-Fluorouracil

1   Framework

1.1 Motivation

Only in 2018, 17 million new cases of cancer appeared worldwide. Some predictions point that by the year 2040, 27.5 million new cases of cancer will emerge annually. From the number of cancer cases diagnosed last year, about 9.6 million people lost their lives (Cancer Research UK, 2019). This, leads to believe that cancer is one of the 21st century's diseases (along with obesity), making it one of the modern medicine's greatest challenges (Kaidar-Person et al., 2011).

Nowadays, there are known to exist more than 200 types of cancer, being the most common and deadliest, the lung cancer, the breast cancer, the pancreatic cancer, the prostate cancer, among others (Cancer Research UK, 2019; Saleh, 2018). Figure 1.1 shows the number of cancer deaths worldwide for the most aggressive types of cancer, in 2018, for both sexes of all ages.
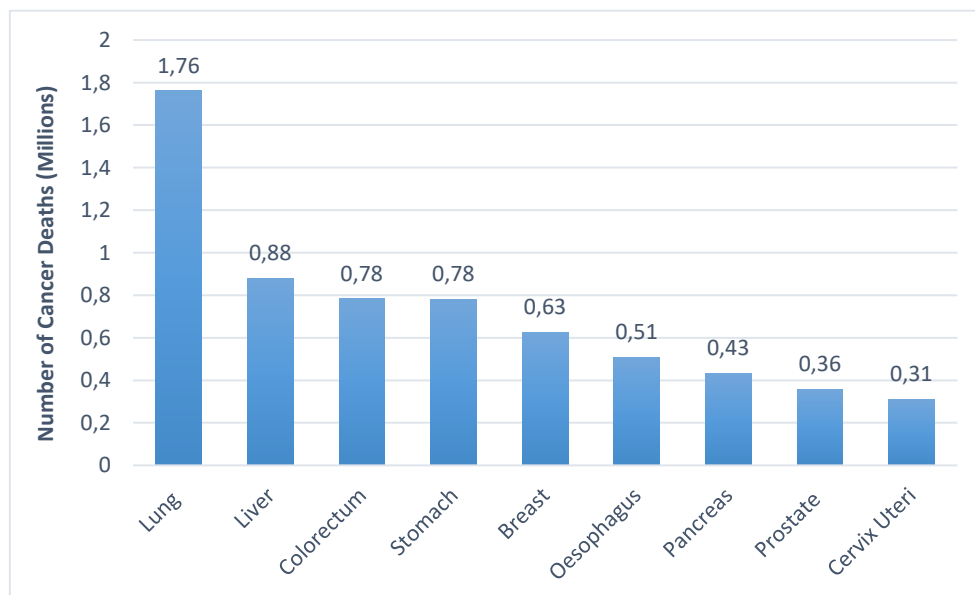
Figure 1.1: Cancer Deaths Worldwide by type, in 2018, adapted from (Statista, 2018)

Since cancer has become a rapid growth disease in the world, researchers have advanced on many different fronts, to develop new ways of preventing, early detect and treat the disease in cancer patients. Studies, however, have not shown very promising results when developing new therapies to target and fight the disease. This is due to the high number of drug test failure in clinical trials for cancer research (Maeda et al., 2018). According to a review form the Nature Magazine in drug development, almost 90% of the failures across all therapeutic areas were attributable to the lack of efficacy (66%) or safety issues (21%). This key factor leads to the necessity of improving the predictability during the preclinical test's development (Arrowsmith, 2011). To better understand the pathway which a new potential drug is subjected to, till its final approval by the Food and Drug Administration (FDA, US), it is represented a diagram in picture 1.2, with all its compulsory steps.

Preclinical	Phase I	Phase II	Phase III	Evaluation
Lab tests of a new drug in animals, to see if it is safe to use in humans.	First trials that try to find the safest dose, the drug's effectiveness and the identify of side effects	Involves more patients and tries to see whether the treatment is effective.	Involves thousand of patients and tries to see if the new treatment is better than the standard one.	The treatment is licensed and approved, becoming the new standard for cancer.
	20-100 Participants	**100-500 Participants**	**1000-10.000 Participants**	

10 to 15 years

Figure 1.2: The Drug Development Cascade in Clinical Trials, adapted from (Brito, 2018)
Pictures from (iStock by Getty Images, 2019; One Person Closer, 2019; Press, 2019; Prime Cirúrgica, 2019; R&D, 2019)

In fact, the lack of predictability in the clinical trials, as already stated before, begins before they even start, more specifically in the laboratories, in the Preclinical stage. Here, experimental mice and rats' models (*in vivo* models) are usually elected to test the drug screening, efficacy and toxicity of candidate drugs. This way, researchers tend to apply the results obtained here in patients at the different phases of the clinical trials and have repeatedly been failing. One of the reasons, is that when a drug is being administrated to a mouse or any other small animal, its readily accessibility throughout the tumoural tissue and the immediate drug action that is experienced, will unlikely be as quick or efficient when it gets administrated in humans. These *in vivo* models are genetically, behaviourally and biologically different from humans, and therefore, totally downplay the complexity of a human solid tumour with complex cellular, stromal and vascular architectural features (cellular clumps, hypoxia, low pH, etc) (Maeda et al., 2018).

Apart from these drawbacks, issues related to financial and ethical reasons using animals as models for cancer research have also raised uncertainties regarding the continuous use of these traditional approaches for drug development. That's why over the last two decades, the

knowledge on cancer biology has been driving researchers to bet in new targeted therapies such as the fields of immunotherapy, genetic engineering, nanotechnology, proteomics or tissue engineering (TE) (American Cancer Society, 2014).

TE, as it will be later described in this chapter, is the field of interest in this dissertation, since it has been considered as one of the most promising approaches when mimicking the real features of a human tumour microenvironment. Especially for the types of cancers that are only diagnosed at stages III or IV in patients that when treated in clinics, often advance to metastatic stages and drug resistance (Maeda et al., 2018). Thus, recreating these cancers' early stages could deeply contribute to understand how a tumour begins to spread and what therapies could be developed to fight it efficiently. One example of these late diagnosed cancers is the Pancreatic Ductal Adenocarcinoma (PDAC), which is the most common type of pancreatic cancer, being incident in 95% of all the pancreatic cancer patients (Pancreatic Cancer UK, 2018).

1.2 Cancer

It is not profitable to talk about cancer without first acknowledge its definition and characteristics. In this subchapter it will be first enunciated what cancer is based on, how it arises and what are the consequences related to its development leading later to the focus of PDAC. As a final part it is also enhanced the importance of studying its microenvironment in the medical research field.

1.2.1 Definition

Cancer is a genetic disease. In other words, it is caused by changes (mutations) in genes that control the way cells function, more specifically, how they grow and divide. These types of changes may lead to an abnormal cell division in an uncontrolled way. In normal circumstances, human cells grow and divide to form new cells and in a cell life cycle, when they grow old or become damaged, they die, in a phenomenon called apoptosis[1] being then replaced by new cells. However, when cancer develops, this ordinary process breaks down and instead of end of life cells die, they survive, leading to the division into new cells with an unstoppable development, ending after in the formation of cellular growths also called tumours (Cancer Research UK, 2019; National Cancer Institute, 2019).

1.2.2 Differences between Cancer and Normal Cells

There are several reasons associated with the fact that cancer cells grow out of control when comparing to normal cells in the body. One of the reasons is that cancer cells are less specialized than normal cells. So, instead of maturing into specific cell types with distinct functions, they divide themselves without stopping. Although there exist in a normal cell division cycle, several signals in each control phase which cells need to go through in order to avoid any errors in their division, cancer cells however, can ignore them and continue to divide even when they are not needed. In addition, cancer cells influence the activity of normal cells and molecules that surround them in order to survive and proliferate. More specifically, these types of cells can induce normal cells to form blood vessels that supply oxygen and nutrients that cancer cells use to feed themselves (angiogenesis). Another consequence that makes cancer cells so difficult to control is that they can easily evade the immune system without being destroyed, gaining consequently the capability of spreading through other parts of the organism in a process called Metastasis. In other words, cancer cells break away from where they were first formed (primary cancer), travel through the blood or lymph system, and form new tumours (metastatic tumours)

---

[1] Apoptosis is a form of cell death in which a programmed sequence of events leads to the elimination of cells without releasing harmful substances into the surrounding area (MedicineNet, 2018).

(National Cancer Institute, 2019). The figure beneath shows the evolution of a tumour in a normal cell tissue.
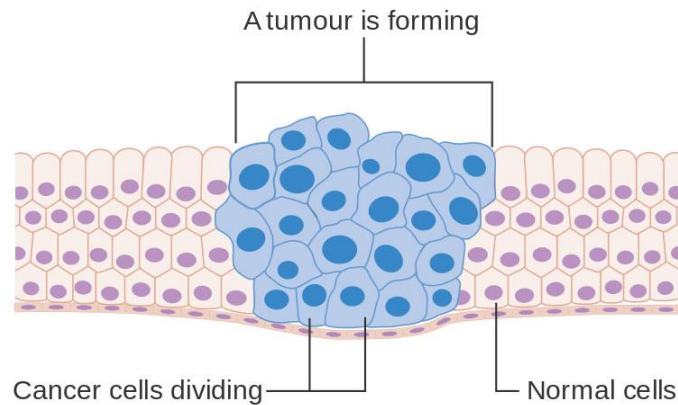
Figure 1.3: Tumour Cells Growth in a Healthy Tissue (Blomquist, 2016)

1.2.3 Pancreatic Ductal Adenocarcinoma

The Pancreatic Cancer is divided into two main groups: the exocrine and endocrine tumours, being the first ones the most common type of pancreatic cancer. The PDAC is among the several known types of pancreatic exocrine tumours and it develops from cells (duct cells) lining small tubes in the pancreas, called ducts. These cellular couplings carry the digestive juices containing enzymes, produced from the acinar cells, to the main pancreatic duct and into the duodenum[2], helping this way with the food digestion. On the other hand, the Pancreatic Neuroendocrine Tumour (PancNET), which is the most common type of pancreatic endocrine tumours, starts from neuroendocrine cells. These ones produce hormones that help control the normal levels of certain components in the body such as sugar levels, with the production of insulin (Pancreatic Cancer UK, 2018).

As already said before, about 95% of the Pancreatic Cancers are PDACs. This tumoral progression is most often found in the head of the pancreas as it is illustrated in figure 1.4.
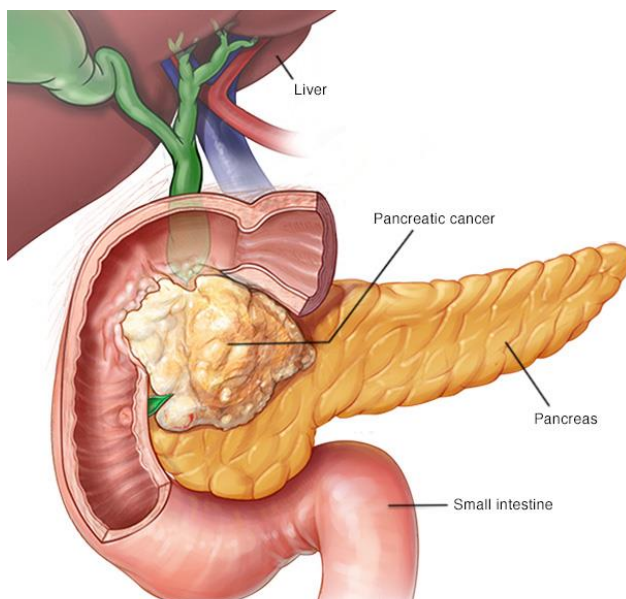
Figure 1.4: Pancreatic Ductal Adenocarcinoma
(Mayo Clinic, 2016)

From the Motivation Section it could be seen that Pancreatic Cancer, more specifically, PDAC, remains one of the leading causes in cancer-related deaths despite its low incidence. This is partly due to the poor prognosis and high resistance to current treatment options such as, chemotherapy, radiotherapy, among others, which makes of pivotal need the improvement of more personalized and effective strategies to fight the disease. Another aggravating topic regarding PDAC is the 5-year survival rate that remains just around 5 to 7%. One of the critical reasons is that around 50% of the diagnosed patients have the disease already metastasized throughout the body, making it much

---

[2] The duodenum is the first part of the small intestine (Pancreatic Cancer UK, 2018).

more difficult to treat and control. This is a major consequence of the lack of tumour's visible and early symptoms and its dense, heterogeneous and complex microenvironment that contributes to the disease's resistance and progression (Adamska et al., 2017).

1.2.3.1 Pancreatic Tumour Microenvironment

The Pancreatic Tumour Microenvironment has been one of the most important study objects in the Pancreatic Cancer field since it is due to its characteristics that the disease development and spreading gets so rapid and aggressive at the same time.

Desmoplasia is one of the most prominent hallmarks of the PDAC. This reaction consists on a dramatic increase in the proliferation of myofibroblasts, also known as activated Pancreatic Stellate Cells (PSCs), accompanied by the increased deposition of many extracellular matrix (ECM) components such as Fibronectin (FN) and Collagen (GLG) I and III. The resulting dense and fibrous connective tissue leads therefore to the reduction of the tumour elasticity and an increase in the tumour Interstitial Fluid Pressure (IFP) (Whatcott et al., 2012). The Desmoplastic Reaction (DR) is so critical that it can reach about 80% of the tumoural mass, leading this way to a high tumour's chemoresistance and inefficient drug delivery (Kuen, 2017). Figure 1.5 shows an illustration of how the desmoplastic pancreatic tumour microenvironment looks like.
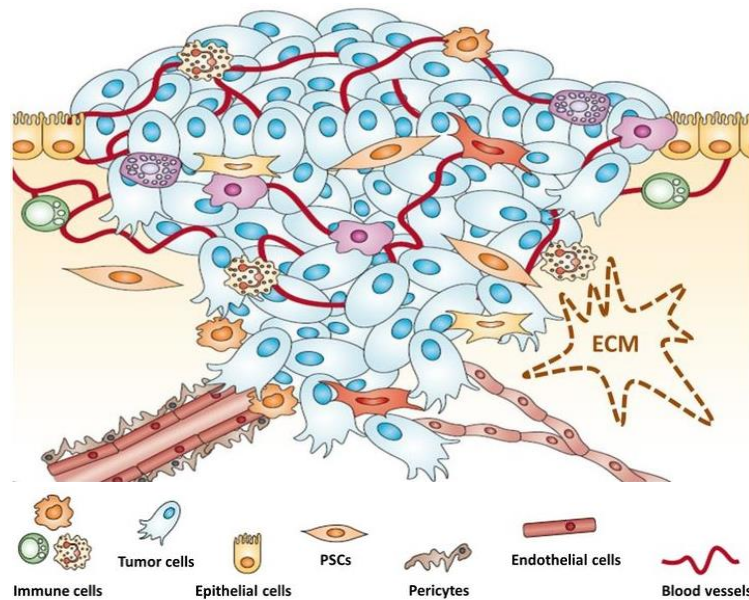
Figure 1.5: Components of the PDAC Microenvironment (Kuen, 2017)

Here, it can be seen how the cancer cells are surrounded by the desmoplastic stroma that tends to accumulate as the primary tumour grows. This is one of the reasons why it is so important to target desmoplasia and understand how its cellular constituents differ, interact and influence drug resistance in order to improve new efficient therapies and control the progression of the cancerous tissue (Kuen, 2017).

1.2.3.1.1 Pancreatic Stellate Cells

PSCs are activated in response to the pancreatic injury and inflammation and play an active role in the stroma's fibrosis, being considered this way as one of the main sources of the malignant tumoural progression. PSCs interact closely with the cancer cells to generate a tumour facilitatory environment that stimulates not only the tumour's growth but also its metastasis. Pancreatic fibrosis is initiated when PSCs become activated and undergo morphological and functional changes so that the rate of ECM deposition exceeds the rate of ECM degradation

(Rasheed et al., 2012). This type of cells can be divided into two biological phenotypes[3]. In physiological conditions, PSCs are rich in intracellular lipid droplets, positive for glial fibrillary acidic protein[4] (GFAP) and desmin expression. These ones are known as Quiescent PSCs. On the other hand, when they are activated from their resting state to myofibroblast-like cells with a concurrent disappearance of lipid droplets, they become known as Activated PSCs. Activated PSCs specifically express the α-smooth muscle actin (α-SMA) and secrete CLG I and III, FN, and other ECM components to promote the formation of pancreatic fibrosis (Zhou et al., 2019).

1.2.3.1.2 Extracellular Matrix

The ECM is composed of two main classes of macromolecules, the fibrous proteins and the proteoglycans. The main fibrous proteins are CLGs, elastins, FN and laminins, being CLG the most abundant fibrous protein within the ECM. This scaffolding protein contributes to the tensile strength and development of the tissue, regulates cell adhesion and supports chemo transportation and migration. Still, the proteoglycans, fill most of the extracellular interstitial space within the tissue in the form of a hydrated gel. These ones are composed of glycosaminoglycan chains (GAGs) covalently linked to a protein core (Venkatasubramanian, 2012). Like the proliferation of PSCs and the infiltration of multiple immune cell types, the deposition of ECM components also contributes significantly to the pathogenic potential of the DR. The various ECM components can enhance the tumour cell proliferation and reduce drug penetration (CLG I, III and IV), increase the IFP (hyaluronan), enhance the resistance to apoptosis (FN and laminin) and can also diffuse nutrients and hormones at the bloodstream. Therefore, in the diseased pancreas, the significant over production of ECM components can be described as the failed resolution of a healing wound, leading towards the fibrosis state (Whatcott et al., 2012).

1.2.3.1.3 Hypoxia

Another important characteristic of the PDAC is its hypoxic environment, in other words the lack of oxygen levels in the tumour microenvironment. In a normal pancreatic tissue, the median oxygen concentration ranges about 6.8% whereas in its tumoural stage the concentrations can drops to 0.4% (McKeown, 2014). This condition is thought to be secondary to the fibrotic microenvironment produced by the PSCs and the expression of several antiangiogenic substances. It has also been linked with worse clinical outcomes in patients, including the increment rates of tumour growth and metastasis. The hypoxic microenvironment in pancreatic cancer has been shown to induce the expression of the Hypoxia-Inducible Factor-1 (HIF1) which has been associated with drug resistance and enhancement of cell invasion (Rasheed et al., 2012).

1.2.3.2 Research Approaches for PDAC

As already said before, the limited therapy efficacy in PDAC due to its dense desmoplastic stroma and hypoxic microenvironment makes it very important to undergo the understanding of its biology background in order to identify early detection strategies, preventive measures and more effective and reliable interventions over the standard ones (Deer et al., 2010).

To date, it has been characterized over 20 different human pancreatic cancer cells. AsPC-1, Capan-1, Capan-2, HPAC and PANC-1 are among the eleven most commonly referenced pancreatic cancer cells. Scientists have not only characterized these cells by their phenotype and

---

[3] Phenotype of a cell is a description of its physical characteristics (Personal Genetics Education Project, 2019).

[4] The GFAP is one of the intermediate filament proteins, which also includes the keratins, vimentin, desmin, peripherin and nestin (Moser et al., 2007).

genotype[5] but also by their adhesion, migration, invasion and even angiogenic potential. Finally, some attention has also been given to their tumorigenicity, which describes the cancer cell line's propensity to produce a tumour *in vivo* (Deer et al., 2010). These cell lines have been being established in the pancreatic cancer research field and have been showing numerous outcomes specially when cultured in 3D models (Kuen, 2017). As it will be enhanced later in this report, several studies using 2D and 3D cultures have been being performed, however the complex chemical, biological, biomechanical and structural *in vivo* situation of the PDAC has only been mainly achieved in 3D cultures.

This ultimately leads to the last section of the Framework Chapter where it will be clarified the importance that TE has been having when predicting models that are more realistic and closer to the ones seen in *in vivo* studies.

1.3 Tissue Engineering

1.3.1 Definition

TE was previously described in 1993 by Robert Langer as "an interdisciplinary field that applies the principles of biology and engineering to the development of functional substitutes for damaged tissue" (Mi et al., 2014). Summarizing, TE refers to the practice of combining biomaterials, such as scaffolds, cells and biologically active molecules in order to assemble functional tissues that can restore, maintain or improve damaged tissues or organs (National Institute of Biomedical Engineering and Bioengineering, 2019). This field has been arising since the 1970's due to the fact it has been answering to the one of the most common and costly problems in human health care which is the loss and failure of organs or tissues in human patients. The increasing number of transplantation surgeries has led to a high donor organ demand which is even more far exceeding the supply. So, alternatively, instead of transplanting living organs, other substitutes such as biocompatible polymers or metals have been being improved to be used for transplantation issues. It is then here, where the role of TE has its greatest impact (Mi et al., 2014).

1.3.2 The Main Elements of Tissue Engineering

When talking about TE it is important to highlight the principle elements involved in its procedure. The three main aspects of TE include the cells, the biological factors (signals) and the scaffolds. Each of these elements play an exclusive role when designing a TE model. The cells are the building blocks of the tissue and play a critical role in its healing and regeneration (Mi et al., 2014). The most common types of cells used in TE models are the stem cells inasmuch as they are undifferentiated, have an unlimited auto renew ability and a high differentiation potential into many different types of cells (Serra, 2018). On the other hand, biological factors can influence the function and behaviour of cells in the scaffold, significantly. These elements mainly consist of hormones, cytokines, growth factors or extracellular matrix molecules. The employment of growth factors can lead cells to perform their normal functions when cultured in TE models. As a final element, the scaffolds recapitulate the normal tissue development process by allowing the cells to formulate the desired microenvironment requirements (Mi et al., 2014). It provides the necessary support for cells to attach, migrate and proliferate and confers the biomechanical and biochemical cues that act on different cell functions. Summing up, the scaffold acts as a synthetic analog of the natural ECM. As such, considering the material

---

[5] Genotype of a cell is a description of its genetic characteristics (genetic identity) (Personal Genetics Education Project, 2019).

properties (weight, viscosity, composition, etc.) is essential to design the best biomimetic cell cultures that assure drug delivery (Mi et al., 2014; Santo et al., 2017).

The figure bellow shows a typical TE cycle where a certain number of cells are isolated form the human body (a) and put in culture to produce more cells (b). The resulting cell culture is seeded onto a porous scaffold along with growth factors (c) and consequently cultured in static or dynamic conditions (d). Finally, it is implanted as a regenerative tissue into the site of the defect of the natural human tissue (e) (Mi et al., 2014).
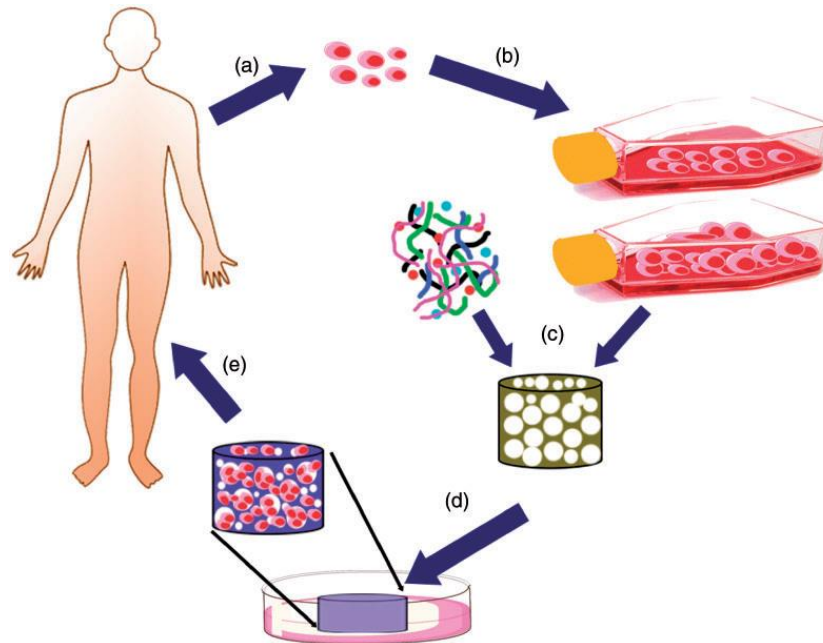
Figure 1.6: The Tissue Engineering Cycle (Mi et al., 2014)

1.3.3 Tissue Engineering in Cancer Research

Over the last years TE has not only evoked new hopes for the cure of organ failure but also provided new technology platforms to study the features of tumour cell growth. The advances in stem cells' technology has allowed to study the interactions that occur when replicating the physiological conditions in TE cancer models. This way it is possible to understand the relevant mechanisms that control cell growth in the tumoural progression since its initial stage. That is why, studying the tissue microenvironment became the key factor since it plays a crucial role in cell signalling and regulation of normal and malignant cell functions (Horch et al., 2013). For the PDAC approach, and even for other types of cancers, featuring its microenvironment in a 3D structure could be the starting point to tailor specific tissue properties of individual patients and help doctors to understand how a specific tumour would be likely to spread or to respond to treatment, potentially improving the outcomes for pancreatic cancer patients (Velliou, 2018). When studying 3D interactions of cells in a TE model it is also important to highlight the critical role of dynamic cultures, more specifically the use of bioreactors, which will also be further enhanced in this report.

1.4 Summary

Summing up, the necessity of improving new cancer models for drug development has considered to be imperative since many of the drug testing failures in clinical trials are due to the lack of predictability existed in the preclinical experiments. The shift from animal models (*in vivo* models), to more realistic approaches (3D *in vitro* models) has challenged researchers to

investigate new solutions in fields such as the TE. The last one has been described as one of the most promising bets in biomedical research, more specifically when mimicking the main physiological features of a tumour microenvironment from its early stages till the moment it starts to spread across other tissues' compartments. Consequently, the improvement of new efficient methods to control cell progression and facilitate drug penetration that is so difficult to oppose in the PDAC, could be easily achieved.

1.5 Objectives

Therefore, the overall aim of this work is settled in developing a 3D pancreatic cancer model that supports the long-term growth of pancreatic cancer cells cultured both in static and dynamic conditions. In order to compare how the cells' behaviour and viability differed, a chemotherapeutic agent was added in both the systems after a long-term culture. The last goal is to prove for the first time that the 3D culture of pancreatic cancer cells in a perfusion bioreactor, closely recapitulates the features of a real pancreatic tumour microenvironment.

2 State of Art

In this chapter are highlighted the different cell culture models where the Pancreatic Cancer Research has been most incident to. These ones range from two-dimensional (2D) *in vitro* models, to three-dimensional (3D) *in vivo* and *in vitro* models. The characteristics and comparisons between each other are specified as well as their advantages and disadvantages. By the end it is also explained why using *in vitro* models, more specifically, polymeric scaffolds, are considered to be of potential use in pancreatic cancer studies. The addition of dynamic systems is also an added value when mimicking a real tumour microenvironment (TME), which is something that static cultures usually fail to recapitulate.

2.1 *In vivo* and *In vitro* Model Systems

Since the last century, the biotechnology field has been trying to target the researcher's attention in order to find novel therapies capable of optimizing the cancer research studies in terms of its drug screening, and biological understating. To make this possible a variety of cell culturing models have been used and improved when cultured and tested with tumoural cells.

2.1.1 2D *in vitro* Models

2D *in vitro* models have been used as cell culture models even before the last decade of the 20th century and consist of growing cells in flat surfaces such as petri dishes or flasks (Mimetas, 2019). Despite the disadvantages associated with these systems, which will be further enhanced, 2D Models have still however been being used in a huge part of the scientific community (Ricci et al., 2014). This is because they are essentially less expensive than any other cell culture model, being its use much more accessible to the research field. Another reason for their high demand is that they are easily reproducible and have a much lower complexity, which makes their analysis and observations easier to perform and understand.

From the studies found regarding pancreatic cancer research in 2D *in vitro* systems, it is exalted the one where Richards et al. showed that cancer-associated fibroblasts (CAFs) are intrinsically chemoresistant to Gemcitabine[6] (GEM) and have an active role in regulating the

---

[6] The Gemcitabine is one of the main chemotherapy drugs used to treat PDAC (Pancreatic Cancer UK, 2017). This chemotherapy agent is a nucleoside analog that replaces one of the building blocks of nucleic acids during the DNA replication (cytidine). Since the new nucleosides cannot be attached to the "faulty" nucleoside, the cell apoptosis occur (DrugBank, 2019).

chemoresistance of pancreatic cancer cells. CAFs exposed to GEM dramatically increased the release of exosomes[7] that potentiated cell proliferation and survival in recipient epithelial cancer cells, leading to a consequent increase of the expression of the chemoresistance-inducing factor, Snail. Treatment of GEM-exposed CAFs with an inhibitor of the exosome release, significantly reduced the survival of drug resistant cells in co-cultured epithelial cells, suggesting that blocking exosome communication may be a promising therapeutic strategy for patients receiving GEM-based treatments (Richards et al., 2017). Additionally, Hashimoto et al. investigated the role of autophagy[8] in pancreatic cancer cells and saw that it was significantly induced in the PDAC when compared to a healthy pancreatic tissue. Autophagy was markedly increased after treatment with 5-Fluorouracil (5-FU) or GEM whereas its inhibition with chloroquine, suppressed the growth of PANC-1 and BxPC-3 cells (Hashimoto et al., 2014). Porcelli et al. illustrated promising results on the role of Rucaparib, a PARP-1 inhibitor of enzymes that cancer cells use to repair strand breaks caused by genotoxic agents. The antitumour effectiveness of combining the PARP-1 inhibitor before, together and after radiotherapy evidenced the first, as the optimal feature in blocking cell growth. Pre-exposure to Rucaparib increased the cytotoxicity of GEM and radiotherapy by heavily inducing the accumulation of cells in G2/M phase of the life cell's cycle, impairing mitosis and finally inducing apoptosis and autophagy (Porcelli et al., 2013).
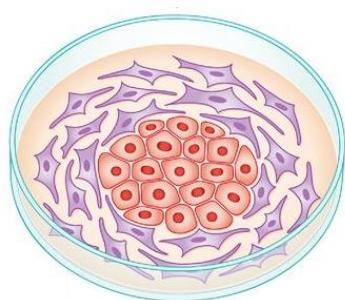
Figure 2.1: 2D Co-Cultured System Model
(Hynds et al., 2017)

Because in a 2D system cells grow in a monolayer, as it can be seen in the picture aside that represents the isolation of human epithelial cells in 3T3[9] mouse embryonic fibroblasts co-culture (Hynds et al., 2017), some implications regarding their predictability in mimicking a real tumour microenvironment are associated. More specifically, 2D cultures do not entirely represent the real cell-cell and cell-ECM interactions occurred in a real *in vivo* system. In a human body, cells do not grow and function in a 2D environment, they are instead surrounded by other cells in a 3D arrangement (Mimetas, 2019; C Ricci et al., 2014). Another implication related to the use of these models is the tendency of the cells to change not only their phenotype (cell shape and morphology) but also their genotype (gene and protein expression), which induces some contradictions in the final results (Mimetas, 2019; Yamada et al., 2007). The exposure of cells to the culture media in 2D systems also brings another relevant disadvantage since the cells are equally exposed to the same concentrations, which is not what happens in the case of cells in a body's tissue. Because here they organized in a 3D layer, the nutrients and drug flows are not spread uniformly throughout the tissue (Jellagen - Marine Biotechnologies, 2019). Therefore, the diffusion limitations that cells experience in *in vivo*, are not well represented in 2D *in vitro* cultures. There is always presented a nutrient gradient which the 2D models practically nullify.

2.1.2 3D *in vivo* Models

One of the other models widely used for many decades to study human diseases are the murine models, more specifically human tumour xenografts. In these models, human tumour

---

[7] Exosomes are small vesicles containing RNA and proteins, which are constantly secreted by cells and have many intriguing functions in the human body, including intercellular communication and signalling (Thermo Fisher Scientific, 2019).

[8] Autophagy is an intracellular degradation system that delivers cytoplasmic constituents to the lysosome (cellular digestion) (Mizushima, 2007).

[9] 3T3 are cell lines whose original growing procedure consisted being transferred (T) every three days (3) and plated at three hundred and thousand (300.000) cells per plate (NCBI, 2019).

cells are transplanted into the organism of immunocompromised mice that do not reject human cells. With this, the tumour inside the mice develops and grows within a certain period of time and the last one is subjected to different therapeutic testings (Richmond et al., 2008).

There are several types of immunocompromised mice that can be used to establish human tissue xenografts. A very common one is the Athymic Nude Mouse (ANM), with a genetic mutation that unables the presence of thymus[10], being consequently incapable of producing thymus-derived-cells (T Cells). The name "nude" comes from the lack of hair growth in their skin (Richmond et al., 2008; River, 2019; Wettersten et al., 2014). Another broadly used mouse is the Severely Compromised Immunodeficient Mouse (SCID) that in addition to the lack of T Cells it also lacks B Cells[11] and are thus characterized by an absence of an adaptive immune response (Richmond et al., 2008; Wettersten et al., 2014). The Non-Obese Diabetic Mouse with the SCID mutation (NOD/SCID) is also another frequent used laboratory mouse, so in addition to impair T and B Cells development, these mouse's background also results in a deficient Natural Killer Cell[12] (NK) function (Richmond et al., 2008; River, 2019). In picture 2.2 it is showed how the phenotypes of the AN and NOD/SCID mice differ between each other.

When talking about xenograft models, it is important to understand that these ones are divided in the Orthotopic and Subcutaneous Xenografts Models and the Experimental Metastasis Model (Wettersten et al., 2014). The Orthotopic Xenografts consist of tumour tissues or cells that are injected into an organ type in which the tumour originated (Richmond et al., 2008). These models might accurately reproduce the tumour microenvironment seen in the human body and allow observations of all the metastatic processes, however, the requirement to undergo animals to a major surgery in order to access the tumoural tissue, makes this procedure, time consuming, expensive and technically challenging (Richmond et al., 2008; Wettersten et al., 2014). The Subcutaneous Xenografts consist of small tissues or cells that are injected subcutaneously on the

Figure 2.2: AN Mouse on the top (River, 2019) **and NOD/SCID Mouse on the bottom** (River, 2019)

flank of animals (under the skin) (ProQinase, 2019; Wettersten et al., 2014). Here, not only the measuring of the tumour size with the use of a caliper[13] without having to subject the animal to surgeries, but also the tumour injection inside the mouse's organism, are much more facilitated. Nevertheless, these models tend to be not as predictive as the orthotopic models, consequently lacking an *in vivo* tumour-like system. Finally, the Experimental Metastasis consists of tumour cells that are injected directly into the venous circulation or highly vascular organs. Following the intravenous injection, it is possible to access the ability of tumour cells to arrest and grow in a particular organ or tissue. Yet, this process limits itself to only certain steps of the metastasis process (circulation, extravasion, formation of metastasis and colonization) whereas the Orthotopic Models have access to the entire one (primary tumour formation, localized invasion,

---

[10] The Thymus is a little organ which is part of the lymphatic system and produces progenitor cells that mature into T-Cells that helps destroy infected or cancerous cells (Live Science, 2018).

[11] B Cells are cells developed from the bone marrow that are involved in immunity defences (Encyclopedia Britannica, 2019).

[12] NK Cells kill virally infected cells and detect or control early signs of cancer (British Society for Immunology, 2019).

[13] Caliper is an instrument that consists of two adjustable legs or jaws for measuring the dimensions of material parts (Encyclopedia Britannica, 2019).

intravasion, circulation, extravasion, formation of metastasis and colonization). However, the controlled number of cells injected as well as the specification of the metastasis sites are beneficial points associated to use of these systems (Wettersten et al., 2014).

Adamska et al. indicated that the ABCC3 gene inhibition (novel target in PDAC) with MCI-715, demonstrated strong antitumour activity. Using mouse models with human cancer cell lines, it was shown that the pharmacological inhibition of ABCC3 significantly decreased the PDAC cell proliferation and clonal expansion, therefore increasing the mice's survival rate (Adamska et al., 2019). Ferro et al. proved that using genetic and pharmacological approaches by inhibiting the G protein-coupled receptor, GPR55, reduced pancreatic cancer cell growth in transgenic mouse models. These ones were treated with a combination of the GPR55 antagonist, Cannabidiol (CBD) and GEM, surviving nearly three times longer when compared to mice treated with GEM alone (Ferro et al., 2018). Furthermore, Costa-Silva et al. showed that PDAC-derived exosomes induced liver pre-metastatic niche formation in naive mice. Uptake of PDAC-derived exosomes by Kupffer cells[14] caused transforming secretion and upregulation of FN by hepatic stellate cells. This fibrotic microenvironment enhanced recruitment of bone marrow-derived macrophages at the same time the macrophage migration inhibitory factor (MIF) was being highly expressed in PDAC-derived exosomes. Its blockade prevented liver pre-metastatic niche formation. This suggested that exosomal MIF may be a prognostic marker for the development of PDAC liver metastasis (Costa-Silva et al., 2015).

Despite the several advantages that 3D *in vivo* models may present when screening a more realistic TME, the use of living organisms induces till today ethical questions that make their use more controversial in the scientific field (Ricci et al., 2014; Richmond et al., 2008). Obtaining concordance between animal models and clinical trials, as already stated before, also remains a challenge for researchers who are starting to seek new techniques that approach a more realistic *in vivo* situation. This is why the use of 3D *in vitro* systems has become an urgent need to study tumoural diseases (Hoarau-Véchot et al., 2018).

2.1.3 3D *in vitro* Models

The development of 3D models using organoids systems has been shown to provide new opportunities in drug testing and understand better the biology background of pancreatic cancer. More specifically, these models can recreate a closer authentic *in vivo* like microenvironment of the human cancer. 3D *in vitro* models are considered to be the gap between 2D cell cultures and whole animal systems (Yamada et al., 2007). Unlike 2D, 3D models reproduce the distinct invasive behaviour of human tumour cells, mimicking not only the tumour-stromal cell interactions, but also the cell-cell and cell-ECM interactions of human carcinomas. In addition, these models also reflect the influence of the microenvironment on cellular differentiation, proliferation, apoptosis and even gene expression (Jong, 2005).

2.1.3.1 Spheroid Models

Spheroids are one of the most widely used 3D model systems which consist of a small aggregate of cells growing freely without adhering to a solid surface (Fennema et al., 2013; Totti et al., 2017).

There are several methods designed to create spheroid models being the most common ones the Hanging Drop, the Forced Floating and the Agitation Based Approach Method. In the first one, cells spontaneously aggregate at the bottom of a plate that was inverted and where

---

[14] Kupffer cells are resident macrophages of the liver and play an important role in its normal physiology and homeostasis as well as participating in the acute and chronic responses of the liver to toxic compounds (Roberts et al., 2007).

were at the beginning, drops of cell suspension (Fennema et al., 2013). In the Forced Floating method, it is prevented the spheroids' attachment to the vessel surface by modifying it, resulting later in a forced-floating of cells. This promotes the cell-cell contact which consequently induces a multicellular sphere formation. Lastly, in the Agitation Based Approach, a cell suspension is placed into a container kept in motion, either stirred (spinner flask bioreactor) or rotated (rotating cell culture bioreactor). The continuous cell suspended motion makes them not to adhere to the container walls and instead they form cell-cell interactions making this way a 3D cell culture arrangement (Breslin et al., 2013). Picture 2.3 gives a proper look of how these spheroid-based methods look like.
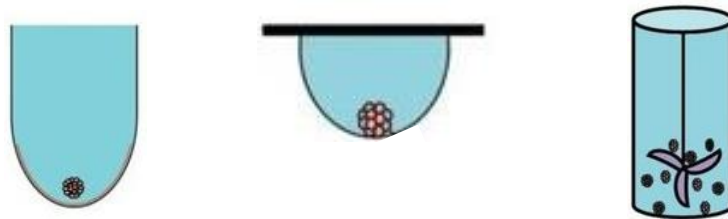
Figure 2.3: Forced Floating on the left, Hanging Drop on the middle and Agitation Based Approach on the right (Breslin et al., 2013)

Several experiments using spheroid models have been being developed over the last years and many of them have proved to be more predictive than 2D cultures. For example, Wong et al. established an efficient 3D tumour spheroid model for PDAC that was made by co-culturing PSCs with MIA PaCa-2 and AsPC-1 cells on hyaluronan grafted chitosan (CS-HA) coated plates which later assembled into tumour-like co-spheroids. These models displayed potent *in vitro* tumourigenicity such as up-regulated expression of stemness and migration markers. The migration rate of cancer cells was much faster in the 3D model than in the 2D co-cultures. This cancer cell structure also contributed to the chemoresistance of pancreatic cancer cells to GEM, turning it into a potential application in personalized and high throughput drug screening for PDAC (Wong et al., 2019). Lazzari et al. characterized a 3D multicellular spheroid tumour model by the liquid overlay technique that consisted of a co-culture of PANC-1 cells, MRC-5 fibroblasts and human umbilical vein endothelial cells (HUVEC). The results revealed the presence of a core rich in fibroblasts and FN in which endothelial cells were homogeneously distributed. The integration of the three cell types enabled to reproduce a complex microenvironment that reduced the sensitivity of cancer cells to chemotherapy thus closely mimicking the resistance to treatments observed in *in vivo* (Lazzari et al., 2018). Ware et al. achieved a spheroid in vitro model by incorporating PSCs into 3D cell culture containing, PANC-1, AsPc-1, BxPC-3, Capan-1 and MIA PaCa-2 cells. This was done using a modified hanging drop method which uses a viscosity-inducing agent called methylcellulose. The increased expression of collagenous regions leaded to the decrease in the GEM's cytotoxicity in the spheroids containing PSCs when compared to spheroids grown without PSCs, which proved that PSCs closely interact with cancer cells to create a tumour facilitatory environment that stimulates local and distant tumour growth. This could potentially provide an insight into pathways that may be therapeutically targeted to inhibit PSCs activation, thereby inhibiting the development of fibrosis in PDAC and its progression (Ware. et al., 2016). Furthermore, Longati et al. developed a spheroid system containing various human PDAC cell lines and compared it to a 2D culture where differences in cell metabolism, and chemoresistance were captured. The lactate accumulation was significantly higher after 6 days in culture in the spheroids system indicating the cells' metabolic pathway' transition from oxidative phosphorylation to aerobic glycolysis induced by the hypoxia phenomena. In addition the production of CLG and FN as well as the resistance to GEM, was increased in these systems (Longati et al., 2013).

Despite the findings mentioned above suggest spheroids to be an attractive system for *in vitro* studies with a distinct cell behaviour from 2D cultures and a higher resistance to traditional treatments, some disadvantages are associated to their usage and designing methods. For instances, in the Hanging Drop Method, culturing cells can be an inexpensive procedure when using standard plates but more expensive if done in specialized ones. Related to this is the fact that when preparing small cultures, the medium change turns up being difficult to handle when trying to avoid disturbing the cells. On the other hand, spheroids produced using this approach can be very suitable for high throughput testing and easily accessible, such as in the other methods. In the Forced Floating Method, despite simplicity and inexpensiveness are its major characteristics, the variability in cell shape and size, as well as the intensive labour requirements needed to run it, are usually current associated problems. In the Agitation Based Approach, there is a great advantage regarding the easily achievable large up production and an induced nutrients' transport in the motion cultures. Nevertheless, there is a necessity of using specialized equipment since the cells can often be exposed to shear stress that can lead to their irregular size and shape. Consequently, these experiments turn up to be more time consuming (Breslin et al., 2013).

2.1.3.2 Hydrogel Models

Hydrogels are characterized as crosslinked 3D polymeric network structures that can absorb and retain considerable amounts of water. These materials, can be formed by either natural or synthetic materials, offering a wide range of mechanical and chemical properties when culturing cells (Rosiak et al., 1999; Tibbitt et al., 2009).

Natural gels are mostly formed of proteins and ECM components such as CLG, FN, fibrin or hyaluronic acid (HA) as well as of materials derived from other biological sources, such as chitosan, alginate or silk fibrils. Since these gels are mainly built from natural compounds, they are inherently biocompatible being therefore very promising in the viability, proliferation and development of many cell types. Still, non-natural gels are formed of poly (ethylene glycol) (PEG), poly (vinyl alcohol) (PVOH) poly (2-hydroxy ethyl methacrylate) (PHEMA), among many other polymers. These types of hydrogels have shown a high ability to maintain the cultured cells viable and induce the ECM deposition. They are also very reproducible and consequently easy to manufacture (Tibbitt et al., 2009).

Although hydrogels reveal to be quite versatile models in cell cultures, they can also show some weaknesses. For example, natural gels may usually become complex, making it difficult to determine which signals are promoting the cellular function. A risk of contamination can also be associated, and their natural properties make them more easily degradable and contractible. In addition, synthetic gels lack factors that promote cell behaviour, permitting only the visualization of the cell function. In figure 2.4 it is demonstrated a specific example of how non-natural gels fail to activate integrins[15] and other surface receptors. Their synthetic environment only permits the cell viability in the 3D microenvironment, whereas in the natural gels, not only the integrin-binding sites can be seen but also the cells' growth factors (Tibbitt et al., 2009).

---

[15] Integrins are transmembrane receptors that mediate cell-adhesion, binding themselves to ECM glycoproteins or connective tissue components (H. J Danen, 2019).
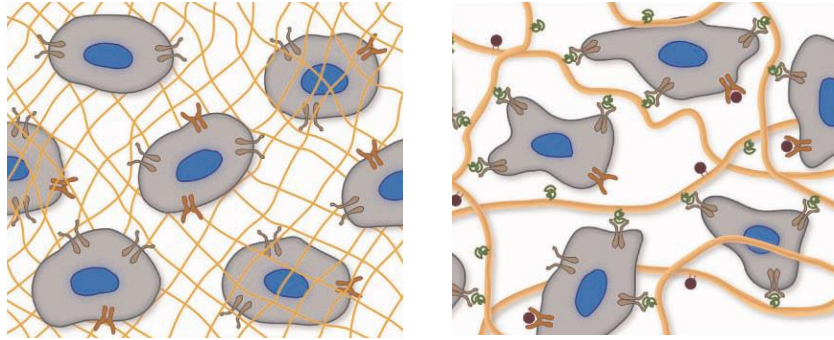
Figure 2.4: Non Natural Hydrogels on the left composed of synthetic polymers (orange) and Natural Hydrogels on the right composed of biological polymers (orange) where it can be seen the integrin binding-sites (green) and the growth factors (red) (Tibbitt et al., 2009).

Liu et al. developed a hydrogel capable of mimicking the diverse biochemical compositions and dynamic microenvironment of pancreatic desmoplasia. The modular thiol-norbornene crosslinking of gelatin, HA and PEG-based macromers, decoupled the influence of HA and matrix stiffness on PDAC cell fate. It was found out that PDAC cells responded to the HA-containing gel with limited cell proliferation and that the HA promoted invasive and matrix-induced epithelial-mesenchymal transition phenotype in PDAC cells (Liu et al., 2018). Liu et al. have also prepared hydrogels capable of being dynamically stiffened through an enzymatic reaction to test if the matrix stiffness affects the myofibroblastic activation of PSCs in pancreatic cancer. Later results evidenced that PSCs encapsulated and cultured in a stiffened matrix expressed higher levels of the α-Smooth Muscle Actin (α-SMA) and HIF-1, suggestive of a myofibroblastic phenotype (Liu et al., 2017). Similar studies were performed by Raza et al. who designed a PEG-based hydrogel prepared by step-growth thiol-ene photopolymerization, where PANC-1 cells were encapsulated. The goal was to illustrate the importance of matrix compositions on cell fate determination. Results showed that the thiol-ene hydrogels provided a cytocompatible environment for encapsulation and culture of PANC-1 cells after 4 days in culture, when comparing to 2D culture surfaces. It was also detected a higher sensitivity of the cellular proliferation to the stiffness of the matrix after 10 days in culture (Raza et al., 2013). Ki et al. characterized a PEG-peptide hydrogel system to demonstrate the influence of matrix properties and epidermal growth factor receptor (EGFR) inhibition on the growth of PANC-1 cell lines. The results showed a higher cell viability and proliferation in softer hydrogels when compared to stiffer ones. In addition, the immobilization of an EGFR peptide inhibitor, in soft hydrogels did not cause cell death whereas in stiff ones, a significant cell apoptosis was induced (Ki et al., 2013).

Hereupon, although hydrogels exhibit numerous advantageous properties in addition to their permeability to oxygen and nutrients for the cells, their high-water content however, presented due to their hydrophilic structure and large pore sizes, often results in a relatively rapid drug release which can be often problematic in 3D cultures. Their low tensile strength also makes them difficult to handle and can result in their premature dissolution. Issues like this can restrict their use in many drug screening test therapies (Hoare et al., 2008; Sudhakar et al., 2015).

2.1.3.3 Polymeric Scaffold Models

Polymeric Scaffolds have been gaining more and more prominence over the last years as a promising approach for *ex vivo* modelling of many cancer diseases. Unlike the other *in vitro* models already described before, polymeric scaffolds can, along with cells, recreate the closest microenvironment characteristics of *in vivo* tumours, more specifically of the pancreatic cancer, since they have been used as scaffolding materials for soft tissues (representative for the PDAC),

cartilage and bone tissue engineering (Fischbach et al., 2007; C Ricci et al., 2014; Totti et al., 2017).

These scaffolds are defined as three-dimension porous or fiber solid biomaterials designed to promote some of the events occurring in a tumour progression (cell adhesion, cell-ECM interactions, ECM deposition, transport of oxygen and nutrients, proliferation, differentiation, etc). Like hydrogels, polymeric scaffolds can also be made of synthetic and biological materials and depending on their fabrication method, the tensile strength, rate of degradation, porosity, shape and size can be easily manipulated. One of the other reasons these 3D models have gained such attention in medical research is due to their high-surface-to-volume ratio, mechanical properties, biodegradation and biocompatibility (Dhandayuthapani et al., 2011).
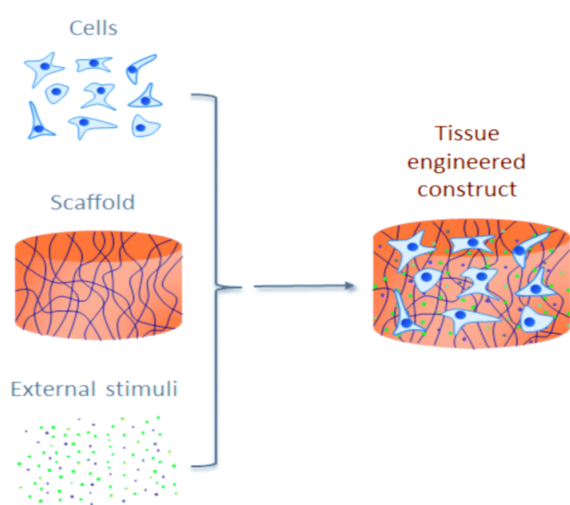
Figure 2.5: Modelling a 3D Tumour Microenvironment in a Polymeric Scaffold
(Querido et al., 2017)

As already seen before in the TE section of the Framework Chapter, the scaffolds are seeded with cells from an *in vivo* environment and with the addition of biomarkers and a culturing media, the *ex vivo* modelling of an *in vivo* system is achieved as it can be seen in the figure aside.

Despite the advantages of polymeric scaffolds, there are however few limited studies investigating the potential of these 3D models in pancreatic cancer research. From the ones found, more recently, Wang et al. developed nanofiber electrospun scaffolds seeded with PANC-1 cells to unveil how the physical attributes of the ECM regulate the mechanics of cell adhesions and intermediate filaments[16] assembly in PANC-1 cells. These scaffolds enhanced the expression of E-cadherin[17] and promoted assembly of keratin intermediate filaments. Meanwhile, the compositional variation showed different preference on up-regulation of the two intermediate filaments (Wang et al., 2019) Additionally, Wang et al. indicated that a highly porous polyglyconate/gelatin electrospun scaffold previously seeded with cancer stem cells (CSCs) enhanced the tumour formation and hepatic metastasis when transplanted into the pancreas of a nude mice. Evidences also showed that FOLFIRINOX[18] had a superior capability of preventing the hepatic metastasis of pancreatic tumour cells than GEM (Wang et al., 2013). Furthermore, Totti et al. fabricated a 3D porous polyurethane (PU) scaffold that was coated with FN to mimic features of the pancreatic cancer tumour microenvironment. The scaffold was able to support the proliferation of the pancreatic tumour cells, formation of dense cellular masses, production of CLG-I and formation of environmental stress gradients similar to the ones reported in *in vivo* studies. This suggested the PU based scaffold to be a great potential for *in vitro* high throughput studies of pancreatic cancer (Totti et al., 2018). Ricci et al. developed 3 scaffolds based on two polymers, the poly (vinyl alcohol)/gelatin (PVA/G) and poly

---

[16] Intermediate filaments are a primary component of the cytoskeleton of a lot of eukaryotic cells. These ones are extended throughout the cytoplasm and the inner nuclear membrane and are composed from a large family of proteins (MBInfo, 2018).

[17] E-cadherin is a key component of the adherent junctions that are integral in cell adhesion and maintaining epithelial phenotype of cells (Mendonsa et al., 2018).

[18] FOLFIRINOX is the name of a combination of drugs that includes folinic acid, 5-FU, irinotecan and oxaliplatin, which is used as a treatment for advanced pancreatic cancer (Cancer Research UK, 2018).

18
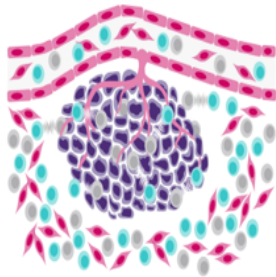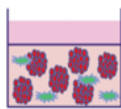
(ethylene oxide terephthalate)/poly (butylene terephthalate) (PEOT/PBT). Primary PDAC cells interfaced with different sponge-like pores and nanofiber interspaces and in all the scaffolds, PDAC cells showed good viability and synthesized tumour-specific metalloproteinases[19] (MMPs). However, only sponge-like pores, obtained via emulsion-based and salt leaching-based techniques allowed for an organized cellular aggregation very similar to the PDAC structure. This suggests that the type of polymer and its formulation technique have a crucial role in the cancer cell growth and MMP synthesis (Ricci et al., 2014). Finally, He et al. cultivated pancreatic CSCs in a poly (glycolide-co-trimethylene carbonate)/gelatin (PGTC/G) electrospun scaffold. The last one supported *in vitro* tumorigenesis from the cells for up to 7 days without inducing apoptosis in addition to an accelerated tumour evolution and proliferation (He et al., 2013).

The studies developed with polymeric scaffolds prove that these 3D models present a major advantage when studying human tissues, comparing to any 2D monolayer or other 3D model. Engineering scaffolds with different polymeric materials has, however, been a huge challenge in this field since depending on the type of cancer studied, there is a need for an optimization of the material's formulation technique and physicochemical properties such as the external geometry, surface properties, porosity, etc. This can further increase the biological performance parameters and guide the tumour tissue formation (Dhandayuthapani et al., 2011). Polymeric scaffolds are also due to their morphology, more complex and time consuming to reproduce making it also difficult to retrieve cells after culture (Breslin et al., 2013; Patel et al., 2011). Nevertheless, due to their high mechanical strength, these models still remain strong tissue engineering candidates for the pancreatic cancer research enabling even the construction of robust perfusion systems (Totti et al., 2017).

2.1.4 Comparison between 2D and 3D Models

Having seen all the characteristics that differentiate 2D from 3D Models, table 1 was constructed in order to sum up all the properties from each model based on the advantages and disadvantages that were stated above.

Table 1: 2D vs 3D Models, adapted from (Ricci et al., 2014)
Figures from (Biolabs, 2011; Burek et al., 2017; Hickman et al., 2014; Jo et al., 2018; Parker Institute for Cancer Immunotherapy, 2019; Place et al., 2009)

TUMOUR	Cell Monolayer	Xenografts	Spheroids	Hydrogels	Polymeric Scaffolds	Caracteristics
						Physical Exemplification
	2D, *in vitro*	3D, *in vivo*	3D, *in vitro*	3D, *in vitro*	3D, *in vitro*	Model Type
	-	+++	+	++	+++	Complexity
	+++	+	++	++	+++	Reproducibility
	-	+++	++	++	+++	Fabrication Cost
	-	+++	++	++	+++	Time Consumption
	+++	+	+++	++	+	High-Throughput
	+++	++	+	++	+++	Long-Term Cultivation
	-	++	+	+	+++	Tumour Phenotype
	-	++	++	++	+++	Tumour Microenvironment

---

[19] Metalloproteinases are involved in wound healing, angiogenesis, and tumour cell metastasis (National Cancer Institute, 2019).

Seeing all the major characteristics of the *in vivo* and *in vitro* models, and what achievements have been obtained with each of them, it is possible to conclude why polymeric scaffolds have most of the advantages when mimicking the tumour microenvironment and the ECM assembly. The reason why it has also become a highly demanded cell culture model despite its complexity and time consumption's factors, was also well specified in this chapter. Although xenografts' properties show to be the most similar to the 3D *in vitro* scaffolds, these models cannot however show such predictive results as well as it brings some involvements to the cancer research (Ricci et al., 2014). This way, polymeric scaffolds have become the potential model to look into the future for PDAC studies.

2.2 Culture Systems

This chapter enhances the two mainly used cell condition cultures: the Static and the Dynamic Culture (UKEssays, 2018). Each of them allows the cultivation of cells in distinct ways with comparable results.

2.2.1 Static Culture

Static Culture Systems were initially developed for the growth of adherent cells and tissue clots. These systems are based on flasks or plates with a flat bottom that operate in static conditions under a controlled atmosphere within an incubator. The cells are commonly seeded with a certain amount of medium that provides nutrients and allows oxygen diffusion for the cells to survive. Nowadays not only adherent cells are being cultivated in these systems but also suspendable cells (Al-Rubeai, 2015).
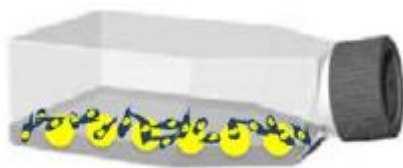
Figure 2.6: 2D Static Culture
(Perez et al., 2014)

With the advances in animal cell technology, static cultures have become less efficient when comparing to the dynamic ones, due to their quite low cell and product concentrations that are a consequence of the low seeding efficiencies and the limited culture medium that only maintains a small number of cells in culture. Furthermore, other problems are related to this type of culturing which are the poor transport of nutrients, oxygen and wastes, that induce the presence of concentration gradients in culture (Al-Rubeai, 2015; Perez et al., 2014).

2.2.2 Dynamic Culture

Dynamic Culture Systems were also developed with the same aim as the static culture ones. Here, adherent cells grow attached to microcarriers[20] in roller bottles which are filled with medium and revolving slowly. The gentle agitation prevents gradients from forming within the medium which does not happen in static cultures and may adversely affect cell growth. The roller bottles were designed to increase the surface area required for the cultivation of large number of adherent cells as well as the further increase in cell and product concentrations (Al-Rubeai, 2015).

---

[20] Microcarriers are matrices in which adherent cells can attach to, allowing them to proliferate while suspended freely in a bioreactor's media (Chemometec, 2019).
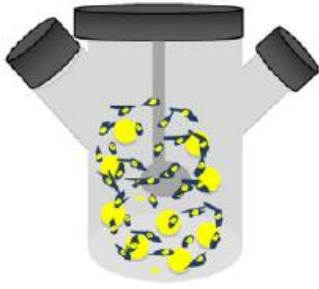
Figure 2.7: 3D Dynamic Culture
(Perez et al., 2014)

There are a bunch of advantages related to dynamic culture systems that are not found in static ones. They range from a better nutrient and waste delivery as well as a larger gas-liquid oxygen transfer, offering the cells a higher survival rate and a high cell number in culture. These systems also allow a more homogenous suspension of cells within the culture medium (Campos et al., 2013; Perez et al., 2014). In the next section there are enhanced some of the most common dynamic culture systems used in the biotechnology field (bioreactors) and what characteristics make them very a very promising approach when culturing cells in 3D in *vitro* models.

2.2.2.1   Bioreactors in Tissue Engineering

Bioreactors are unit operations defined as devices that use mechanical stimuli to influence biological processes in cell culture. They can aid the *in vitro* development of new tissues by providing the biochemical and physical regulatory signals that cells need to undergo differentiation or to allow the production and deposition of ECM. As already said before, the development of new dynamic culture's equipments was essential to overcome the problems associated in static. This way, bioreactors are supposed to perform several functions that range from the uniform cell distribution, the maintenance of the optimal concentration of gases and nutrients, the facility of the mass transport to the tissue and the exposition of the construct to physical stimuli to purvey information about the expansion of the 3D tissue (Partap et al., 2010).

2.2.2.1.1   Spinner Flask Bioreactors
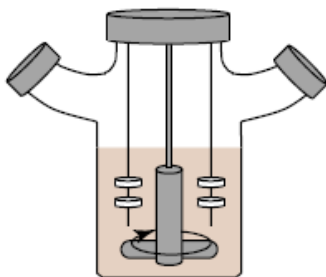
Figure 2.8: Spinner Flask
(Martin et al., 2004)

Spinner Flask Bioreactors are one of the most used and basic bioreactors in TE. They induce the mixing of oxygen and nutrients throughout the medium and reduce the concentration boundary layer at the construct surface. Here, a magnetic stirrer mixes the media and the scaffolds are fixed in place with respect to the moving fluid. These bioreactors are commonly associated with turbulent flow, having this way lead to an improvement on cartilage grown experiments. However, they are still not much appropriate for some clinical uses due to their lack of mass transfer that could prevent homogeneous cell distribution. In addition, cells predominantly reside on the construct periphery (Partap et al., 2010).

2.2.2.1.2   Rotating Wall Bioreactors
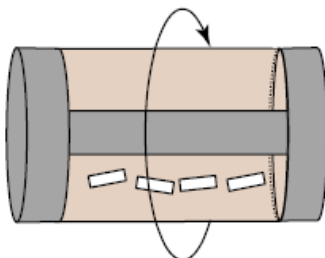
Figure 2.9: Rotating Wall Bioreactor
(Martin et al., 2004)

Rotating Wall Bioreactors consist of cylindrical chambers in which the vessel walls (outer and inner) are both capable of rotating at a constant speed. This rotational speed is such that a balance is reached between the downward gravitational force and the upward hydrodynamic drag force acting on the scaffolds and allowing them to move freely in the media. These equipments own a much more versatile option than spinner flasks due to their dynamic laminar flow generated by the rotating fluid that reduces the diffusional limitations of nutrients and wastes while producing low levels of shear stress. Fluid transport is enhanced in a similar mechanism as the spinner flasks and gas transport occurs through a gas

exchange membrane. As the tissue grows in the bioreactor, the rotational speed must be increased in order to balance the gravitational force and ensure that the scaffolds remain in suspension (Partap et al., 2010).

2.2.2.1.3 Compression Bioreactors
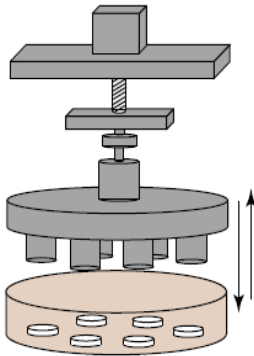
Figure 2.10: Compression Bioreactor
(Martin et al., 2004)

Compression Bioreactors are a class of bioreactors that are designed in a way that both static and dynamic loading can be performed. The bioreactors consist of a motor, a system providing linear motion and a controlling mechanism used to provide displacements of different magnitudes and frequencies. Due to the dynamic compression, fluid flows in the scaffolds making this way an improvement in the mass transfer and an upgrading in aggregate tissues to levels approaching those of in *in vivo*. However, some care must be taken when stimulating multiple scaffolds simultaneously, in order to make sure that the constructs are of similar height or the compressive strain applied will vary as the scaffold height does (Partap et al., 2010).

2.2.2.1.4 Flow Perfusion Bioreactors
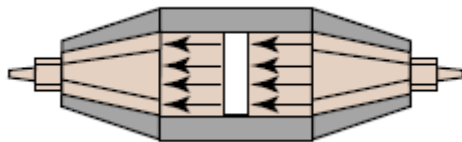
Figure 2.11: Flow Perfusion Bioreactor
(Martin et al., 2004)

Beyond the bioreactors described above and other ones also commonly used (Tensile Strain and Hydrostatic Pressure Bioreactors), the Flow Perfusion Bioreactors are currently considered to be the most valuable in many TE areas (Campos et al., 2013). One of the reasons, is that cultures using flow Perfusion Bioreactors have been shown to provide more homogeneous cell distribution throughout the scaffolds, whereas in the Spinner Flask Bioreactors, as already seen before, most of the viable cells are placed on the periphery. These equipments consist of a pump and a scaffold chamber joined together by tubing. A fluid pump is used to force media flow through the cell seeded scaffold, and the last one is kept in position across the direct flow path of the device. The media is consequently perfused through the scaffold, enhancing fluid transport within the internal pores (Partap et al., 2010). This way, the system is capable of performing both seeding of the scaffold and subsequent culturing of the construct (Martin et al., 2004).

When comparing this dynamic culture system to other bioreactors, the first one has proved to be the best for fluid transport. However, it is important to consider that the effects of direct perfusion can be highly dependent on the medium flow rate. Optimizing a perfusion bioreactor must address a careful balance between the mass transfer of nutrients and waste products, the retention of newly synthesized ECM components and the fluid induced shear stress within the scaffold pores (Partap et al., 2010). To date it is unknown any perfusion bioreactor system used for pancreatic cancer studies, however, this device has shown its potentialities in other tumour diseases such as breast and colorectal cancer that along with pancreatic cancer represent a similar tissue stiffness and TME characteristics. For example, Manfredonia et al. investigated the suitability of a perfusion-based bioreactor for 3D culture of primary colorectal cancer cells where these ones were fragmented and put between 2 GLG scaffolds in a "sandwich-like" format. The 3D model was cultured for 3 days both in a perfusion and static system. Results showed that cultures under perfusion resulted in significantly higher maintenance of the tissue integrity when compared to the static cultures, with preservation of the whole TME components (cancer,

mesenchymal stromal and immune cells). This tumour tissues also displayed an almost intact architecture with viable and proliferating tumour cells in similar proportions to those of original tumours. In addition, immune cells were capable to release effector cytokines[21] upon activation (Manfredonia et al., 2018). Additionally, Muraro et al. cultured primary breast cancer cells in the same "sandwich-like format" between CLG porous scaffolds and cultured it under a perfusion flow. The viability of the breast cancer specimens in perfusion was preserved and promoted the expansion of breast cancer cells along with stromal and immune cells into the scaffolds. The cancer cells were also viable and recapitulated the initial histology formation of glands after 21 days (Muraro et al., 2017). Several studies using perfusion systems have also been tested for bone tissue engineering as it is the example of Warren et al. who designed PU scaffolds, previously seeded with murine preosteoblasts[22] and loaded them in dynamic culture. Results showed a significantly improved core cell activity and density (maintained at approximately 80%), compared to the static culture and the periphery ratio also showed steady till the end of the experience (Warren et al., 2009). In addition to other studies, the scaffold-based perfusion bioreactors proved to represent a successful organotypic tumour model for the long-term *in vitro* cell culture, even for thick tissues such as bone, and suitable for testing the sensitivity of primary tumour cells to different treatments.

2.3 Summary

Compacting all that was stated in the State of Art Chapter, it was firstly approached the different types of cell culture models that have been used through the years by researchers, leading to the conclusion that 3D models are currently, the potential candidates in the TE field. More specifically, the 3D polymeric scaffolds seem to have a suitable role when studying and mimicking the tumour's microenvironment and ECM progression. Secondly it was broached the importance of having dynamic cultures when culturing mammalian cells and its benefits over static cultures (longer-term cell culture and survival rate). Lastly, it was enhanced the use of perfusion bioreactors that stimulate the cellular growth complexity similar to *in vivo* tumours.

---

[21] Effector Cytokines mediate host defensive mechanisms to various infections and are involved in the pathogenesis of many autoimmune diseases. These receptors are broadly expressed on various epithelial tissues (Ouyang et al., 2008).

[22] Preosteoblasts are mesenchymal cells that originate osteoblasts which are bone building cells (Rutkovskiy et al., 2016).

3 Materials and Methods

When designing a biological experimental work, the main things to have into account are the variables of the system that was settled to be implemented. The variables are the unknown part of all the overall experiment. In this case, there were two uncharted parameters of interest: the Addition of Perfusion and the Addition of Drugs in a 3D model. Each variable has, therefore, its Experimental and Control experience that will be then combined between the other variable's Experimental and Control experiences. Supposing that the Addition of Perfusion's variable is given by **P** and the Addition of Drugs' variable is given by **D**, the following table shows in a clear way what do the Experimental, **E**, and Control, **C**, experiences mean for each variable:

Table 2: System's Variables and Experimental and Control Experiences

	Variables	
	P	**D**
E	Perfusion Culture	Addition of Drugs
C	Static Culture	Non addition of Drugs

Figure 3.1 helps simplifying the planning of the experimental work, allowing this way the visualization of how the main experiences will look like, as it is represented in table 3:
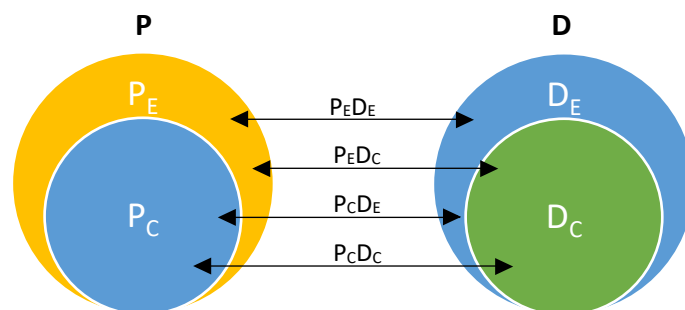
Figure 3.1: Experimental Planning Scheme

Table 3: Main Experiences to be Performed

P_ED_E	Perfusion Culture with Drugs
P_ED_C	Perfusion Culture without Drugs
P_CD_E	Static Culture with Drugs
P_CD_C	Static Culture without Drugs

It is important to enhance that due to a coccus bacterial contamination in the third week of culture of the Perfusion Culture without Drugs, no available data regarding this experience is presented in the Results and Discussion Chapter of this report.

Furthermore, other procedures were also considered as part of this dissertation's work. These ones are:

- The Culture of PANC-1 Cells in Hydrogels
- The Culture of PANC-1 Cells in CLG Coated Scaffolds

To perform all the experiments stated, a series of protocols had to be carefully followed and each of them is described in the next subchapters below. Since all the experiments where the cells were being used were done inside the Biological Safety Cabinet (BSC, Triple Red, UK), it was assured that the laminar flow was switched on and the hood was sterilized as well as all the materials used. During the procedures, all the plastic wares used were from Thermo Fisher Scientific, UK. Some of the lab's compounds and equipments stated, are further described in Appendix A and B, respectively.

3.1 Cell Maintenance

The Cell Maintenance concerns to all the basic necessary procedures in animal cell culture. From the ones introduced bellow, the Media Change and Cell Passaging are periodically repeated (every two or three days). This is to assure the cells have their growth environment (media) rich in the nutrients necessary for their development and that they have enough space to continue to grow freely in the culture vessels.

3.1.1 Preparation of Media

A fresh bottle of Dulbecco's Modified Eagle Medium (DMEM) with high glucose (Sigma-Aldrich, UK) is taken out from the -4°C and warmed up in the water bath (Thermo Fisher Scientific, UK) at 37˚C. Secondly, a falcon with 1 aliquot of 50ml of Fetal Bovine Serum (FBS, Thermo Fisher Scientific, UK), another with 5ml of L-glutamine (Sigma-Aldrich, UK) and another with of 5ml of Penicillin-Streptomycin Solution (Pen Strep, Sigma-Aldrich, UK) are taken out from the -20˚C to the water bath too.

All the aliquots from the falcon are gently poured out in the DMEM bottle or with the help of a pipette gun and the bottle is mixed and labelled with the user's initials and date of preparation. Finally, a certain amount of the freshly made media is added to a well plate and put in the in a humidified CO_2 incubator (Thermo Fisher Scientific, UK) at 37˚C and 5% CO_2 for 24 hours to verify its sterility under the microscope (Zeiss, Germany).

3.1.2 Media Change

The DMEM is warmed up in the water bath at 37˚C. The medium inside the T-flask is poured out in a waste box and an appropriate volume of medium, depending on the culture vessel's size, is added to it. Lastly, the PANC-1 cells (Sigma-Aldrich, UK, ECAAC 87092802) are

visualized under the microscope to confirm if everything is sterile and the vessel is put inside the humidified CO_2 incubator at 37˚C and 5% CO_2.

3.1.3   Cell Passaging

The Cell Passaging is a technique usually done to keep cells alive and growing for extended periods of time. During the Cell Maintenance's Procedures this was done every time the cells showed a confluency[23] of 80 to 90%, as seen in figure 3.2.

The DMEM, the Phosphate-Buffered Saline (PBS, Sigma-Aldrich, UK) and the Trypsin-EDTA (Sigma-Aldrich, UK) are warmed up in the water bath at 37˚C. The medium inside the T-flask is poured out in a waste box and an appropriate volume of PBS is added to remove all traces of medium by swirl the vessel around. This is because, the medium already contains FBS that stops the Trypsin-EDTA's action from detaching the cells from the vessel walls. The added PBS is poured out in the waste box and it is added an appropriate amount of trypsin-EDTA in the vessel. The culture vessel is then incubated for 5 minutes and after this period, it is certified under the microscope that the cells are well detached from the vessel walls. If not, the vessel can be incubated for another few minutes or tapped/swung gently.

Consequently, a certain amount of medium is added to neutralize the trypsin-EDTA, action and the medium is pipetted to remove all adherent cells. The cell suspension is then added to a falcon and 1ml of it, is taken out and put in an eppendorf for cell counting procedures. The falcon is centrifuged for 5 minutes at a spin rate of 1500rpm. Finished this time, the resulting supernatant is poured out in the waste box and the cells are resuspended in a new medium volume. The cells are added to a new culture vessel with fresh medium, previously labelled with the cell name, passage number, user's initials and date, always having into account that the volume taken from the falcon must have about 1 million cells. Finally, the cells in the culture vessel are visualized under the microscope and placed in the humidified CO_2 incubator at 37˚C and 5% CO_2.
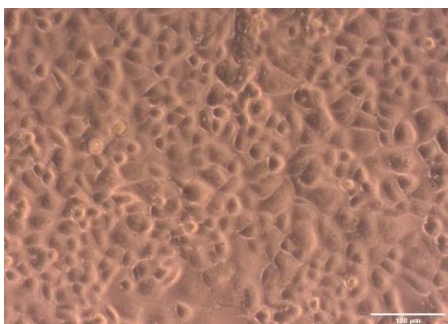
Figure 3.2: PANC-1 Cells in a T-75 Flask with ~ 90% Confluency

3.1.3.1 Cell Counting

The Cell Counting is a procedure made to have an approximate estimation of how many cells are in a volume suspension.

After taking 1ml of the cell suspension from the falcon to an eppendorf in the Cell Passaging subchapter, it is taken from here 500µl of cell suspension to a new eppendorf. 500µl of Trypan Blue (BioWhittaker, Lonza, Switzerland) is also added to the new eppendorf and the resulting solution is well mixed. Then, 10µl of the solution is taken from the eppendorf and introduced in one of the chambers of the haemocytometer (Bright-Line, Sigma-Aldrich, UK) that will be looked under the microscope. During the cell counting the PANC-1 cells are counted in

---

[23] Confluency is a measure of the number of the cells in a cell culture vessel, and refers to the coverage of the vessel by the cells (Definitions, 2019).

the 4 squares presented inside the haemocytometer's chambers as it is presented in figure 3.3. After knowing the number of cells, a calculation is made to know the cell number presented in the falcon where the 1ml of cell suspension was taken from.

$$T_{number\ of\ cells} = \frac{(number\ of\ cells\ counted)\ (dillution\ factor)\ (10^4)\ (volume\ of\ original\ cell\ suspension)}{4} \quad (1)$$

Knowing the number of cells in suspension and exact amount of medium where the cells will be resuspended again, it can then be calculated what volume, containing 1 million cells, needs to be taken out from the falcon to the T-Flask.
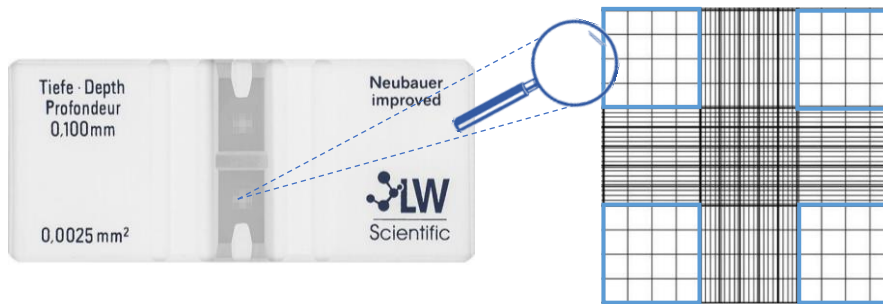
Figure 3.3: Haemocytometer where the cells are counted in the 4 squares highlighted in blue
(Joshi, 2014; LW Scientific, 2019)

3.1.4 Cell Freezing

Depending on the number of cells required to freeze, several 1ml cryovials are labelled with the cell name, passage number, number of cells frozen, user's initials and date. Following the steps of the Passaging Procedure and after centrifuge the falcon for 5 minutes, the supernatant is dropped out in the waste box. A specific amount of medium is added to the falcon to create cell suspension, having into account that in this one will be added 10% of Dimethyl Sulfoxide (DMSO, Sigma-Aldrich, UK) quickly mixed. The DMSO acts like a cryoprotectant when freezing cells allowing them to freeze gradually at negative temperatures. Later, 1ml of cell suspension volume is added to each of the cryovials that are then stored in a freezing container (Mr Frosty) at -80°C for 24 hours. The container is used to achieve a rate of cooling very close to -1°C/min, the optimal rate for cell preservation (Thermo Fisher Scientific, 2019). After this time, the cryovials are taken out from the Mr Frosty and put in a new box at -80°C.

3.1.5 Cell Thawing

The DMEM is warmed up in the water bath at 37°C. A cell culture vessel is labelled and prepared with a certain amount of medium and 9ml of medium is added to a 15ml falcon. A cryovial is defrosted manually in the water bath until 90% of the vial is thawed out. Very quickly, the cell suspension is taken out from the cryovial using a 1ml pipette and added to the falcon tube. The procedures need to be done quickly because the freezing medium contains DMSO which is harmful to the cells at room temperature. The falcon is then centrifuge for 5 minutes at a spin rate of 1500rpm. After this, the resulting supernatant is dropped out in the waste box and an appropriate amount of medium is added to the falcon and pipetted to mix the cell pellet. The cell suspension is then added to the culture vessel prepared before and the cells are visualized under the microscope. The culture vessel is finally placed in the humidified CO_2 incubator at 37°C and 5% CO_2 and after 24 hours the medium is changed to remove all remnants of DMSO.

3.2 Preparation of the 3D Scaffolds

The PU scaffolds are the frame of the cell structure. Their preparation goes from the moment when they are fabricated as a PU pie, by the Thermally Induced Phase Separation Method (TIPS), to the moment when they are seeded with PANC-1 cells. Between these two steps the scaffolds are coated with FN from bovine plasma (1mg/ml, Sigma-Aldrich, UK) *via* adsorption, not only to mimic one of the most prominent ECM proteins in pancreatic cancer, but also to enhance the cell adhesion on the PU matrix (Totti et al., 2018). All the followed procedures are described below:

3.2.1 Fabrication of the PU Pie

3g (5% w/v) of PU beads (Noveon, Belgium) are dissolved in 60ml of Dioxane (99.8% anhydrous pure, Sigma-Aldrich, UK) in a glass recipient with the help of a magnetic stirrer, at room temperature for 3 hours to make a homogenous polymer solution. The solution is transferred to a petri dish inside a lyophilisation flask which is then quenched at -80°C, for 3 hours. The phase separation takes place when the solvent is removed by freeze drying (sublimation) in a PEG bath at -15°C under 0.01mbar vacuum pressure, for 48 hours. The solvent is sublimated from the system and goes to a glass column placed inside a liquid nitrogen bucket. The presence of liquid nitrogen at -196°C makes the dioxane to condensate from the gas to the liquid state being this way possible to retrieve it. The glass column is changed every two times per day till the initial volume of dioxane is mostly retrieved in the previous mixing recipient.

a   **b**   **c**
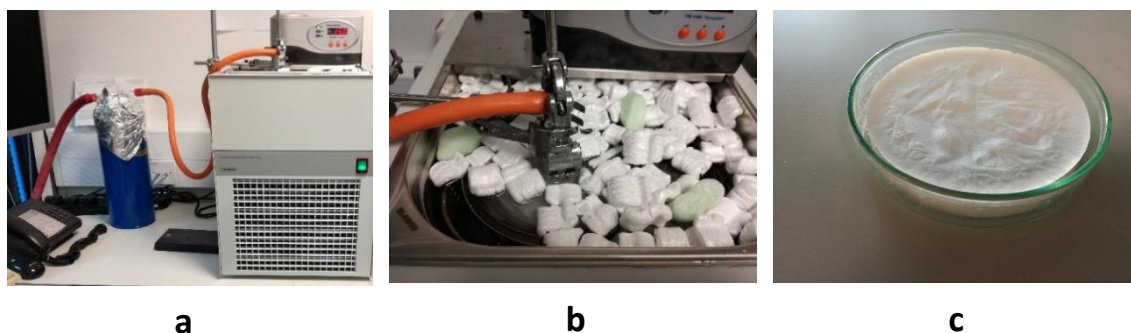
Figure 3.4: (a) TIPS System installed in the lab with the PEG bath at the right and the glass column covered with aluminium foil inside the liquid nitrogen bucket at the left. (b) Lyophilisation flask inside the PEG bath. (c) Resulting PU Pie inside the petri dish.

3.2.2 Cutting the PU Scaffolds

Figure 3.5: Final cubic dimension required for each scaffold

About half of the PU pie is introduced in a liquid nitrogen bucket at -196°C for a few seconds. This will make the scaffold material more rigid, making it easier to cut than in its natural spongy shape. With the help of a blade and a drawn scale, half of the PU pie is cut into small pieces of 5×5×5mm^3 dimension. The scaffolds' average pore size is 100-150µm, the porosity of 85-90%, which was previously determined by Mercury Intrusion Porosimetry (PoreMaster33, Quantachrome, USA), the specific volume of 2.3±0.48 cm^3/g, which was previously obtained using Helium Displacement Pycnometry (AccuPyc, 1330 V3.00, Micromeritics, USA) and the compression modulus of 28±3 kPa, as previously reported (Safinia et al., 2006).

3.2.3   Sterilization of the PU Scaffolds

After cutting the PU scaffolds, they are placed in a well plate in order to be sterilized with 70% v/v ethanol solution under the UV light inside the BSC, for at least 3 hours. After this period, the ethanol solution is taken out from the wells with a pipette and the scaffolds are dipped twice with PBS and immersed in medium. The well plate is placed in the humidified CO_2 incubator at 37˚C and 5% CO_2 overnight to verify later under the microscope if the scaffolds are well sterilized.

3.2.4   Surface Modification of the PU Scaffolds

The FN is taken out from the -4˚C and warmed up at room temperature and a 30ml FN solution with PBS is prepared in a 50ml falcon. Knowing that the Working Solution Concentration of the FN is 25µg/ml, by using equation number 2 it is known the volume that needs to be taken out from the stock solution.

$$C_1 V_1 = C_2 V_2 \qquad\qquad (2)$$

In another 50ml falcon is added 30ml of PBS and a certain number of scaffolds are transferred with the help of a sterilized tweezer. The falcon is centrifuge for 10 minutes at a spin rate of 2500rpm. This is to assure the scaffold's pores get widely open to adsorb the highest FN concentration as possible. After this time, the scaffolds are taken out from the falcon and introduced in the one where the FN solution was previously prepared. The falcon where the scaffolds are now introduced is centrifuge for 20 minutes at a spin rate of 2000rpm to ensure the better penetration and uniform distribution of the FN in the PU matrix. After this time, the scaffolds are taken out from the falcon and introduced in the falcon previously used with a new 30ml volume of PBS. The falcon is centrifuge for 10 minutes at a spin rate of 1500rpm. This is to assure that the remnants of the FN that were not adsorbed by the scaffold's are washed out from surface in order to unblock the pores. Consequently, the scaffolds are taken out from the falcon and introduced in a 24 well plate topped up with 1.5ml of medium in each well. The well plate is introduced in the humidified CO_2 incubator at 37˚C and 5% CO_2 overnight and the scaffolds are later looked under the microscope to check their sterility.

3.2.5   3D Cell Culture in the PU Scaffolds
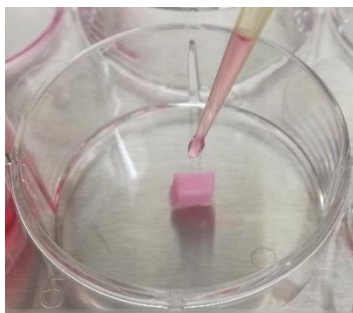
Figure 3.6: PANC-1 cell suspension seeding onto the PU scaffold

After having the scaffolds sterilized, they are taken out from the medium where they were and put in new fresh wells from a 24 well plate, by squeezing them properly in order to eliminate the medium's excess and make them as dried as possible. The more dried they are, the better they will soak the cells and the more attached the cells will become after seeding. Following the steps of the Passaging Procedure, a certain amount of volume suspension is taken out from the falcon to a new one having into account the number of cells required for the seeding procedure (0.5 million cells in each scaffold). The new falcon is introduced in the centrifuge at a spin rate of 1500rpm for 5 minutes. The volume suspension is poured out in the waste box and a certain amount of medium is introduced in the falcon, knowing that only 30µl of cell suspension will be seeded in each scaffold. Then, 0.5 million PANC-1 cells (in 30µl of cell suspension) are carefully seeded into each scaffold. This method is achieved by adding the cell solution dropwise, waiting between each drop for the scaffold to soak the cells. The scaffolds are then left in the humidified CO_2 incubator at 37˚C and 5% CO_2 for a period of 1 hour and after this, 1.5ml of medium is added in each of the wells. The 24 well plate is again introduced in the humidified CO_2 incubator at 37˚C and 5% CO_2 (Appendix C).

3.3 3D Dynamic Cell Culture

The Dynamic Cell Culture had place in a Perfusion Bioreactor (Cellab GmbH, Germany) where a set of different experiments were performed over time. The first ones consisted in preliminary experiments where the main goal was to optimize the perfusion flow rate that kept the highest cell's viability in the scaffolds. Furthermore, a long-term culture of 4 weeks took place and a chemotherapy reagent was added after 28 days in culture. All the followed procedures are described below:

3.3.1 Preliminary Experiments

In these experiments 5 different flow perfusion rates were tested: 4.60ml/min, 0.46ml/min, 2.5m/min, 1.5ml/min and 3.5ml/min. For each experience, 3 uncoated scaffolds are previously seeded with PANC-1 cells and kept in the humidified CO_2 incubator at 37˚C and 5% CO_2 for a period of 24 hours in static culture. Each bioreactor's bag is filled with the help of a syringe, with 50ml of medium that will be run through the scaffolds. After 24 hours in static, the scaffolds are introduced in a 24 well plate with a previous prepared solution of the cell viability reagent for 3 hours straight in the humidified CO_2 incubator at 37˚C and 5% CO_2. The solution absorbance is then measured, and the scaffolds are introduced in the bioreactor's scaffold holders where a chosen flow rate will be run through for 48 hours straight. After this time, the scaffolds are taken out from the bioreactor and introduced again in a 24 well plate with a previous prepared solution of the cell viability reagent for new cell viability assays. The scaffolds are then washed in medium to clean any remnants of the cell viability solution and introduced inside cryovials to be snap frozen[24] in liquid nitrogen at -196˚C during approximately 15 minutes. The cryovials are then placed at -80˚C.

3.3.1.1 The Perfusion Bioreactor

The Perfusion Bioreactor used while running the experiments consisted of a Docking Station and a Disposable Set that are meant for artificial tissue culture. While running, this equipment is integrated inside the humidified CO_2 incubator at 37˚C and 5% CO_2 and connected to a standard PC where a software, The Cellab Control Centre, designs all the experimental control (Cellab GmbH, 2017).

3.3.1.1.1 The Docking Station

The Docking Station can operate for automated control of the cell tissue culture as it was performed in all the bioreactor experiments. This equipment is available with either a 1-channel or 5-channel media pump. The last one, was the elected for this work's purpose (Cellab GmbH, 2017). The peristaltic pump operates with a 5-channel disposable pump head from the disposable set. This one, offers a standard work range for the flow rate between 0.46 to 4.60ml/min per pump channel. The flow rate, that is determined with zero pressure and no suction height can be adjusted in the control centre software with a resolution of 0.01ml/min (Cellab GmbH, 2017).

---

[24] Snap Freezing is the technique in which a sample is rapidly frozen using dry ice or liquid nitrogen. This procedure reduces the chance of water present in the sample forming ice crystals during the freezing process maintaining this way all the sample's integrity and structure (Biocision, 2019).
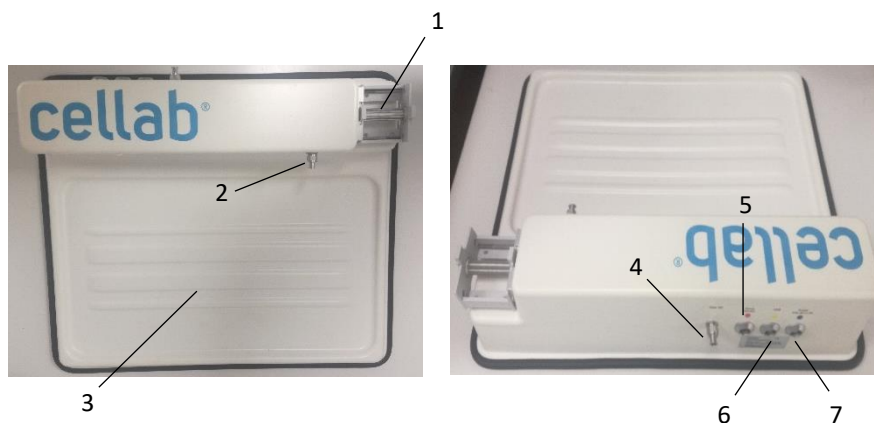
Figure 3.7: The Docking Station

The Docking Station, in the picture above, is constituted by:

1. 5-channel Media Pump Head
2. Gas outlet connector (not used in the experiments)
3. Disposable Set receiving Frame
4. Gas inlet connector (not used in the experiments)
5. Temperature Sensor Plug
6. USB Plug
7. Power Plug

3.3.1.1.2 The Disposable Set

The Disposable Set designed for the tissue culture experiments consists of a closed tubing system assembled with a 5-channel disposable pump head, 5 scaffold holders and 5 media bags where the media is introduced before starting the experiences (Cellab GmbH, 2017).

Figure 3.8: The Disposable Set
(News Medical Life Sciences, 2019)

3.3.2 4 – Weeks' Cell Culture in the PU Scaffolds

5 coated scaffolds are previously seeded with PANC-1 cells and kept in the humidified CO_2 incubator at 37˚C and 5% CO_2 for a period of 24 hours in static culture. Each of bioreactor's bags are filled with the help of a syringe, with 50ml of medium that will be run through the scaffolds when they are placed in. After 24 hours in static, the scaffolds are introduced in a 24 well plate with a previous prepared solution of the cell viability reagent for 3 hours straight in the humidified CO_2 incubator at 37˚C and 5% CO_2. The solution absorbance is then measured,

and the scaffolds are introduced in the bioreactor's scaffold holders where the best flow rate will be run through, for 4 weeks. Once a week, at day 7, 14, 21 and 28, a new cell viability assay is measured in the scaffolds.

Figure 3.9: Long-Term Dynamic Culture in the Perfusion Bioreactor

3.3.3 Addition of Chemotherapy after 4 weeks in Perfusion

At day 28, the GEM (hydrochloride ≥98% (HPLC), 50mM, Sigma-Aldrich, UK) is taken out from the -20˚C and warmed up at room temperature. Knowing that the Working Solution Concentration of the GEM is 50µM, by using equation number 2 it is known the volume that needs to be taken out from both the stock solution to be mixed in a specific volume of DMEM. The perfusion with GEM is then run for 24 hours, and after this time there are chosen 2 scaffolds to be subjected to the cell viability assay while the others are kept in the perfusion system for another 24 hours. At the end of the additional 24 hours, the GEM is taken out and the remaining scaffolds are kept in culture till day 7 after adding the GEM. Once the cell viability in each scaffold is tested, these ones are then washed in medium to clean any remnants of the cell viability solution and introduced inside cryovials to be snap frozen in liquid nitrogen at -196˚C during approximately 15 minutes. The cryovials are then placed at -80˚C.
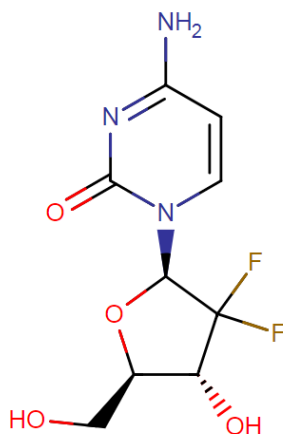
Figure 3.10: GEM Compound Structure (DrugBank, 2019)

3.4 3D Static Cell Culture

The Static Cell Culture had place in well plates where a set of different experiments were performed over time. The first one consisted in the control of the preliminary experiments performed in the perfusion bioreactor while the 2 others consisted in a 4 – weeks' culture where a chemotherapy reagent was added after 28 days in culture in one of the well plates. In addition,

a static culture using 5 different types of hydrogels (Manchester BIOGEL, UK) and a static culture using 4 jellyfish CLG coated scaffolds (Jellagen, Marine Biotechnologies, UK) were also developed for future work approaches. All the followed procedures are described below:

3.4.1 Preliminary Experiments

3 uncoated scaffolds are previously seeded with PANC-1 cells and kept in the humidified CO_2 incubator at 37˚C and 5% CO_2 for a period of 24 hours in static culture. After 24 hours in static, the scaffolds are introduced in a 24 well plate with a previous prepared solution of the cell viability reagent for 3 hours straight in the humidified CO_2 incubator at 37˚C and 5% CO_2. The solution absorbance is then measured, and the scaffolds are introduced in a 24 well plate previously topped up with 1.5ml of medium for a period of 48 hours straight. After this time, the scaffolds are taken out from culture and introduced again in a 24 well plate with a previous prepared solution of the cell viability reagent for new cell viability assays. The scaffolds are then washed in medium to clean any remnants of the cell viability solution and introduced inside cryovials to be snap frozen in liquid nitrogen at -196˚C during approximately 15 minutes. The cryovials are then placed at -80˚C.

3.4.2 4 – Weeks' Cell Culture in the PU Scaffolds

7 coated scaffolds are previously seeded with PANC-1 cells and kept in the humidified CO_2 incubator at 37˚C and 5% CO_2 for a period of 24 hours in static culture. After 24 hours in static, the scaffolds are introduced in a 24 well plate with a previous prepared solution of the cell viability reagent for 3 hours straight in the humidified CO_2 incubator at 37˚C and 5% CO_2. The solution absorbance is then measured, and the scaffolds are introduced in a 24 well plate previously topped up with 1.5ml of medium. For a period of 28 days the scaffolds are kept in static having their media change in the wells every 3 times a week. Once a week, at day 7, 14, 21 and 28, a new cell viability assay is measured in the scaffolds.

Figure 3.11: Long-Term Static Culture in one of the 24-Well Plates

3.4.3 Addition of Chemotherapy after 4 weeks in Static

At day 28, the GEM is taken out from the -20˚C and warmed up at room temperature. Knowing the Working Solution Concentration of the GEM is 50μM, by using equation number 2 it is known the volume that needs to be taken out from both the stock solution to be mixed in a specific volume of DMEM. The static culture with GEM is then settled for 24 hours, and after this time there are chosen 2 scaffolds to be subjected to the cell viability assay while the others are kept in the static system for another 24 hours. At the end of the additional 24 hours, the GEM is taken out and the remaining scaffolds are kept in culture till day 7 after adding the GEM. Once the cell viability in each scaffold is tested, these ones are then washed in medium to clean any remnants of the cell viability solution and introduced inside cryovials to be snap frozen in liquid nitrogen at -196˚C during approximately 15 minutes. The cryovials are then placed at -80˚C.

3.4.4 3D Cell Culture in the Hydrogels

The hydrogels and the DMEM are warmed up in the water bath at 37°C. Following the steps of the Passaging Procedure, a certain amount of volume suspension is taken out from the falcon to a new one having into account the number of cells required for the seeding procedure, which will be 6 times more concentrated than the final cell concentration solution required (0.5 million cells in each ml of hydrogel) (Manchester BIOGEL, 2019). 500μl of each hydrogel is transferred into a 15ml falcon and centrifuged for 1 minute at a spin rate of 3000rpm. Knowing the dilution factor (0.2ml of cell suspension in 1.2ml of solution), 100μl of cell suspension volume is added to each hydrogel in the falcon (Manchester BIOGEL, 2019). The solution is gently mixed pulling the pipette upwards in a stirring motion, towards the surface of the hydrogel, making sure the pipette tip doesn't leave the hydrogel. In a 48 well plate, 4 replicas from each hydrogel falcon are placed inside the wells making sure the hydrogel-cell mixture is spread enough to cover the bottom surface of the well. Then a certain amount of medium is pipetted in each well onto the surface of the gel. Finally, the cells in the well plate are visualized under the microscope and this one is placed in the humidified CO_2 incubator at 37°C and 5% CO_2. The medium is kept changing every 3 time per week.

3.4.5 3D Cell Culture in the CLG Scaffolds

A 96 well plate with 4 jellyfish CLG coated scaffolds is placed inside the BSC. Following the steps of the Passaging Procedure, a certain amount of volume suspension is taken out from the falcon to a new one having into account the number of cells required for the seeding procedure (0.25 million cells in each scaffold). The new falcon is introduced in the centrifuge at a spin rate of 1500rpm for 5 minutes. The volume suspension is poured out in the waste box and a certain amount of medium is introduced in the falcon, having into attention that only 30μl of cell suspension will be seeded in each scaffold. Then, 0.25 million PANC-1 cells (in 30ul of cell suspension) are carefully seeded into each scaffold. This method is made adding the cell solution dropwise, waiting between each drop that the scaffold soaks the cells. Having this completed, the scaffolds are left in the humidified CO_2 incubator at 37°C and 5% CO_2 for a period of 1 hour and after completed, a certain amount of medium is added in each of the wells. The 96 well plate is again introduced in the humidified CO_2 incubator at 37°C and 5% CO_2. The medium is kept changing every 3 time per week.

3.5 Bioprocessing Analysis

The Bioprocess Analysis are a set of techniques designed to measure the viability and apoptotic pathways of the cultured PANC-1 cells. Since the reagents used in these procedures are light sensitive it is important to perform the experiments in the darkest environment possible. In this sub-chapter it is also presented the statistical analyses measured for the experiments under study.

3.5.1 Cell Viability

3.5.1.1 alamarBlue Assay

The DMEM is warmed up in the water bath at 37°C and the resazurin[25] compound (7-hydroxy-10-oxidophenoxazin-10-ium-3-one, sodium) alamarBlue reagent (Thermo Fisher Scientific, UK) is taken out from the -4°C and warmed up at room temperature (STEMCELL Technologies, 2019). It is prepared a solution containing an appropriate volume of medium and alamarBlue reagent and in a 24 well plate is added 1.5ml of the solution in each well, having into account that only 10% of the alamarBlue reagent is presented in it. After adding the scaffolds to the well plate, this one is incubated for 3 hours in the humidified CO_2 incubator at 37°C and 5% CO_2. Then, 3 replicas of 100µl from each well are pipetted in a 96 well plate that will be introduced in a microplate reader (Cytation 5 Imaging Reader, BioTek, USA) and processed with the Gen 5 software (BioTek, USA), for absorbance measures.
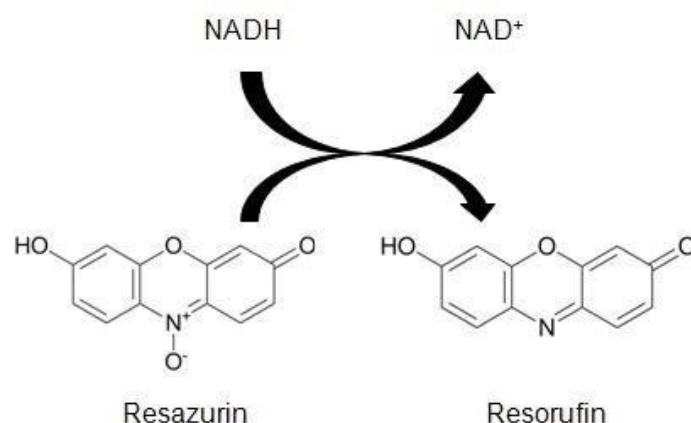
Figure 3.12: Reduction of Resazurin into Resorufin in Viable Cells
(Riss et al., 2016)

3.5.1.2 Live/Dead Cell Assay

The DMEM is warmed up in the water bath at 37°C and the Calcein-AM[26] (2µM, Thermo Fisher Scientific, UK) and Ethidium Homodimer-1[27] reagents (4µM, Thermo Fisher Scientific, UK) are taken out from the -20°C and warmed up at room temperature. The cryovials with the previously snap frozen scaffolds are taken out from the -80°C and put in a liquid nitrogen bucket at -196°C. The scaffolds are introduced in the BSC and cut into thin slices with the help of a blade. The harder the scaffolds are by being put in the liquid nitrogen, the easier it is to cut them. The resulting slices are placed in a 48 well plate and immersed with an appropriate amount of live/dead staining solution. The live/dead staining solution is prepared by mixing both the reagents in an appropriate volume of medium. Knowing that the Working Solution Concentration of the Calcein-AM and the Ethidium-Homodimer-1 are 4mM and 2mM, respectively, by using equation number 2 it is known the volume that needs to be taken out

---

[25] Resazurin is a blue indicator dye that undergoes colorimetric change in response to cellular metabolic reduction resulting from cell growth. The Resazurin gets reduced to Resorufin, a pink and highly fluorescent reagent which the fluorescence's intensity produced is proportional to the number of viable living cells (BIO RAD, 2019).

[26] Calcein-AM is a cell-permeant dye that when contacted with live cells emits green fluorescence, indicating intracellular esterase activity (Thermo Fisher Scientific, 2019).

[27] Ethidium-Homodimer-1 is a cell-impermeant dye with high-affinity to the nucleic acid stain that when bounds to the DNA emits red fluorescence, indicating the loss of plasma membrane (Thermo Fisher Scientific, 2019).

from both the stock solutions to be mixed in a specific amount of DMEM with the help of a vortex. A certain amount of the live/dead staining solution is added to each of the wells from the 48 well plate and the last one is covered with aluminium foil and placed in the humidified CO_2 incubator at 37˚C and 5% CO_2 for 1 hour. After this time, the wells are washed twice with PBS and the presence of live and dead cells is evaluated with the Nikon Eclipse Ti Confocal Microscope and processed with the Nikon NIS-Elements Software (Nikon Instruments Inc., Japan). The cell viability analysis is measured in the ImageJ software and the following equation was used to determine the percentage of viable cells.

$$\% \, of \, Viable \, Cells = \frac{Live \, Cells}{Total \, Number \, of \, Cells} \times 100 \qquad (3)$$

3.5.2 Cell Distribution

3.5.2.1 DAPI Staining

The DMEM is warmed up in the water bath at 37°C and the DAPI[28] compound (4',6-diamidino-2-phenylindole) (1mg/ml, Thermo Fisher Scientific, UK) is taken out from the -4°C and warmed up at room temperature. The cryovials with the previously snap frozen scaffolds are taken out from the -80˚C and put in a liquid nitrogen bucket at -196˚C. The scaffolds are introduced in the BSC and cut into thin slices with the help of a blade. The resulting slices are placed in a 48 well plate previously pipetted with an appropriate amount of paraformaldehyde. A waiting time of 20min is settled for the Cell Fixation[29] to occur and the paraformaldehyde is taken out from the wells and these ones are washed twice with PBS before adding the DAPI staining solution. Knowing the Working Solution Concentration of the DAPI is 2μg/ml, by using equation number 2 it is known the volume that needs to be taken out from the stock solution to be mixed in a specific amount of PBS with the help of a vortex. A certain amount of the DAPI staining solution is added to each of the wells from the 48 well plate and the last one is covered with aluminium foil and placed in the humidified CO_2 incubator at 37˚C and 5% CO_2 for 1 hour. After this time, the wells are washed twice with PBS and the sections are ready to be imaged.

3.5.3 Cell Apoptosis

3.5.3.1 Caspase 3/7 Staining

The DMEM is warmed up in the water bath at 37°C and the CellEvent Caspase 3/7 green detection reagent[30] (2mM, Thermo Fisher Scientific, UK) is taken out from the -20°C and warmed up at room temperature. The cryovials with the previously snap frozen scaffolds are taken out from the -80˚C and put in a liquid nitrogen bucket at -196˚C. The scaffolds are introduced in the BSC and cut into thin slices with the help of a blade. The resulting slices are placed in a 48 well plate and immersed with an appropriate amount of Caspase 3/7 staining solution. The Caspase 3/7 staining solution is prepared by mixing both the reagents in an appropriate volume of medium. Knowing the Working Solution Concentration of the Caspase 3/7 green detection reagent is 5μM, by using equation number 2 it is known the volume that needs to be taken out

---

[28] DAPI is fluorescent stain that binds to the AT (adenine-thymine) regions of the cell´s DNA, thus emitting a blue fluorescence (Thermo Fisher Scientific, 2019).

[29] The Cell Fixation is a method essential for immunohistochemistry that preserves and stabilizes the cell morphology and tissue architecture as well as protects the samples against microbial contamination and possible degradation. The Paraformaldehyde is the most widely used chemical fixative in samples to be used in fluorescence studies (Thermo Fisher Scientific, 2019)

[30] The Caspase 3/7 green detection reagent is a fluorogenic substrate for activated caspase-3/7 that is compatible with both live cell and fixed imaging. Activation of caspase-3 is an essential event during apoptosis, making this an optimized reagent for analysis of apoptotic cells (Thermo Fisher Scientific, 2019).

from the stock solutions to be mixed in a specific amount of DMEM with the help of a vortex. At this stage it can also be added the DAPI stain in a concentration of 1:200 to have a proper estimation of the total number of cells in the scaffold's section. A certain amount of the Caspase 3/7 staining solution is added to each of the wells from the 48 well plate and the last one is covered with aluminium foil and introduced in the humidified CO_2 incubator at 37°C and 5% CO_2 for 1 hour. After this time, the wells are washed twice with PBS and the presence of apoptotic cells is evaluated with the Nikon Eclipse Ti Confocal Microscope and processed with the Nikon NIS-Elements Software. The cell viability analysis is measured in the ImageJ software and the following equation was used to determine the percentage of apoptotic cells.

$$\% \, of \, Apoptotic \, Cells = \frac{Apoptotic \, Cells}{Total \, Number \, of \, Cells} \times 100 \qquad (4)$$

3.5.4 Statistical Analysis

Statistical analyses were performed in 3 independent cultures (N = 3) where 5 replicate scaffold measurements were averaged in one of the experiments and 7 replicate scaffolds measurements were averaged in the other two (n = 5 - 7). Error bars represent standard error of the mean (SEM) and the analysis of variance (Two-way ANOVA) was performed using the Graph-Pad Prism software (GraphPad Software, USA) with a *p*-value threshold 0.05 to evaluate whether there was any statistical difference between the experimental conditions.

4 Discussion and Analysis of Results

This chapter will focus on the results' presentation and its further analysis and discussion. The next subchapters below show the main experiments' outcomes.

4.1 Flow Rate's Optimization in the Perfusion Bioreactor

The first set of experiments designed in the Perfusion Bioreactor consisted in preliminary trials where different flow rates were run during the same amount of time (48 hours). The goal was to see which perfusion flow rate kept the highest cell's viability in culture and the best cell's distribution throughout the scaffolds' layers. The same was also studied in static culture (control) for better comparable results.

The flow rates ran in the bioreactor are listed in table 4 along with the respective cell passage number that the previous seeded cells had at that time.

Table 4: Flow Rates ran in the Preliminary Experiments

Flow Rate Number	Flow Rate (ml/min)	Passage Number
F1	4.60	11
F2	0.46	11
F3	2.5	11
F4	1.5	12
F5	3.5	12
Static	0	11

After measuring the cell viability for each experiment with the help of the alamarBlue reagent, variations in fluorescence were seen between all the flow rates as it can be visualized in the graphic from figure 4.1.

.
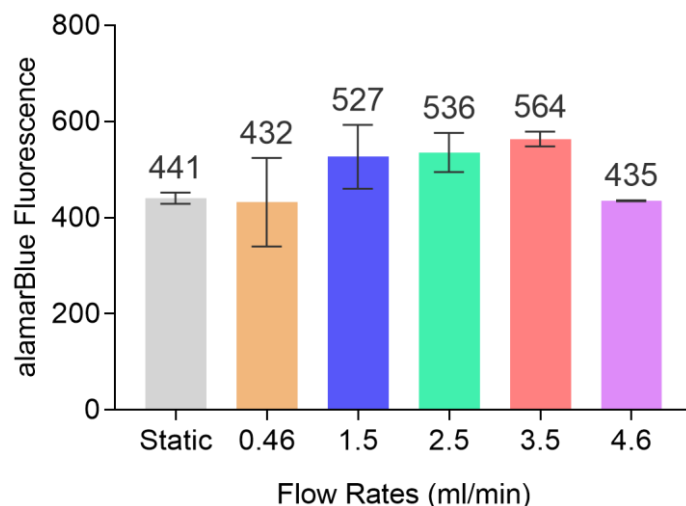
Figure 4.1: Growth of PANC-1 cancer cell lines in uncoated PU scaffolds for 48 hours at different flow rates. Data are presented as mean ± SEM (N=3, n=3). N = number of independent experiments; n = number of replicas.

From the results shown it is possible to see that the 3.5ml/min flow rate was the one that kept the highest alamarBlue fluorescence value leading then to the highest cell viability in culture. The 4.6ml/min and the 0.46ml/min which represent the maximum and lowest flow rate, respectively, showed a lower cell viability than the static culture. These last results turned up being contradictory to the current literature since it has been proved in several studies the enhancement of the cell viability in dynamic cultures when comparing to static ones. However, these discrepancies cannot be taken as certain since the cells were only cultured for a period of 48 hours which is not enough for them to get adapted to a system different from the one where they have been used to grow (2D). It would probably be necessary to culture the cells for longer periods to actually see a higher cell viability in all the flow rates, when compared to the static culture. Another consequence of the short-term culture is the lack of significant differences in the alamarBlue fluorescence's values between the flow rates which make these results inconclusive.

Therefore, it was necessary to resort information given by microscopy imaging where cells from different sections of the scaffolds used in each flow rate, were stained with the DAPI reagent. This would make possible the visualization of the cells' distribution throughout the layers and then conclude where they were more uniformly spread. Different images were taken for several samples from each flow rate and a montage was made to ensure the total visualization of the layer where the cells were scattered and more accurate comparisons. After their analysis, the most representative ones were chosen and are presented in figure 4.2.

After comparing the data given by the alamarBlue fluorescence and the images where the cells were stained with the immunofluorescent stain it is possible to predict that the images give a much more realistic vision of how the cells grow after 2 days in culture. This is grounded by the significant differences between what is seen in static culture till the moment the scaffolds are run at a flow rate of 4.6ml/min. In figure 4.2a, the cells are mainly spread at the edges of the scaffold which, as seen in previous results, is very characteristic of cells cultured in a static system. The absence of a flow rate doesn't allow the cells to migrate to other areas of the material. Similar results are also seen in figure 4.2b. Despite here the cells had already experienced the presence of a flow (0.46ml/min), this one was however too low to make the cells starting to migrate to other locations. On the other hand, in figure 4.2c, representative of the 1.5ml/min, the situation is already different.
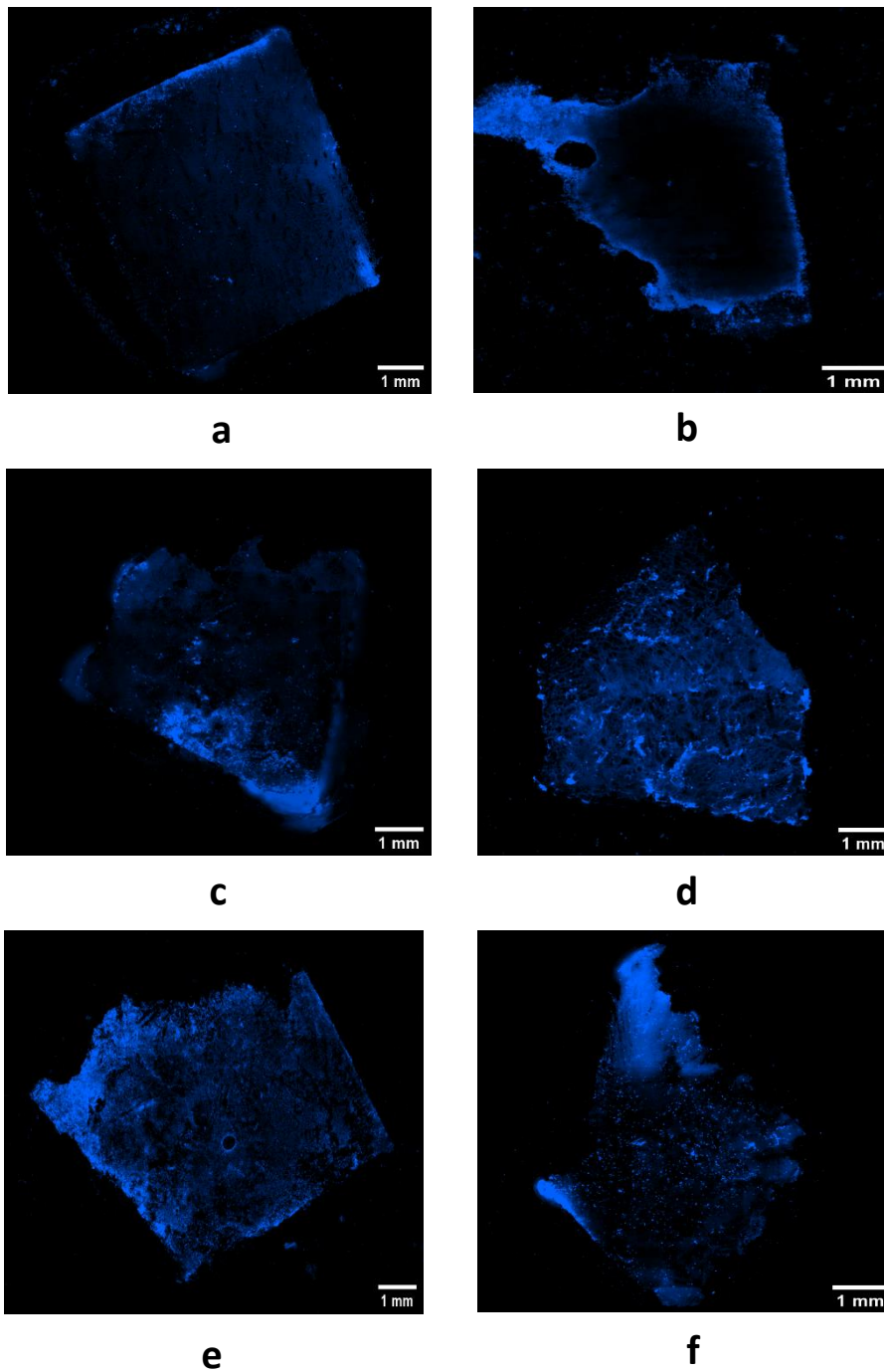
**Figure 4.2: (a-f) Representative immunofluorescence images of the PANC-1 cells'
distribution throughout the scaffold's layer with fluorescent DNA staining (DAPI)
after 48 hours in static, at 0.46 ml/min, at 1.5 ml/min, at 2.5ml/min, at
3.5ml/min and at 4.6ml/min, respectively.**

Here, it can be noticed a migration of the cells to the inner part of the scaffold's layer as
well as in figure 4.2d where the cells were run at flow rate of 2.5ml/min. When comparing the
two last figures however (4.2e and f) which represent the flow rates of 3.5ml/min and
4.6ml/min, respectively, it is seen that in image e, the cells were able to have a much higher
grow and distribution throughout the layer, occupying the majority of the scaffold's section in

addition to a more uniform distribution, when comparing to the 4.6ml/min. This is in accordance to the previous seen alamarBlue fluorescence values. The subjection of the PANC-1 cells to the highest flow rate would then probably lead to much worse outcomes after a long-term culture, also because the cells could be much more easily washed out from the surface of the scaffold.

Thus, analysing both the cell viability and distribution results in the preliminary experiments it was decided to choose the 3.5ml/min as the best perfusion flow rate to carry on in the long-term experiments. Hence, after knowing which flow rate to run in the cell-polymer 3D model, some calculations regarding relevant parameters of the dynamic flow were able to be determined, as it is further described. All calculations were done assuming that the flow was ran in a single direction, perpendicular to the scaffold's cubic structure.

4.1.1 Reynolds Number

For the Reynolds number, a value of 13.07 was reached, which suggests that the flow regime was laminar (<<2300) (Docs, 2019). The equation used for this calculus is presented below (Boschetti et al., 2006). The DMEM was stipulated as an incompressible Newtonian fluid with a density of 997.04 kg/m^3 and a viscosity of 0.00089 Pa/s^{-1} (Dhall et al., 2016).

$$Re = \frac{d\rho v}{\mu} \Leftrightarrow Re = \frac{0.005 \times 997.04 \times 0.0023}{0.00089} \Leftrightarrow \boldsymbol{Re = 13.07} \tag{5}$$

Where,

d is the diameter/length of the scaffold (m)
ρ is the culture medium density (kg/m^3)
μ is the culture medium viscosity (Pa/s^{-1})
v is the superficial fluid velocity within the construct (m/s)[31]

4.1.2 Interstitial Fluid Flow

The interstitial fluid flow, which consists in the fluid flowing through the 3D matrix, around interstitial cells (tumour cells, fibroblasts, immune cells etc) that helps with the transport of nutrients throughout the tissue, is another important parameter when studying the properties of a dynamic system in tissue engineering (Rutkowski et al., 2007). Therefore, this average value was determined as 5303μm/s by equation number 6 (Radisic et al., 2008). The void fraction was determined has the average porosity, which was comprehend between 85 and 90%, as already stated in the Materials and Methods Chapter. The pores were assumed as cylindrical, following a tortuous pathway.

$$U = \frac{2HQ}{\varepsilon V} \Leftrightarrow U = \frac{2 \times 0.005 \times \frac{0.0000035}{60}}{0.88 \times 0.005^3} \Leftrightarrow U = 0.005303 \, m/s \Leftrightarrow \boldsymbol{U = 5303 \, \mu m/s} \tag{6}$$

Where,

H is the scaffold thickness (m)
Q is the volumetric flow rate (m^3/s)
ε is the void fraction
V is the scaffold volume (m^3)

---

[31] The volumetric flow rate (Q) is given in m^3/s, so the **v** parameter is given by: $Q = v \times A$, where A is sectional area where the flow passes through (5×5mm^2).

4.1.3 Shear Stress

Finally, the shear stress on the cell surface, which is imparted from the interstitial flow and plays mechanical stimulus in the tissue, was also calculated and an average value of 2.9dyn/cm^2 was achieved (Rutkowski et al., 2007). Equation number 7, based on Poiseuille flow, shows how this parameter was calculated (Radisic et al., 2008). The porous diameter was determined has the average porous size, which was comprehend between 100 and 150µm, as already stated in the Materials and Methods Chapter.

$$\tau = \eta \frac{4U}{R} \Leftrightarrow \tau = \frac{0.00089 \times 4 \times 0.005303}{\dfrac{0.00000130}{2}} \Leftrightarrow \tau = 0.29 \, kg/m.s^2 \Leftrightarrow \boldsymbol{\tau = 2.9 \, dyn/cm^2} \, (7)$$

Where,

η is the culture medium viscosity (Pa/s^{-1})
R is the pore radius (m)

The determined value for the flow regime is known to be in accordance to what is seen in biological systems since it is prevalent the existence of a laminar fluid flow (Huang et al., 2018). On the contrary, the interstitial fluid velocity was different from the ones believed to be seen in a real tumour microenvironment, ranging from values between 0.1 to 10µm/s (Munson et al., 2014). However, the majority of the few experimental measures, were based on animal models that constitute tumours which have their surrounding microenvironment substantially different from human tumours, as already said before (Munson & Shieh, 2014). As for the case of the cell surface shear stress, it is currently assumed to be in the order of 0.1dyn/cm2 in real *in vivo* tumours (Mitchell et al., 2013). Nevertheless, the achieved values were dependent from the perfusion flow rate velocity, as it is clearly seen in the three equations.

Therefore, the optimization of a flow rate turns up being very important when the aim is to use a bioreactor to keep a dynamic culture for a specific cell line. The relevance of a bioprocessing optimization is even more evidenced when comparing the range of values used in this experiment to previous literature results that have between each other's a huge lack of consensus. For example, Magrofuoco et al. used image analysis to study the scaffold morphology of a porous collagen disk sponge and the cell distribution within the construct. The experiments were carried out for 7 days in a perfusion bioreactor using a medium flow rate of 0.65ml/min and a mathematical model representing the cell growth heterogenicity was also performed (Magrofuoco et al., 2019). Furthermore, Starokozhko et al. induced hepatic differentiation of human-induced pluripotent stem cell (hiPSCs) under perfusion conditions to compare with *in vivo* tissues. Polydimethylsiloxane (PDMS) porous scaffolds were used as the cell frame structure and medium was perfused at flow rates of 1µl/min and 5µl/min for a period of 25 days (Starokozhko et al., 2018). In addition, Kim et al. designed and fabricated a perfusion bioreactor to study the differentiation and proliferation of intestinal epithelial organoid units seeded onto 3D porous scaffolds tubes made of polyglycolic acid fibers (PGA). The culture medium was pumped at a flow rate of 1.5ml/min for 2 consecutive days (Kim et al., 2007). These results would then consequently lead to different values in the dynamic flow's parameters, as it was the case in this study.

Summing up, when designing a dynamic flow rate, the different system's properties need to be taken into attention (type of cell line, type of 3D scaffold and bioreactor, peristaltic pump, scaffold holders, etc) since different variables lead to different results. Thereupon, one experimental procedure cannot be applicable to the ones under development.

4.2 Long-term Culture in a Dynamic and Static System

The long-term experiments consisted in a period of 4 weeks where the PANC-1 cells were cultured in the previous coated PU scaffolds (Passage 14) both in the perfusion bioreactor and in the 24 well plates. As already said in the Materials and Methods' Section the alamarBlue was measured every week and the evolution of the cell viability can be seen in the graphic from figure 4.3.
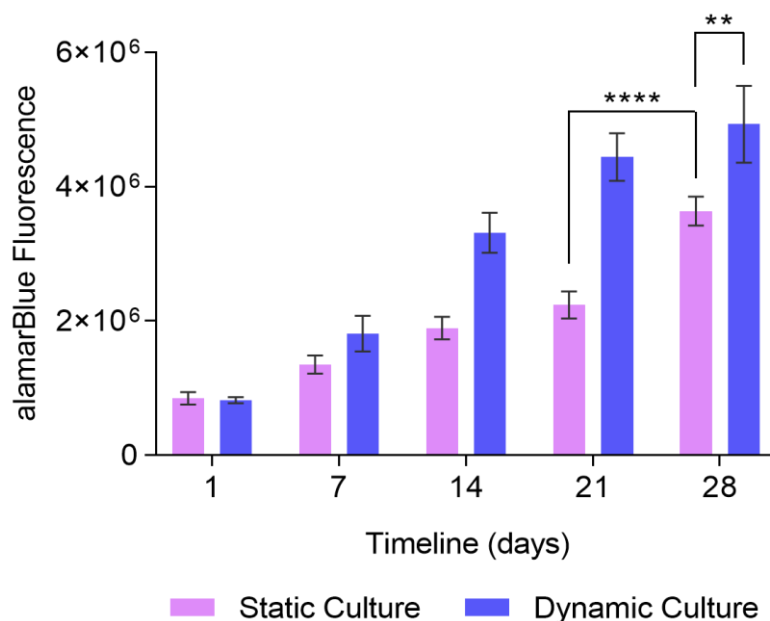
Figure 4.3: Growth of PANC-1 cancer cell lines in coated PU scaffolds for 28 days both in static and dynamic culture. Data are presented as mean ± SEM. For the static culture it was used 2 well plates and the final values are presented as the average of both the well plates' results (N=2, N=7). For the dynamic culture it was used 1 disposable set (N=1, n=5). Statistical differences for the cell growth are marked by asterisks (p<0.0018; ****p<0.0001). N = number of independent experiments; n = number of replicas.**

From figure 4.3 it can be seen a clear evolution of the cell growth in both the different systems along the 4 weeks in culture, however the dynamic culture shows a significantly higher cell viability increment when compared to the static one. At day 1 both the systems represent approximately the same cell viability number which is in accordance to the expected data since this day represents the measured value after 24 hours in static culture before being introduced in the perfusion bioreactor and in the respective well plates. At day 7 and 14 the viability measurements turned to be higher in the dynamic system, however the significant differences only started to be seen from day 14 with a p-value below 0.0005. As for the static culture, the significant difference between two consecutive weeks was only seen from day 21 to day 28. Similar findings were reported by Stella et al. where the growth of PANC-1 cells in FN coated scaffolds during 29 days in culture didn't show significant differences throughout the weeks, except between day 21 and 28 (Totti et al., 2018). The greater number of live cell masses in the perfusion system remained to be significant when compared to the static one even in the last day of culture (day 28) with a p-value below 0.0018. However, between day 21 to day 28, the difference in the cell viability of the dynamic system showed a much lower difference, with no significant difference, when compared to the previous weeks. This could lead to questions on whether it would be necessary to keep the PANC-1 cells in culture for an additional fourth week in a dynamic system since they seem to reach the optimal cell viability number much faster than

the static culture. Nevertheless, to reach a conclusion regarding the less time consumption of the dynamic system, it would be necessary to go through studies regarding the ECM secretion (distribution of CLG I and Ki-67, which is associated to the cellular proliferation) and the analysis of oxidative stress (expression of HIF1-α) to see if they are significantly different between day 21 and day 28 in culture. Since it has not been reported in literature similar studies using pancreatic cancer cells in dynamic systems, comparisons using other types of cancer cells are hence specified to suggest the versatility of the dynamic culture in forming higher cellular masses and real tissues-like structures. Hirt et al. cultured colorectal cancer HT-29 cells on CLG scaffolds and showed that the perfused 3D cultures resulted in a significantly higher cell numbers after 4 days in culture when compared to the static ones. The 3D perfusion culture also produced tissue-like-structures with morphology and phenotypes similar to xenografts (Hirt et al., 2015). In addition, Wan et al. revealed that neuroblastoma cells SY5Y cultured in a 3D Matrigel sandwich, showed significantly higher cell viability at day 14 in culture in the perfusion bioreactor (Hirt et al., 2015). Furthermore, Muraro et al. saw that the viable number of breast cancer cells cultured in a "sandwich-like format" scaffold was significantly higher both at day 7 and 14 in the perfusion system than in the static one (Muraro et al., 2017).

These findings can thus evidence the fact that using a perfusion system contributes to a significantly higher cell proliferation and viability after a certain period when comparing to the static culture system. A better cell distribution through the scaffold material and a more homogenous spatial organization is also achieved, as it was previously seen in the Flow Optimization Subchapter. These outcomes make the use of perfusion bioreactors as one of the keys to achieve a 3D culture system that more closely mimics the features seen in *in vivo* tissues.

4.3 Addition of Gemcitabine after 28 days in Culture

The addition of GEM, the drug of care in the PDAC, took place after 28 days in culture for both the dynamic and static systems. The drug's concentration in both the systems was higher than its water solubility value of 22.3g/L (Human Metabolome Database, 2019). The differences on the cell viability measurements were studied at day 1 and 7 after adding the drug.

4.3.1 Variations on the Cells' Behaviour in Static Culture

The alamarBlue results for the cell viability at day 1 and day 7 after adding the Gem are presented in figure 4.4 and the results for both the Live/Dead and Apoptotic Cell Assays are presented in figures 4.5. and 4.7, respectively. Both the results were compared to the control experiment where no treatment was added in culture

In the next figure it is noticed a decrease both in the treated and the control culture. This effect however should have only been seen in the culture where the GEM was added (Figure 4.4a). The cell viability's results regarding the control system can suggest that the cells were stressed before being measured with the alamarBlue solution. Possible events might have been the occurrence of mechanical stress when transferring the cells from the media to the alamarBlue solution in a new well plate (extra strength using the sterile tweezer) or when changing media through the 4 weeks' culture (cells could have been washed out from the scaffold's surface when immersed in 1.5ml of medium). Chemical stress could have also occurred during the procedures (the tweezer could have had some remnants of the GEM reagent) and therefore, a big percentage of the cell in the control system could have died. No significant differences were seen in the treated cell culture after adding the GEM between day 0 and day 1. At day 7 however, it can be seen an increment in the cell viability, despite this event doesn't show to be the same in the images taken from the confocal microscopy, both for the viable and apoptotic cells.
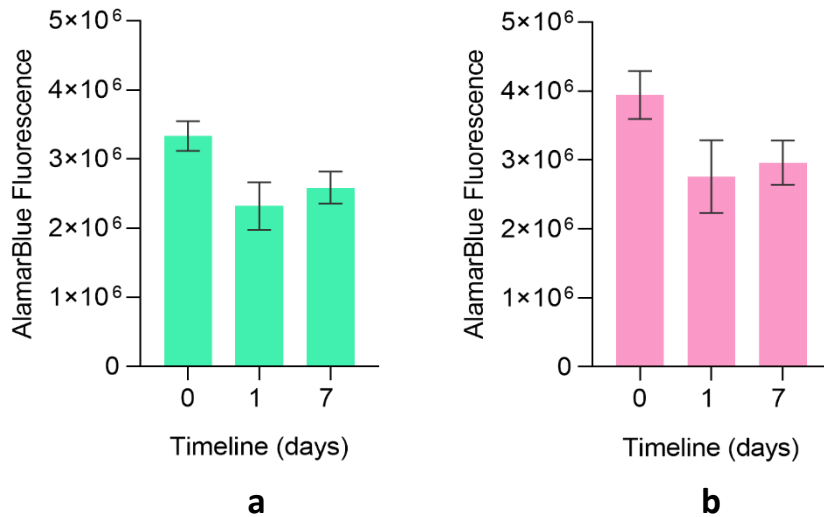
Figure 4.4: Cell growth's variation after adding the GEM (a) and without adding the GEM (b). Data are presented as mean ± SEM (N=2, n=7). N = number of independent experiments; n = number of replicas.
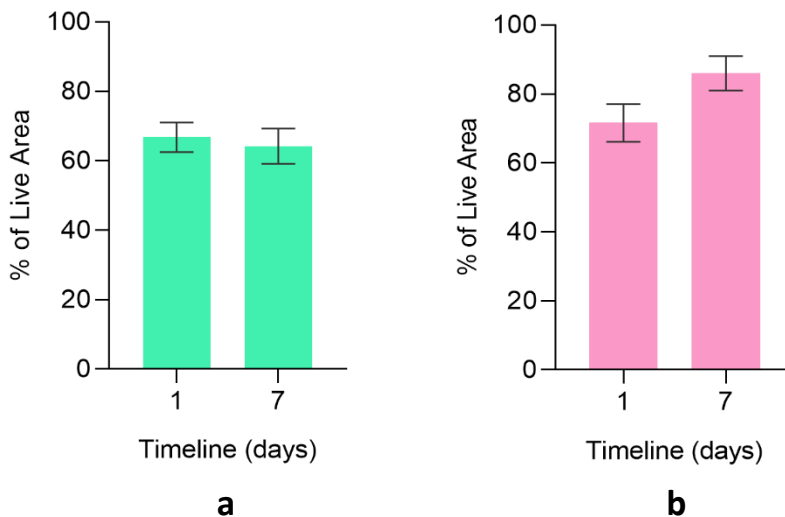
Figure 4.5: Percentage of Live Area after adding the GEM (a) and without adding GEM (b). Data are presented as mean ± SEM (N=2, n=6). N = number of independent experiments; n = number of replicas.

From the two graphics above in figure 4.5, it can be seen, as already mentioned before, that the percentage of live cells at day 7 (64%), in the treated culture, was lower than at day 1 (67%) although the decrease was not significant enough to assume that the cells can continue to die even after 5 days without being in contact with the GEM. Additional replicates should be measured, or the cells should have remained in culture for longer periods to retain more accurate results. That is why, the requirement to the use of Caspase 3/7 green detection reagent was necessary, where all the apoptotic cells could be identified and a more accurate information about the remaining cell's life period could be given. For the control analysis (Figure 4.5b) the results show however a different tendency where the number of live cells increased at day 7 (86%) when compared to day 1 (72%). The percentage at day 1 however, should not have such

a low percentage of live area as it was already noticed in the alamarBlue results. In a normal situation, when comparing to previous results, the value should be between 80 to 100% as it is seen on day 7. This suggestion is supported by Stella et al. who visualized that about 90% of the PANC-1 cells in FN coated scaffolds after 29 days in culture, were marked as positive for the Calcein-AM reagent (Totti et al., 2018). The next figure shows how the cells for both the static and control systems look live when stained for Live/Dead Viability Assays.

a

c

b

d
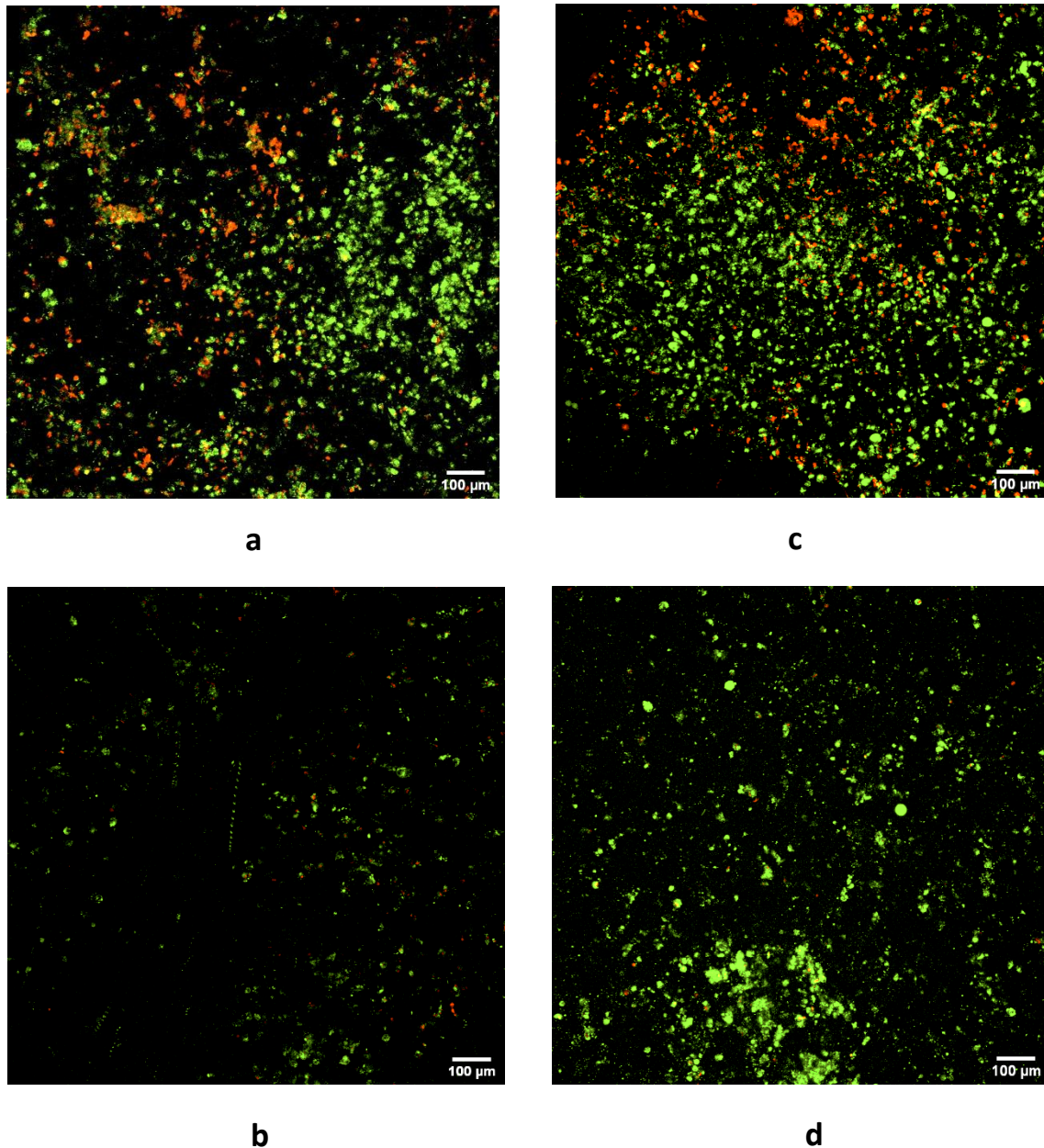
Figure 4.6: (a and b) Visualization of PANC-1 cells in FN coated scaffolds with fluorescence Live (green, Calcein-AM) and Dead (red, Ethidium Homodimer-1) viability assays at day 1 and 7 in culture after adding the GEM, respectively. (c and d) Visualization of PANC-1 cells in FN coated scaffolds with fluorescence Live (green, Calcein-AM) and Dead (red, Ethidium Homodimer-1) viability assays at day 1 and 7 with no addition of GEM, respectively.

After comparing both the Live/Dead confocal images and the alamarBlue plot with the post-treatment viability assays, it is proposed that metabolic activity dependent assays like the AlamarBlue or even MTT assay[32] might be affected by cytotoxic agents. This leads to a lack of sensitivity when identifying differences in cell population within the scaffolds, especially for very high cell numbers, as it was the case. This is further supported by Ulukaya et al. that checked in a cell-free system the possible chemical interactions between the MTT assays and 22 different anti-cancer drugs. Some of the drugs caused a relatively significant increase in absorbance values in the MTT assays, giving rise to false results (Ulukaya et al., 2004).

For the apoptotic cell analysis, the next image shows how the percentage of apoptotic cells varied between day 1 and day 7 after adding the gem in both the static and control cultures.
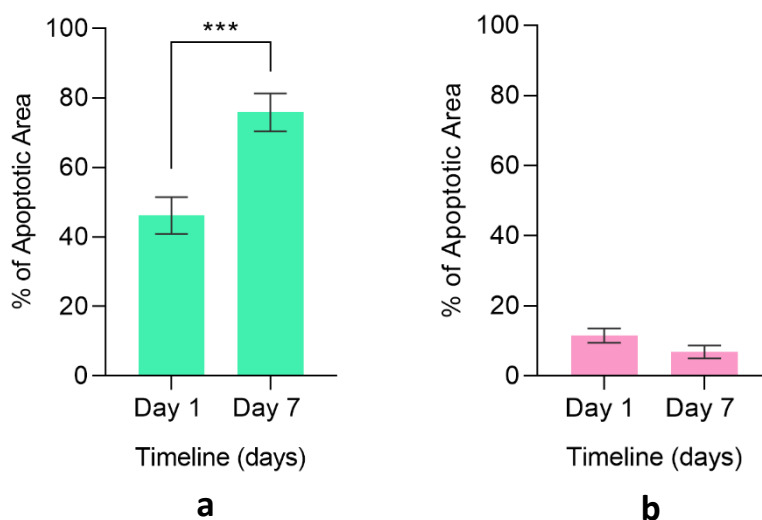

Figure 4.7: Percentage of Apoptotic Area after adding the GEM (a) and without adding GEM (b). Data are presented as mean ± SEM (N=2, n=6). Statistical differences for the cell growth are marked by asterisks (***p<0.0002). N = number of independent experiments; n = number of replicas.

From figure 4.7a, it was shown a significant difference in the percentage of apoptotic area between day 1 and day 7 after adding the GEM in static with a consequent increment of 30% (from 46% to 76%) between the two days. This event gives more accurate conclusions about the cell's life cycle 7 days after being contacted for the first time to the GEM. While in the Live/Dead Cell Viability Assay it was not clear if the cells continued to die on this day, from this analysis it is already possible to conclude that the fraction of live area would significantly decrease if the cells were left in culture for additional days. On the other hand, the apoptotic area in the control system (Figure 4.7b), although not significant, decreased from day 1 to day 7. However, as said for the Live/Dead Cell Viability Assay's analysis, it would be expected a much lower value of apoptotic area on day 1 like the one seen at day 7 (5 to 10%). The next figure shows how the cells for both the static and control systems look live when stained with the Caspase 3/7 green detection reagent.

---

[32] The MTT tetrazolium reduction assays is one of the most used cell viability assays for high throughput screening. The quantity of purple colored formazan converted from the MTT (proportional to the number of viable cells) is measured by recording changes in absorbance using a microplate reader (Riss et al., 2016).

a

c

b

d
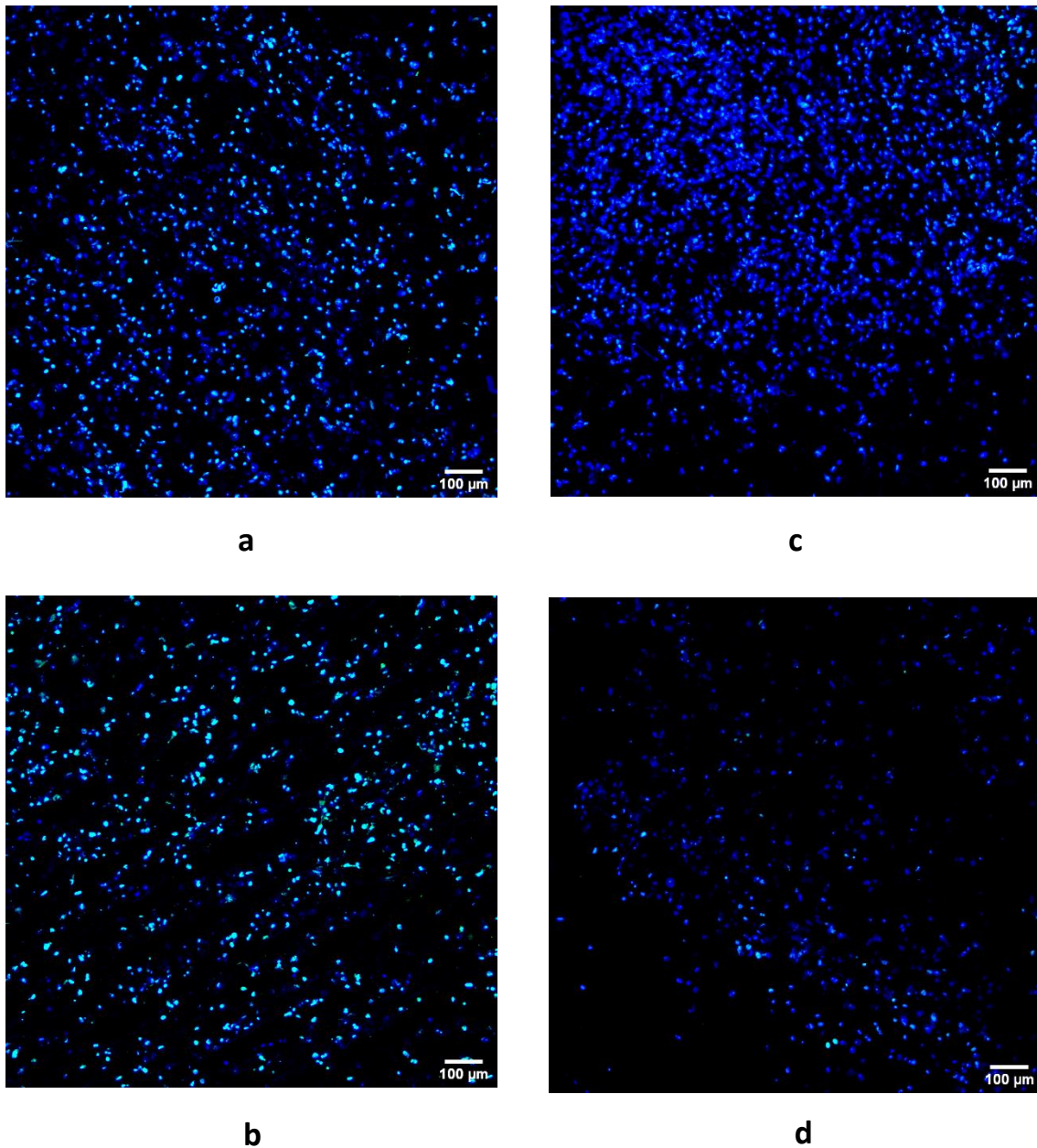
Figure 4.8: (a and b) Visualization of PANC-1 cells in FN coated scaffolds with fluorescent DNA staining (DAPI) and Caspase 3/7 activation reagent staining (green) at day 1 and 7 in culture after adding the GEM, respectively. (c and d) Visualization of PANC-1 cells in FN coated scaffolds with fluorescent DNA staining (DAPI) and Caspase 3/7 activation reagent staining (green) at day 1 and 7 with no addition of GEM, respectively.

4.3.2 Variations on the Cells' Behaviour in Dynamic Culture

The alamarBlue results for the cell viability at day 1 and day 7 after adding the Gem are presented in figure 4.9 and the results for both the Live/Dead and Apoptotic Cell Assays are presented in figures 4.10. and 4.12, respectively.
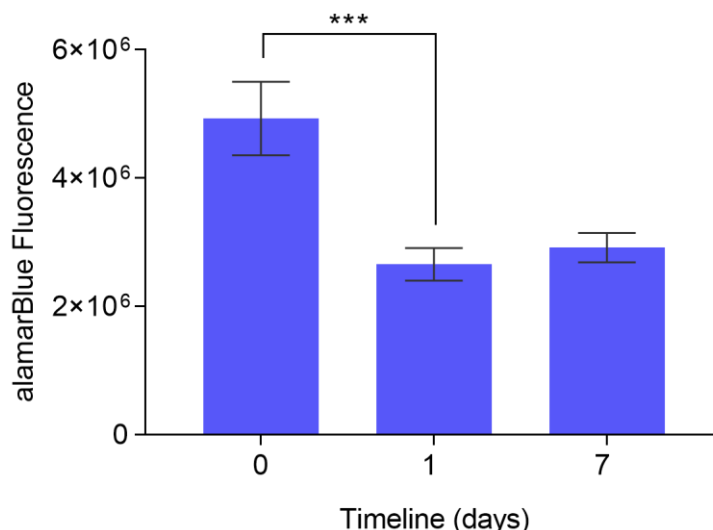
Figure 4.9: Cell growth's variation after adding the GEM. Data are presented as mean ± SEM (N=1, n=5). Statistical differences for the cell growth are marked by asterisks (***p<0.0002). N = number of independent experiments; n = number of replicas.

As it can be seen from the previous figure it is noticed a significant decrease on the alamarBlue measurements between day 0 before adding the GEM (28 days in culture) and at day 1 after adding it in the bioreactor, where the *p*-value is below 0.0002. When comparing both the alamarBlue fluorescence between the dynamic and static system after treatment, both reached a very similar cell viability measurement on day 1, in a range of values between $2x10^6$ and $3x10^6$. At the same time, the dynamic culture was the one that had the highest cell viability drop on this day. This leads to believe that the chemotherapy flow had a much higher effect on the dynamic system rather the static one, since the dynamic flow running through the cells distributed along the scaffold's material might have had a potential role on the PANC-1 cells' death. However, as for the images analysed in the static and control systems which showed completely different values from the alamarBlue that lead to distinct conclusions, the same happened in the dynamic system's confocal images. These findings give an additional prove of why the alamarBlue induces a lot of biological errors when working with cytotoxic agents.

From the graphic on figure 4.10 it is noticed an increment on the percentage of live area in the perfusion bioreactor between day 1 and 7, which is in accordance to what was seen in the alamarBlue plot. However, on day 1 a value of 83% of the live area reaches the conclusion that the GEM action didn't have such an impact in the cells' physiological functions as it had in the static culture, which showed only 67% of live area on day 1. It is important to enhance however, that the number of viable cells at day 0 in the perfusion bioreactor was significantly higher than in the well plates as it was already seen in the graphic from picture 4.3. Due to this and knowing that the added concentration of the GEM reagent was the same in both cases (50μM) it is profitable to admit that the number of viable cells would be also higher in the post-treatment images taken from the dynamic culture. The same amount of drug would be penetrating the scaffolds' layers and destroy approximately the same number of cancer cells. Nevertheless, the potentiality of the perfusion system cannot be underestimated because of this assumption. Another explanation for the lower sensitivity from the cells to the drug, could be because of the greater cellular masses formed in culture that could have prevented the drug penetration. Other studies have reached similar conclusions such as the case of Wan et al. that showed lower cytotoxicity of the 5-FU drug (10μM) and consequently a higher cell viability on spheroids previously cultured with colorectal cancer cell lines, DLD-1, and breast cancer cell lines, NCI/ADR (ATCC), over a long-

term culture of 17 days in perfusion (Wan et al., 2016). Furthermore, Hirt et al. discovered that the treatment with 5-FU in HT-29 colorectal cancer cell 2D culture, induced apoptosis, which consequently lead to a low cell viability number as well as the down-regulation of anti-apoptotic genes. As for the case of 3D cultures under perfusion in porous scaffolds, the drug treatment only induced nucleolar stress[33] (Hirt et al., 2015).

a
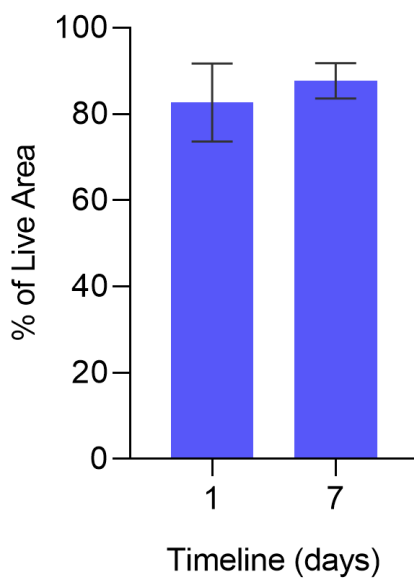
Figure 4.10: Percentage of Live Area after adding the GEM. Data are presented as mean ± SEM (N=1, n=7). N = number of independent experiments; n = number of replicas.
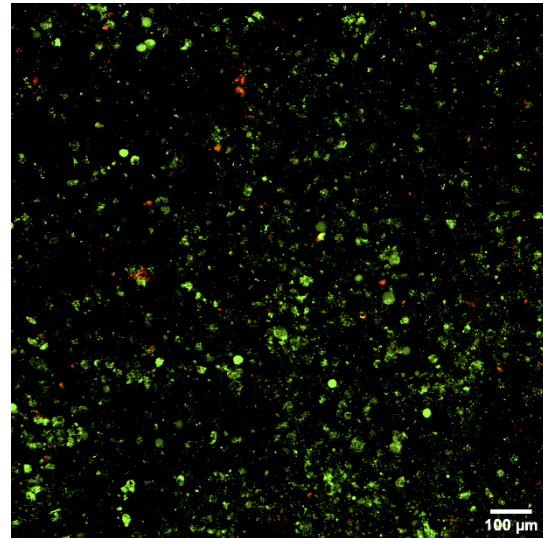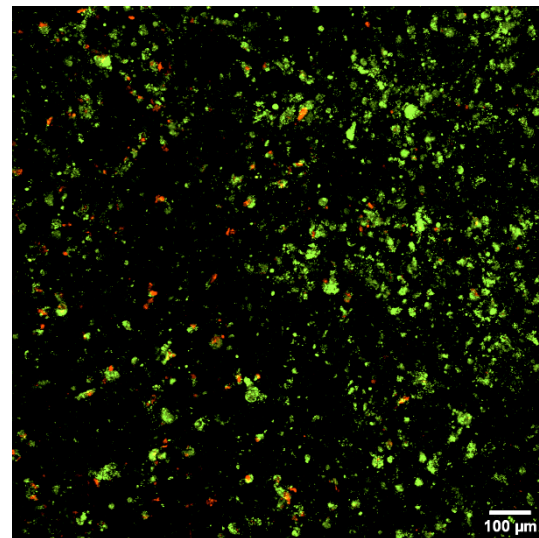
b

Figure 4.11: (a and b) Visualization of PANC-1 cells in FN coated scaffolds with fluorescence Live (green, Calcein-AM) and Dead (red, Ethidium Homodimer-1) viability assays at day 1 and 7 in culture after adding the GEM, respectively.

---

[33] Nucleolar stress is characterized by cellular insult-induced abnormalities in nucleolar structure and function that leads to alterations in cell behaviour (Yang et al., 2018).

Since the control experiment of the bioreactor (without the drug) was not possible to take till the end due to a bacterial contamination already stated before, it is unknown the percentage of live area that the system would have at day 1. Without this is not possible to compare the system under study to its control and conclude if the decrease on the value of the percentage of live area was significant after the GEM action. However, since it would be expected, as it is for the static culture, a percentage of live area between 90 to 100%, an 83% cellular viability value can support the argument regarding the efficacy of the dynamic culture in the cells' resistance to chemotherapeutic stress. Nevertheless, for more accurate results, in future experiments should be added a higher concentration of GEM into the bioreactor that when compared to the one added in the static system, could be proportional to the number of viable cells in culture.

a
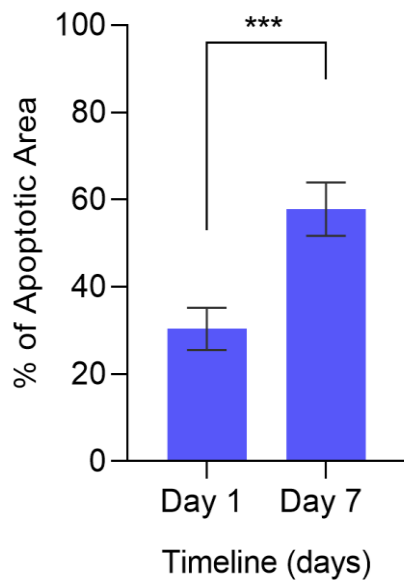
Figure 4.12: Percentage of Apoptotic Area after adding the GEM. Data are presented as mean ± SEM (N=1, n=6). Statistical differences for the cell growth are marked by asterisks (***p<0.0009). N = number of independent experiments; n = number of replicas.
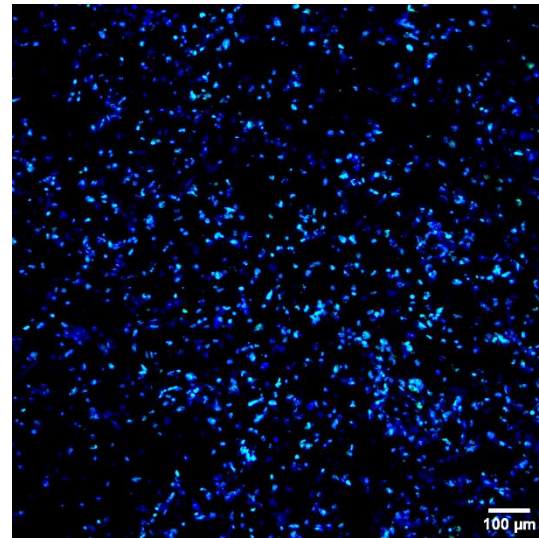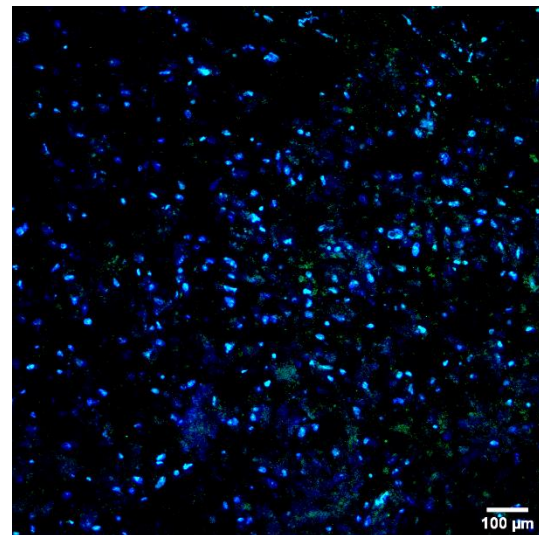
b

Figure 4.13: (a and b) Visualization of PANC-1 cells in FN coated scaffolds with fluorescent DNA staining (DAPI) and Caspase 3/7 activation reagent staining (green) at day 1 and 7 in culture after adding the GEM, respectively.

Figure 4.12 shows a significant difference on the apoptotic area between day 1 and 7 with a *p*-value lower than 0.0009, representing an increment of 28% from day 1 to day 7 after adding the GEM. The percentage of apoptotic area in the bioreactor however, at day 1 is lower (30%) than what was shown in the well plate (46%) which consequently leads to lower apoptotic values on day 7. Therefore, the dynamic and static culture show on this day an apoptotic area's percentage of 58% and 76%, respectively. The increment of the apoptotic are in both the systems on day 7 suggests once more, that if the cells were kept in culture for a few more days the number of dead cells would potentially be higher. Yet, it is important to mention that both the live and apoptotic area range of values suggest the effectiveness of the perfusion bioreactor, in enhancing higher cellular concentrations along the scaffolds and thereafter a higher cell resistance to drug treatment. Consequently, conclusions regarding its closer recapitulation of a real tumoural PDAC tissue are easily sustained. The same is not seen in cells cultured in a static system where it lacks the presence of shear stress, interstitial flow (inducing a better distribution of oxygen and nutrients) and even diffusional limitations.

4.4 Cell Viability's Studies in other Biomaterials

The long-term culture of the PANC-1 cell line in other biomaterials endured for 3 weeks and was done as part of future work's experiments. In the Framework Chapter it was enhanced the heterogenicity that characterizes the PDAC, which is partly due to the DR. Therefore, due to the increasing number of other cell types, it turns up being necessary to study other biomaterials and biochemical cues that support other cells' growth, adhesion and proliferation as the PU coated scaffolds makes for the PANC-1 cells. In other words, it is mandatory to synthetize a hybrid polymeric scaffold's system that enables not only the viability of PANC-1 cells but also of other known pancreatic cells such as the PSC's, immune cells, endothelial/epithelial cells, fibroblasts, etc. Not all cells adapt to a certain material the same way, some of them can continue to grow and proliferate while others can stop their division cycle and even die. Because of this, it is necessary to study how cells behaviour in other materials or biomarkers and discover which ones contribute to their highest viability, that can lead to the production of more robust, heterogeneous and versatile biosystems. For this reason, two different systems were selected to study the PANC-1 cells' growth.

4.4.1 Long-term Culture in a Hydrogel Static System

The first system consisted in a set of 5 different hydrogels that were cultured for 3 weeks along with the cancer cells (Passage 18). From the Live/Dead image's analysis it was seen that each one of them kept a different cell proliferation after the 3 weeks in culture. Since the hydrogels also differed in mechanical and functional properties, the cells consequently adapted in different ways to each one of them. The table below shows how the Storage Modulus (G'), also known as Elastic Modulus, which represents the energy stored in the elastic structure of the sample, and the Charge, vary in each of the peptides (Franck, n.d.).

Table 5: PeptiGels' Mechanical and Functional Properties, adapted from (Manchester BIOGEL, 2019)

PeptiGel	Alpha 1	Alpha 2	Alpha 3	Alpha 4	Alpha 5
G' (kPa)	5	10	5	1	14
Charge	Neutral	Medium	Low	High	High

The next figure shows how the PANC-1 cells' morphology and proliferation would look like with the cells cultured in a control system, more specifically only in DMEM. It is important to notice that this image was once to be analysed with the presence of the Alpha1 Hydrogel, however, after a few days in culture it was seen that the hydrogel started to desegregate and

after a week of changing medium it got completely washed out from the culture. Because of this, the images taken from the cells cultured in Alpha 1 were labelled as the control since what it is shown are the cells attached to the bottom of the well where they were cultured in medium.
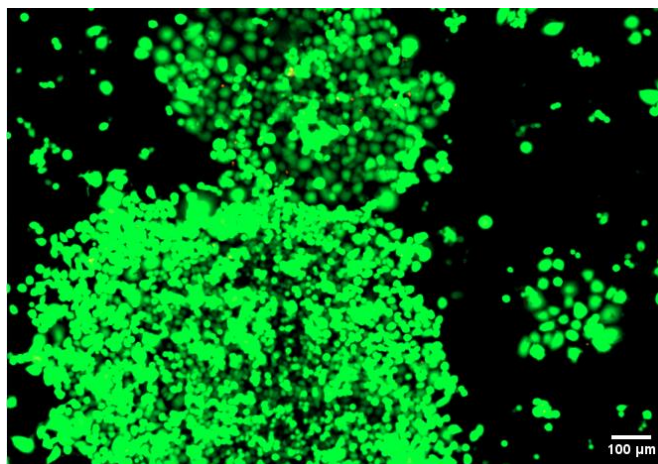

Figure 4.14: Visualization of PANC-1 cells after a 3-weeks' culture in DMEM with fluorescence Live (green, Calcein-AM) and Dead (red, Ethidium Homodimer-1) viability assays

It is seen after the culturing period, the formation of big cellular clumps in the medium, as the PANC-1 cells have the tendency to do. In addition, almost all the cells presented were marked as positive for the Calcein-AM. The same happened for the Alpha 2 cell culture (figure 4.15a), although here, the cellular masses were not as big as the ones seen in the control system, suggesting that a lower number of cells is achieved with the presence of the Alpha 2 peptide. In the case of the Alpha 3 peptide (figure 4.15b), the image shows that the cells were able to proliferate and migrate along the material and remained viable during the 3 weeks in culture. The opposite happened however, for both the Alpha 4 and Alpha 5's peptides (figure 4.15c and d, respectively). Culturing these hydrogels with the pancreatic cancer cells resulted in the cells death, with a very low number of viable cells in both the systems after the 3 weeks' period. From all the images analysed, the Alpha 5 peptigel was however the system where most of the present cells were marked as positive for the Ethidium Homodimer-1.

These results propose that the PANC-1 cells have a higher ability of attaching and proliferate in materials with a lower storage modulus and charge as it is the case of the Alpha 3 which describes, along with the Alpha 4, one of the materials with less solid-like properties and mechanical rigidity. What reinforces the fact that the PANC-1 cell line grows better in lower charge peptides is the fact that despite the Alpha 4 has a storage modulus similar to the Alpha 3, the first one, which has a higher charge, potentiated the death of a bigger percentage of cells. The conclusions taken from the Alpha 5 peptigel also evidence that a peptide with a very high modulus and charge prevent the development of the PANC-1 cells. Thence, in theory, if the Alpha 2 peptigel presented a lower storage modulus and charge, the images would show not only a much higher cell adhesion but also a higher number of live cells.

Other studies using hydrogels, have suggested different results from the experiments performed in this study. For example, Kumar et al. has reported that peptide hydrogels with low charge and storage modulus (like Alpha 3) as well as with high charge and storage modulus (like Alpha 5) can support the adhesion, proliferation and typical *in vivo* morphology of mouse oe-sophageal epithelial cells (mOECs). These hydrogels were also proved to support the 3D homog-enous distribution of viable rat oesophageal stromal fibroblasts (rOSFs) (Kumar et al., 2017).

Furthermore, Mujeeb et al. studied how the chondrocytes culture was affected when cultured in a peptide with similar characteristics to the Alpha 1 peptigel and saw that the first one could encapsulate chondrocytes, maintaining the cell viability and proliferation for up to 35 days *in vitro* without the use of growth factors. The deposition of CLG type II was also observed along with the increment of the gel's stiffness (Mujeeb et al., 2013). These findings therefore emphasize the fact that different hydrogel's properties lead to different cell morphology, ECM deposition and proliferation outcomes. Due to the reported range of values seen for the gels' stiffness, water content, charge, pH etc., each system ends up offering specific microenvironment properties that enhance the growth of certain types of cells that would not develop if cultured under different systems' conditions.
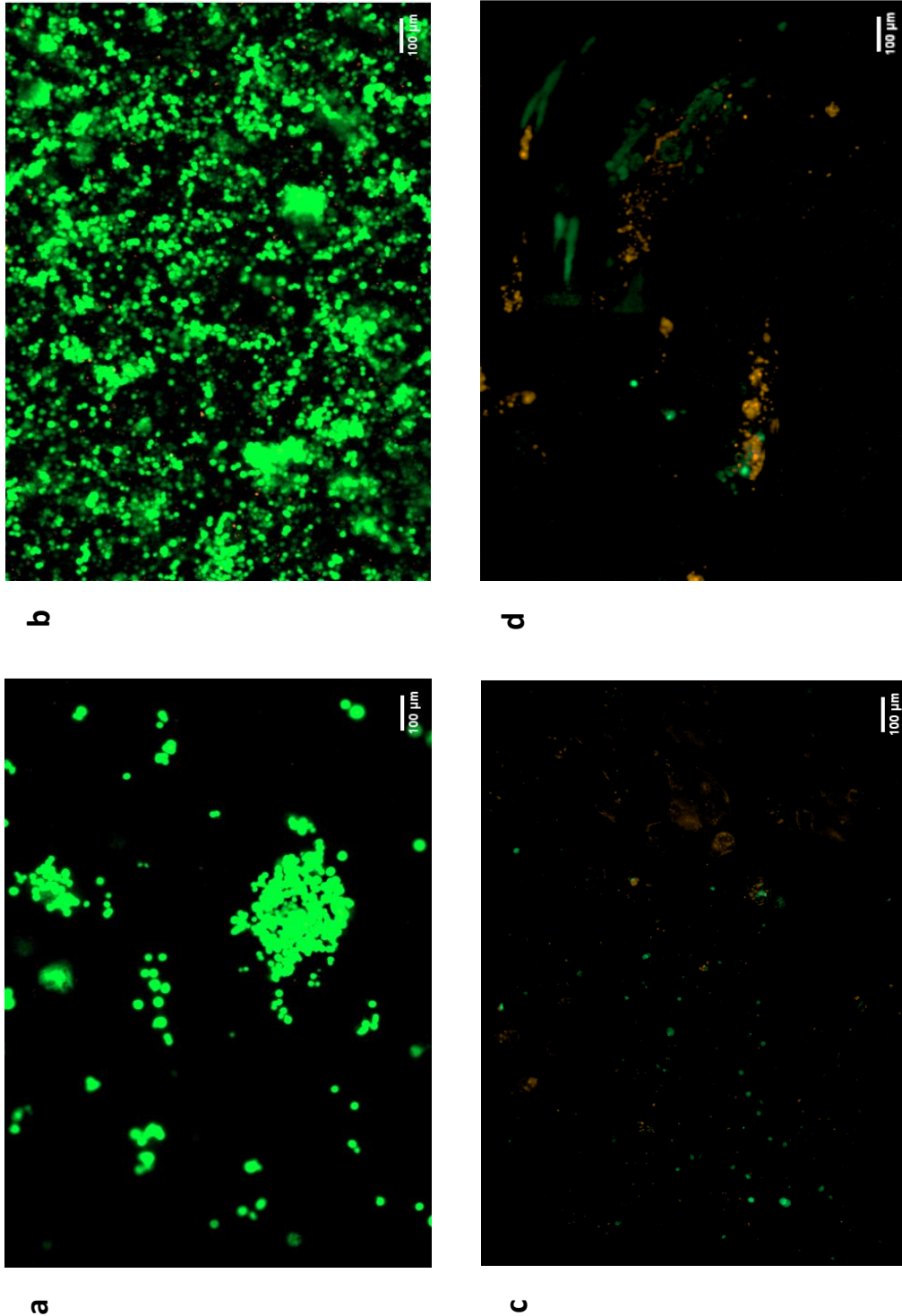
Figure 4.15: (a-d) Visualization of PANC-1 cells in 4 different hydrogels with fluorescence Live (green, Calcein-AM) and Dead (red, Ethidium Homodimer-1) viability assays in Alpha 2, 3, 4 and 5, respectively.

4.4.2 Long-term Culture in a 3D CLG Scaffold System

The second system selected to study the PANC-1 cells' growth, consisted in 4 jellyfish CLG coated 3D scaffolds that were cultured for 3 weeks along with the cancer cells (Passage 18). From the Live/Dead Cell Assays image's analysis (Figure 4.16) it was seen that the CLG presented in the scaffolds provided a proper environment for the cells to grow and migrate, therefore enhancing their cellular performance. The formation of large cellular masses is observed as well as the maintenance of the cells' *in vivo* morphology and responsiveness. Since the scaffolds are also characterized of a porous network within the sponge (similar to the PU scaffolds), they allow an efficient nutrient uptake and a better cell attachment (Jellagen - Marine Biotechnologies, 2019). Similar findings have also suggested the need to incorporate this ECM protein when mimicking the tumour niches as it is the case of Puls et al. who embedded PANC-1 cells in a 3D Matrigel made of CLG I and showed the growth on this cell line as tight clusters with the expression of both E-cadherin and vimentin proteins as well as the visualisation of a rounded cell morphology. It was also revealed the higher resistance of the PANC-1 cell line to treatment with GEM than in 2D cultures and in lower fibril density systems (Puls et al., 2017). In addition, previous work regarding experiments of the PANC-1 cell culture in PU scaffolds with the presence of CLG I, showed significant differences in the cell viability measurements along 28 days in culture.

a

b

Figure 4.16: (a-b) Visualization of PANC-1 cells in the CLG coated scaffolds with fluorescence Live (green, Calcein-AM) and Dead (red, Ethidium Homodimer-1) viability assays

At day 14 a significant higher cell proliferation was seen in scaffolds containing CLG as well as in the last day of culture (Appendix D). With these results, it is proposed that not only the presence of FN in polymeric scaffolds is important to enhance the cell-cell and cell-ECM interactions as well as the consequent cell proliferation. CLG has also proved to recapitulate the cell behaviour from *in vivo* tumoural microenvironments and to contribute to high cell density values.

5 Conclusions and Future Work

The main goal of this work was to design a dynamic perfusion system capable of support the long-term growth of pancreatic cancer cells, functional performances and therapy screening in a mechanically-robust 3D model. All the conclusions taken out from this study are stated below.

5.1 Conclusions

Preliminary tests showed that the perfusion bioreactor was able to culture the PANC-1 cells in PU scaffolds and make the cells achieve their highest metabolic viability at a flow rate of 3.5ml/min. This finding was further supported by the visualization of microscopy images where the cell's distribution along the scaffold layer was able to be compared with other flow rates' and static culture's images. These evidences proved that using a perfusion system not only increases the cell viability in culture but also enables the migration of the cells throughout the tissue's overall area which in static culture is more difficult to achieve since the cells are mainly distributed at the edges of the scaffold.

After a long-term culture experiment both in a dynamic and static system, comparable results between the alamarBlue assays showed a significant increase of the cell viability after 2 weeks in culture in perfusion and at the end of the 4 weeks when comparing to the static system. The cells were able to proliferate much faster in the bioreactor than in the well plates, thus suggesting the efficacy towards cell culture when subjecting them to perfusion.

With the addition of GEM, for chemotherapeutic treatment, both the results regarding Live/Dead Cell and Caspase3/7 Cell Assays showed that the resistance of cells to treatment is significantly enhanced in the perfusion system. At day 7 of culture, after adding the chemotherapeutic agent, the static system revealed about 24% less live cells than the dynamic one. In addition, the number of apoptotic cells at day 7 in the dynamic system was lower than in static with about 20% difference. However, to have a proper comparison between the decrease of the cell viability in the perfusion system after adding the GEM, with a system where the drug was not added, it is necessary to perform a control experiment in future studies for the dynamic culture. It would also be relevant to take into attention the concentration of drug added into both the systems since the number of viable cells in the dynamic culture is much higher than in the static one after a 4 weeks' period.

Seeking new possible materials and biological factors for the co-culture of PANC-1 cells also reveals to be mandatory since the PDAC tumour is constituted by several types of cells that differ biologically and functionally between each other. Therefore, each cell has different physiological properties that cause them to adapt differently to biomaterials synthetized to make them grow and attach in *in vitro* cultures. Different biochemical cues, (ECM proteins, peptides) could also be used to modify the surface of the scaffold in order to enhance other cells' biological performances.

Summing up, engineering for the first time a 3D *in vitro* perfusion system for PDAC studies resulted in a versatile system capable of a higher long-term cell proliferation than traditional studies (2D) that lead not only to higher cell viability outcomes but also to closer recapitulations of a real tumoural tissue. This platform also proved to be efficient for drug and test screening.

5.2 Future Work

As part of the future work, several experiments will be focused in mimicking the complex tumoural microenvironment with the co-culture of different cell types seen in the PDAC tissue (PSCs, fibroblasts, endothelial cells, etc). This approach will be capable of recreating the different cell-type interactions seen in *in vivo* studies and the first experiences will focus in 3D static cultures, shifting later to a 3D dynamic culture in the perfusion bioreactor.

Furthermore, it will be also necessary to optimize the scaffolds' structural and physicochemical properties to access and optimize the culture of other cell types. This might not only be required for culturing other cells but also to study other types of malignancies. Therefore, customizing the biochemical, biological and mechanical characteristics of the scaffold must be considered. For the ovarian cancer for example, which is one of the malignancies that is currently being looked for future studies, the decrease of the scaffold's stiffness turns up being important since the disease has its origins in the ovaries, which are known to be a very soft tissue, when comparing to the pancreatic one.

Bibliography

Adamska, A., Domenichini, A., Capone, E., Damiani, V., Akkaya, B. G., Linton, K. J., … Falasca, M. (2019). Pharmacological inhibition of ABCC3 slows tumour progression in animal models of pancreatic cancer, *7*, 1–14.

Adamska, A., Domenichini, A., & Falasca, M. (2017). Pancreatic ductal adenocarcinoma: Current and evolving therapies. *International Journal of Molecular Sciences*, *18*(7). https://doi.org/10.3390/ijms18071338

Al-Rubeai, M. S. E. (2015). *Cell Engineering 9: Animal Cell Culture*. https://doi.org/10.1007/978-3-319-10320-4

American Cancer Society. (2014). Cancer in the Twenty-first Century. Retrieved April 11, 2019, from https://www.cancer.org/cancer/cancer-basics/history-of-cancer/twenty-first-century-and-beyond.html

Arrowsmith, J. (2011). Trial watch: Phase III and submission failures: 2007-2010. *Nature Reviews Drug Discovery*, *10*(2), 87. https://doi.org/10.1038/nrd3375

Binder. (2015). Everything worth knowing about CO2 incubators. Retrieved June 12, 2019, from https://pages.binder-world.com/en/co2-incubator-function

BIO RAD. (2019). What is alamarBlue. Retrieved June 19, 2019, from https://www.bio-rad-antibodies.com/alamarblue-cell-viability-assay-resazurin.html

Biocision. (2019). Snap Freezing Product Applications. Retrieved June 19, 2019, from http://biocision.com.s219960.gridserver.com/applications/snap-freezing

Biolabs, C. (2011). Subcutaneous Tumor Models. Retrieved April 4, 2019, from https://www.creative-biolabs.com/drug-discovery/therapeutics/subcutaneous-tumor-models.htm

Blomquist, M. (2016). Cooperation in Cancer Cells. Retrieved April 16, 2019, from https://askabiologist.asu.edu/evmed-edit/cancer-cooperation

Boschetti, F., Raimondi, M. T., Migliavacca, F., & Dubini, G. (2006). Prediction of the micro-fluid dynamic environment imposed to three-dimensional engineered cell systems in

bioreactors. *Journal of Biomechanics*, *39*(3), 418–425. https://doi.org/10.1016/j.jbiomech.2004.12.022

Breslin, S., & O'Driscoll, L. (2013). Three-dimensional cell culture: The missing link in drug discovery. *Drug Discovery Today*, *18*(5–6), 240–249. https://doi.org/10.1016/j.drudis.2012.10.003

British Society for Immunology. (2019). Natural Killer Cells. Retrieved April 10, 2019, from https://www.immunology.org/public-information/bitesized-immunology/cells/natural-killer-cells

Brito, C. (2018). In vitro models for preclinical research - the power of human stem cells (pp. 1–10). Animal Cell Technology Unit, ITQB-UNL/iBET.

Burek, M., Waśkiewicz, S., Lalik, A., Student, S., Bieg, T., & Wandzik, I. (2017). Thermoresponsive microgels containing trehalose as soft matrices for 3D cell culture. *Biomaterials Science*, *5*(2), 234–246. https://doi.org/10.1039/c6bm00624h

Campos, D. M., Soares, G. A., & Anselme, K. (2013). Role of culture conditions on in vitro transformation and cellular colonization of biomimetic HA-Col scaffolds. *Biomatter*, *3*(2), 1–10. https://doi.org/10.4161/biom.24922

Cancer Research UK. (2018). FOLFIRINOX. Retrieved August 19, 2019, from https://www.cancerresearchuk.org/about-cancer/cancer-in-general/treatment/cancer-drugs/drugs/folfirinox

Cancer Research UK. (2019a). What is cancer? Retrieved April 11, 2019, from https://www.cancerresearchuk.org/about-cancer/what-is-cancer

Cancer Research UK. (2019b). Worldwide Cancer Statistics. Retrieved April 11, 2019, from https://www.cancerresearchuk.org/health-professional/cancer-statistics/worldwide-cancer#heading-One

Cellab GmbH. (2017). *Cellab Docking Station*. Radeberg.

Chemometec. (2019). Monitor Microcarrier Cultures. Retrieved April 10, 2019, from https://chemometec.com/counting-cells-microcarriers/

Costa-Silva, B., Aiello, N. M., Ocean, A. J., Singh, S., Zhang, H., Thakur, B. K., … Lyden, D. (2015). Pancreatic cancer exosomes initiate pre-metastatic niche formation in the liver. *Nature Cell Biology*, *17*(6), 816–826. https://doi.org/10.1038/ncb3169

Deer, E. L., Gonzalez-Hernandez, J., Coursen, J. D., Shea, J. E., Ngatia, J., Scaife, C. L., … Mulvihill, S. J. (2010). Phenotype and Genotype of pancreatic cancer. *Pancreas*, *39*(4), 425–435. https://doi.org/10.1097/MPA.0b013e3181c15963.Phenotype

Definitions. (2019). Confluency. Retrieved May 14, 2019, from https://www.definitions.net/definition/confluency

Dhall, A., Masiello, T., Butt, L., Strohmayer, M., Hemachandra, M., Tokranova, N., & Castracane, J. (2016). Simulating Fluid Flow through a Culture Chip for Cell Migration Studies in Microgravity, 2016.

Dhandayuthapani, B., Yoshida, Y., Maekawa, T., & Kumar, D. S. (2011). Polymeric scaffolds in tissue engineering application: A review. *International Journal of Polymer Science*, *2011*(ii). https://doi.org/10.1155/2011/290602

Docs. (2019). What is the Reynolds Number? Retrieved May 6, 2019, from https://www.simscale.com/docs/content/simwiki/numerics/what-is-the-reynolds-number.html

DrugBank. (2019). Gemcitabine. Retrieved June 28, 2019, from https://www.drugbank.ca/drugs/DB00441

Encyclopedia Britannica. (2019a). B Cell. Retrieved April 10, 2019, from https://www.britannica.com/science/B-cell

Encyclopedia Britannica. (2019b). Caliper. Retrieved April 10, 2019, from https://www.britannica.com/technology/caliper-measurement-instrument

Fang, J., & Trewyn, B. (2012). Trypan Blue. Retrieved June 17, 2019, from https://www.sciencedirect.com/topics/medicine-and-dentistry/trypan-blue

Fennema, E., Rivron, N., Rouwkema, J., van Blitterswijk, C., & De Boer, J. (2013). Spheroid culture as a tool for creating 3D complex tissues. *Trends in Biotechnology*, *31*(2), 108–115. https://doi.org/10.1016/j.tibtech.2012.12.003

Ferro, R., Adamska, A., Lattanzio, R., Mavrommati, I., Edling, C. E., Arifin, S. A., … Falasca, M. (2018). GPR55 signalling promotes proliferation of pancreatic cancer cells and tumour growth in mice, and its inhibition increases effects of gemcitabine. *Oncogene*, *37*(49), 6368–6382. https://doi.org/10.1038/s41388-018-0390-1

Fischbach, C., Chen, R., Matsumoto, T., Schmelzle, T., Brugge, J. S., Polverini, P. J., & Mooney, D. J. (2007). Engineering tumors with 3D scaffolds. *Nature Methods*, *4*(10), 855–860. https://doi.org/10.1038/nmeth1085

Franck, A. (n.d.). *Viscoelasticity and dynamic mechanical testing*.

H. J Danen, E. (2019). Integrins: An Overview of Structural and Funcional Aspects. Retrieved April 10, 2019, from https://www.ncbi.nlm.nih.gov/books/NBK6259/

Hashimoto, D., Bläuer, M., Hirota, M., Ikonen, N. H., Sand, J., & Laukkarinen, J. (2014). Autophagy is needed for the growth of pancreatic adenocarcinoma and has a cytoprotective effect against anticancer drugs. *European Journal of Cancer*, *50*(7), 1382–1390. https://doi.org/10.1016/j.ejca.2014.01.011

He, Q., Wang, X., Zhang, X., Han, H., Han, B., Xu, J., … Yin, H. (2013). A tissue-engineered subcutaneous pancreatic cancer model for antitumor drug evaluation. *International Journal of Nanomedicine*, *8*, 1167–1176. https://doi.org/10.2147/IJN.S42464

Hickman, J. A., Graeser, R., de Hoogt, R., Vidic, S., Brito, C., Gutekunst, M., … Imi Predect consortium. (2014). Three-dimensional models of cancer for pharmacology and cancer cell biology: Capturing tumor complexity in vitro/ex vivo. *Biotechnology Journal*, *9*(9), 1115–1128. https://doi.org/10.1002/biot.201300492

Hirt, C., Papadimitropoulos, A., Muraro, M. G., Mele, V., Panopoulos, E., Cremonesi, E., … Spagnoli, G. C. (2015). Bioreactor-engineered cancer tissue-like structures mimic phenotypes, gene expression profiles and drug resistance patterns observed "in vivo." *Biomaterials*, *62*, 138–146. https://doi.org/10.1016/j.biomaterials.2015.05.037

Hoarau-Véchot, J., Rafii, A., Touboul, C., & Pasquier, J. (2018). Halfway between 2D and animal models: Are 3D cultures the ideal tool to study cancer-microenvironment interactions? *International Journal of Molecular Sciences*, *19*(1). https://doi.org/10.3390/ijms19010181

Hoare, T. R., & Kohane, D. S. (2008). Hydrogels in drug delivery: Progress and challenges. *Polymer*, *49*(8), 1993–2007. https://doi.org/10.1016/j.polymer.2008.01.027

Horch, R. E., Boos, A. M., Quan, Y., Bleiziffer, O., Detsch, R., Boccaccini, A. R., … Arkudas, A. (2013). Cancer research by means of tissue engineering - is there a rationale? *Journal of Cellular and Molecular Medicine*, *17*(10), 1197–1206. https://doi.org/10.1111/jcmm.12130

Huang, Q., Hu, X., He, W., Zhao, Y., Hao, S., Wu, Q., … Zhang, S. (2018). Fluid shear stress and tumor metastasis. *American Journal of Cancer Research*, *8*(5), 763–777.

Human Metabolome Database. (2019). Showing metabocard for Gemcitabine (HMDB0014584). Retrieved October 27, 2019, from http://www.hmdb.ca/metabolites/HMDB0014584

Hynds, R. E., Bonfanti, P., & Janes, S. M. (2017). Regenerating human epithelia with cultured stem cells: feeder cells, organoids and beyond. *EMBO Molecular Medicine*, *10*(2), 139–150. https://doi.org/10.15252/emmm.201708213

ibidi. (2019). Microscopy Techniques and Culture Surfaces: Find the Perfect Match. Retrieved from https://ibidi.com/content/216-confocal-microscopy

iStock by Getty Images. (2019). Employment and Labor. Retrieved July 25, 2019, from https://www.istockphoto.com/gb/illustrations/employment-and-labor?license=rf&assettype=image&sort=mostpopular&mediatype=illustration&family=creative&phrase=employment and labor

Jellagen - Marine Biotechnologies. (2019a). 3D Scaffolds. Retrieved September 16, 2019, from https://www.jellagen.co.uk/products/cell-culture-reagents/3d-scaffolds/

Jellagen - Marine Biotechnologies. (2019b). What is the difference between the 2D and 3D Cell Culture. Retrieved March 29, 2019, from https://www.jellagen.co.uk/blog/what-is-the-difference-between-2d-and-3d-cell-culture/

Jo, Y., Choi, N., Kim, K., Koo, H. J., Choi, J., & Kim, H. N. (2018). Chemoresistance of cancer cells: Requirements of tumor microenvironment-mimicking in vitro models in anti-cancer drug development. *Theranostics*, *8*(19), 5259–5275. https://doi.org/10.7150/thno.29098

Jong, B. K. (2005). Three-dimensional tissue culture models in cancer biology. *Seminars in Cancer Biology*, *15*(5 SPEC. ISS.), 365–377. https://doi.org/10.1016/j.semcancer.2005.05.002

Joshi, G. (2014). Hemocytometer. Retrieved June 17, 2019, from https://www.slideshare.net/GovardhanJoshi/hemocytometer

JoVE Science Education Databse. (2019). Introduction to the Microplate Reader. Retrieved September 19, 2019, from https://www.jove.com/science-education/5024/introduction-to-the-microplate-reader

Kaidar-Person, O., Bar-Sela, G., & Person, B. (2011). The two major epidemics of the twenty-first century: Obesity and cancer. *Obesity Surgery*, *21*(11), 1792–1797. https://doi.org/10.1007/s11695-011-0490-2

Ki, C. S., Shih, H., & Lin, C. C. (2013). Effect of 3D matrix compositions on the efficacy of EGFR inhibition in pancreatic ductal adenocarcinoma cells. *Biomacromolecules*, *14*(9), 3017–3026. https://doi.org/10.1021/bm4004496

Kim, S. S., Penkala, R., & Abrahimi, P. (2007). A Perfusion Bioreactor for Intestinal Tissue Engineering. *Journal of Surgical Research*, *142*(2), 327–331.

https://doi.org/10.1016/j.jss.2007.03.039

Kuen, J. (2017). *Influence of 3D tumor cell/fibroblast co-culture on monocyte differentiation and tumor progression in pancreatic cancer*.

Kumar, D., Workman, V. L., O'Brien, M., McLaren, J., White, L., Ragunath, K., … Gough, J. E. (2017). Peptide Hydrogels—A Tissue Engineering Strategy for the Prevention of Oesophageal Strictures. *Advanced Functional Materials*, *27*(38). https://doi.org/10.1002/adfm.201702424

Labcompare. (2019). Water Baths. Retrieved June 17, 2019, from https://www.labcompare.com/General-Laboratory-Equipment/80-Water-Baths/

Lazzari, G., Nicolas, V., Matsusaki, M., Akashi, M., Couvreur, P., & Mura, S. (2018). Multicellular spheroid based on a triple co-culture: A novel 3D model to mimic pancreatic tumor complexity. *Acta Biomaterialia*, *78*, 296–307. https://doi.org/10.1016/j.actbio.2018.08.008

Liu, H. Y., Greene, T., Lin, T. Y., Dawes, C. S., Korc, M., & Lin, C. C. (2017). Enzyme-mediated stiffening hydrogels for probing activation of pancreatic stellate cells. *Acta Biomaterialia*, *48*, 258–269. https://doi.org/10.1016/j.actbio.2016.10.027

Liu, H. Y., Korc, M., & Lin, C. C. (2018). Biomimetic and enzyme-responsive dynamic hydrogels for studying cell-matrix interactions in pancreatic ductal adenocarcinoma. *Biomaterials*, *160*, 24–36. https://doi.org/10.1016/j.biomaterials.2018.01.012

Live Science. (2018). Thymus: Facts, Function & Diseases. Retrieved April 10, 2019, from https://www.livescience.com/62527-thymus.html

Longati, P., Jia, X., Eimer, J., Wagman, A., Witt, M. R., Rehnmark, S., … Heuchel, R. L. (2013). 3D pancreatic carcinoma spheroids induce a matrix-rich, chemoresistant phenotype offering a better model for drug testing. *BMC Cancer*, *13*, 1–13. https://doi.org/10.1186/1471-2407-13-95

LW Scientific. (2019). Hemacytometer. Retrieved June 17, 2019, from https://www.lwscientific.com/products/hemacytometer

Maeda, H., & Khatami, M. (2018). Analyses of repeated failures in cancer therapy for solid tumors: poor tumor-selective drug delivery, low therapeutic efficacy and unsustainable costs. *Clinical and Translational Medicine*, *7*(1), 1–20. https://doi.org/10.1186/s40169-018-0185-6

Magrofuoco, E., Flaibani, M., Giomo, M., & Elvassore, N. (2019). Cell culture distribution in a three-dimensional porous scaffold in perfusion bioreactor. *Biochemical Engineering Journal*, *146*(August 2016), 10–19. https://doi.org/10.1016/j.bej.2019.02.023

Manchester BIOGEL. (2019a). *How to perform 3D cell culture*. https://doi.org/10.1017/CBO9781107415324.004

Manchester BIOGEL. (2019b). Hydrogel Products. Retrieved September 16, 2019, from https://manchesterbiogel.com/products/peptigels

Manfredonia, C., Muraro, M. G., Hirt, C., Mele, V., Governa, V., Papadimitropoulos, A., … Iezzi, G. (2018). Maintenance of primary human colorectal cancer microenvironment using a perfusion bioreactor-based 3D culture system. In *AACR Annual Meeting 2018*. Chicago. Retrieved from https://cancerres.aacrjournals.org/content/78/13_Supplement/4097.short

Martin, I., Wendt, D., & Heberer, M. (2004). *The role of bioreactors in tissue engineering*. *Trends in Biotechnology* (Vol. 22). https://doi.org/10.1016/j.tibtech.2003.12.001

Mayo Clinic. (2016). Pancreatic Cancer. Retrieved April 16, 2019, from https://www.mayoclinic.org/diseases-conditions/pancreatic-cancer/symptoms-causes/syc-20355421

MBInfo. (2018). What are intermediate filaments? Retrieved August 19, 2019, from https://www.mechanobio.info/cytoskeleton-dynamics/what-is-the-cytoskeleton/what-are-intermediate-filaments/

McKeown, S. R. (2014). Defining normoxia, physoxia and hypoxia in tumours - Implications for treatment response. *British Journal of Radiology*, *87*(1035), 1–12. https://doi.org/10.1259/bjr.20130676

MedicineNet. (2018). Medical Definition of Apoptosis. Retrieved April 10, 2019, from https://www.medicinenet.com/script/main/art.asp?articlekey=11287

Mendonsa, A. M., Na, T. Y., & Gumbiner, B. M. (2018). E-cadherin in contact inhibition and cancer. *Oncogene*, *37*(35), 4769–4780. https://doi.org/10.1038/s41388-018-0304-2

Mi, H. Y., Jing, X., & Turng, L. S. (2014). Fabrication of porous synthetic polymer scaffolds for tissue engineering. *Journal of Cellular Plastics*, *51*(2), 165–196. https://doi.org/10.1177/0021955X14531002

MicroscopyU. (n.d.). Introduction to Phase Contrsat Microscopy. Retrieved June 21, 2019, from https://www.microscopyu.com/techniques/phase-contrast/introduction-to-phase-contrast-microscopy

Mimetas. (2019). 2D Versus 3D Cell Cultures. Retrieved March 29, 2019, from https://mimetas.com/article/2d-versus-3d-cell-cultures

Mitchell, M. J., & King, M. R. (2013). Computational and experimental models of cancer cell response to fluid shear stress. *Frontiers in Oncology*, *3 MAR*(March), 1–11. https://doi.org/10.3389/fonc.2013.00044

Mizushima, N. (2007). *Autophagy: process and function*. Tokyo Medical and Dental University.

Moser, H. W., & Naidu, S. (2007). The Leukodystrophies. In *Neurology and Clinical Neuroscience* (pp. 1065–1092). https://doi.org/10.1016/B978-0-323-03354-1.50084-5

Mujeeb, A., Miller, A. F., Saiani, A., & Gough, J. E. (2013). Self-assembled octapeptide scaffolds for in vitro chondrocyte culture. *Acta Biomaterialia*, *9*(1), 4609–4617. https://doi.org/10.1016/j.actbio.2012.08.044

Munson, J. M., & Shieh, A. C. (2014). Interstitial fluid flow in cancer: Implications for disease progression and treatment. *Cancer Management and Research*, *6*(1), 317–318. https://doi.org/10.2147/CMAR.S65444

Muraro, M. G., Muenst, S., Mele, V., Quagliata, L., Iezzi, G., Tzankov, A., … Soysal, S. D. (2017). Ex-vivo assessment of drug response on breast cancer primary tissue with preserved microenvironments. *OncoImmunology*, *6*(7), 1–12. https://doi.org/10.1080/2162402X.2017.1331798

National Cancer Institute. (2019a). NCI Dictionary of Cancer Terms. Retrieved August 19, 2019, from https://www.cancer.gov/publications/dictionaries/cancer-terms/def/matrix-metalloproteinase

National Cancer Institute. (2019b). What is Cancer? Retrieved April 11, 2019, from https://www.cancer.gov/about-cancer/understanding/what-is-cancer

National Institute of Biomedical Engineering and Bioengineering. (2019). Tissue Engineering and Regenerative Medicine. Retrieved April 29, 2019, from https://www.nibib.nih.gov/science-education/science-topics/tissue-engineering-and-regenerative-medicine

NCBI. (2019). 3T3 Cells. Retrieved April 10, 2019, from https://www.ncbi.nlm.nih.gov/mesh/68016475

News Medical Life Sciences. (2019). Scaffold Holder-Disposable Set from Cellab. Retrieved June 28, 2019, from https://www.news-medical.net/Scaffold-Holder-Disposable-Set-from-Cellab

One Person Closer. (2019). One Person Closer. Retrieved July 25, 2019, from https://twitter.com/onepersoncloser

Online, P. (2016). Phosphate buffered saline. Retrieved June 12, 2019, from https://www.protocolsonline.com/recipes/phosphate-buffered-saline-pbs/

Ouyang, W., Kolls, J. K., & Zheng, Y. (2008). The Biological Functions of T Helper 17 Cell Effector Cytokines in Inflammation. *Immunity*, *28*(4), 454–467. https://doi.org/10.1038/jid.2014.371

Pancreatic Cancer UK. (2017). Gemcitabine (Gemzar). Retrieved June 28, 2019, from https://www.pancreaticcancer.org.uk/information-and-support/treatments-for-pancreatic-cancer/chemotherapy-for-pancreatic-cancer/main-drugs-for-pancreatic-cancer/gemcitabine-gemzar/

Pancreatic Cancer UK. (2018). Types of Pancreatic Cancer. Retrieved April 11, 2019, from https://www.pancreaticcancer.org.uk/information-and-support/facts-about-pancreatic-cancer/types-of-pancreatic-cancer/

Parker Institute for Cancer Immunotherapy. (2019). Tumor Microenvironment. Retrieved July 25, 2019, from https://www.parkerici.org/research_focus/tumor-microenvironment/

Partap, S., Plunkett, N. A., & O'Brien, F. J. (2010). Bioreactors in Tissue Engineering. In D. Eberdi (Ed.), *Tissue Engineering* (pp. 323–336). InTech. Retrieved from https://www.intechopen.com/books/tissue-engineering/bioreactors-in-tissue-engineering%0Ahttp://www.intechopen.com/books/tissue-engineering/bioreactors-in-tissue-engineering

Patel, H., Bonde, M., & Srinivasan, G. (2011). Biodegradable Polymer Scaffold for Tissue Engineering. *Trends in Biomaterials & Artificial Organs*, *25*(1), 20–29.

Perez, R. A., Riccardi, K., Altankov, G., & Ginebra, M. P. (2014). Dynamic cell culture on calcium phosphate microcarriers for bone tissue engineering applications. *Journal of Tissue Engineering*, *5*(January). https://doi.org/10.1177/2041731414543965

Personal Genetics Education Project. (2019). What is Genotype? What is Phenotype? Retrieved April 29, 2019, from https://pged.org/what-is-genotype-what-is-phenotype/

Place, E. S., George, J. H., Williams, C. K., & Stevens, M. M. (2009). Synthetic polymer scaffolds for tissue engineering. *Chemical Society Reviews*, *38*(4), 1139–1151. https://doi.org/10.1039/b811392k

Porcelli, L., Quatrale, A. E., Mantuano, P., Leo, M. G., Silvestris, N., Rolland, J. F., … Azzariti, A.

(2013). Optimize radiochemotherapy in pancreatic cancer: PARP inhibitors a new therapeutic opportunity. *Molecular Oncology*, *7*(3), 308–322. https://doi.org/10.1016/j.molonc.2012.10.002

Press, T. (2019). How many people in the UK share your name? Retrieved July 25, 2019, from https://www.yorkpress.co.uk/news/ryedale/15085294.how-many-people-in-the-uk-share-your-name/

Prime Cirúrgica. (2019). Tubo de Ensaio 12*75 mm Estéril com Tampa c/50 Kasvi. Retrieved July 25, 2019, from https://www.google.com/search?biw=1366&bih=576&tbm=isch&sa=1&ei=cMo4Xf_8H5L BlwSegbxI&q=tubo+de+ensaio&oq=tubo+de+ensaio&gs_l=img.3..0j0i67j0l2j0i5i30l2j0i30l 4.123567.123567..123728...0.0..0.87.87.1......0....1..gws-wiz-img.W43UkJvGdU8&ved=0ahUKEwj_9O33vM7

ProQinase. (2019). Subcutaneous Tumor Models (Xenograft Models & Syngeneic Models)/Xenograft Models. Retrieved April 1, 2019, from https://www.proqinase.com/products-services-vivo-testing-services/subcutaneous-tumor-models-xenograft-models

Puls, T. J., Tan, X., Whittington, C. F., & Voytik-Harbin, S. L. (2017). 3D collagen fibrillar microstructure guides pancreatic cancer cell phenotype and serves as a critical design parameter for phenotypic models of EMT. *PLoS ONE*, *12*(11), 1–25. https://doi.org/10.1371/journal.pone.0188870

Querido, W., Falcon, J. M., Kandel, S., & Pleshko, N. (2017). Vibrational spectroscopy and imaging: Applications for tissue engineering. *Analyst*, *142*(21), 4005–4017. https://doi.org/10.1039/c7an01055a

R&D. (2019). Bacterial Skin Infection Antibiotic Approved by FDA. Retrieved July 25, 2019, from https://www.rdmag.com/news/2017/06/bacterial-skin-infection-antibiotic-approved-fda

Radisic, M., Marsano, A., Maidhof, R., Wang, Y., & Vunjak-Novakovic, G. (2008). Cardiac tissue engineering using perfusion bioreactor systems. *Nature Protocols*, *3*(4), 719–738. https://doi.org/10.1038/nprot.2008.40

Rasheed, Z., Matsui, W., & Maitra, A. (2012). Pathology of pancreatic stroma in PDAC. In P. J. Grippo & H. G. Munshi (Eds.), *Pancreatic Cancer and Tumor Microenvironment*. Retrieved from https://www.ncbi.nlm.nih.gov/books/NBK98933/#ch1.Pancreatic_cancer_stellate_cells_ and

Raza, A., Ki, C. S., & Lin, C. C. (2013). The influence of matrix properties on growth and morphogenesis ofhuman pancreatic ductal epithelial cells in 3D. *Biomaterials*, *34*(21), 5117–5127. https://doi.org/10.1016/j.biomaterials.2013.03.086

Ricci, C., Moroni, L., & Danti, S. (2014). Cancer tissue engineering - new perspectives in understanding the biology of solid tumours - a critical review. *OA Tissue Engineering*, *1*(1), 1–7. https://doi.org/10.13172/2052-9643-1-1-607

Ricci, C., Mota, C., Moscato, S., D'Alessandro, D., Ugel, S., Sartoris, S., … Danti, S. (2014). Interfacing polymeric scaffolds with primary pancreatic ductal adenocarcinoma cells to develop 3D cancer models. *Biomatter*, *4*, e955386. https://doi.org/10.4161/21592527.2014.955386

Richards, K. E., Zeleniak, A. E., Fishel, M. L., Wu, J., Littlepage, L. E., & Hill, R. (2017). Cancer-

associated fibroblast exosomes regulate survival and proliferation of pancreatic cancer cells. *Oncogene*, *36*(13), 1770–1778. https://doi.org/10.1038/onc.2016.353

Richmond, A., & Su, Y. (2008). Mouse xenograft models vs GEM models for human cancer therapeutics. *Disease Models and Mechanisms*, *1*(2–3), 78–82. https://doi.org/10.1242/dmm.000976

Riss, T. L., Moravec, R. A., Niles, A. L., Duellman, S., Benink, H. A., Worzella, T. J., & Minor, L. (2016). Cell Viability Assays. In *The Assay Guidance Manual* (pp. 1–25). Retrieved from http://www.ncbi.nlm.nih.gov/pubmed/23805433

River, C. (2019a). Athymic Nude Mouse. Retrieved April 1, 2019, from https://www.criver.com/products-services/find-model/athymic-nude-mouse?region=3671

River, C. (2019b). NOD/SCID Mouse. Retrieved April 1, 2019, from https://www.criver.com/products-services/find-model/nod-scid-mouse?region=3671

Roberts, R. A., Ganey, P. E., Ju, C., Kamendulis, L. M., Rusyn, I., & Klaunig, J. E. (2007). Role of the Kupffer cell in mediating hepatic toxicity and carcinogenesis. *Toxicological Sciences*, *96*(1), 2–15. https://doi.org/10.1093/toxsci/kfl173

Rosiak, J. M., & Yoshii, F. (1999). Hydrogels and their medical applications. *Nuclear Instruments and Methods in Physics Research, Section B: Beam Interactions with Materials and Atoms*, *151*(1–4), 56–64. https://doi.org/10.1016/S0168-583X(99)00118-4

Rutkovskiy, A., Stensløkken, K.-O., & Vaage, I. J. (2016). Osteoblast Differentiation at a Glance. *Medical Science Monitor Basic Research*, *22*, 95–106. https://doi.org/10.12659/msmbr.901142

Rutkowski, J. M., & Swartz, M. A. (2007). A driving force for change: interstitial flow as a morphoregulator. *Trends in Cell Biology*, *17*(1), 44–50. https://doi.org/10.1016/j.tcb.2006.11.007

Safinia, L., Mantalaris, A., & Bismarck, A. (2006). Nondestructive technique for the characterization of the pore size distribution of soft porous constructs for tissue engineering. *Langmuir*, *22*(7), 3235–3242. https://doi.org/10.1021/la051762g

Saleh, N. (2018). A Closer Look at the Top 5 Deadliest Cancers. Retrieved April 11, 2019, from https://www.verywellhealth.com/top-deadliest-cancers-1123927

Santo, V. E., Rebelo, S. P., Estrada, M. F., Alves, P. M., Boghaert, E., & Brito, C. (2017). Drug screening in 3D in vitro tumor models: overcoming current pitfalls of efficacy read-outs. *Biotechnology Journal*, *12*(1). https://doi.org/10.1002/biot.201600505

ScienceDirect. (2012). Laminar Flow Cabinet. Retrieved June 13, 2019, from https://www.sciencedirect.com/topics/immunology-and-microbiology/laminar-flow-cabinet

Serra, M. (2018). Células Estaminais e Terapia Celular (pp. 1–25).

Sigma-Aldrich. (2019a). Cell Dissociation with Trypsin. Retrieved June 13, 2019, from https://www.sigmaaldrich.com/technical-documents/articles/biology/cell-dissociation-with-trypsin.html

Sigma-Aldrich. (2019b). Dimethyl Sulfoxide. Retrieved June 17, 2019, from https://www.sigmaaldrich.com/chemistry/solvents/products.html?TablePage=17292420

Sigma-Aldrich. (2019c). Dimethyl Sulfoxide. Retrieved June 17, 2019, from https://www.sigmaaldrich.com/catalog/product/sial/276855?lang=en&region=GB&gclid= EAIaIQobChMIoc_Sl-3-4AIVr7ftCh3YZwCAEAAYASAAEgJidvD_BwE

Sigma-Aldrich. (2019d). DMEM (Dulbecco's Modified Eagle Medium). Retrieved June 12, 2019, from https://www.sigmaaldrich.com/life-science/cell-culture/classical-media-salts/dmem.html?gclid=EAIaIQobChMIz93shPnj4gIVx4jVCh0QtQexEAAYAiAAEgJa0fD_BwE

Sigma-Aldrich. (2019e). Dulbecco's Modified Eagle's Medium (DME) Formulation. Retrieved June 12, 2019, from https://www.sigmaaldrich.com/life-science/cell-culture/learning-center/media-formulations/dme.html

Sigma-Aldrich. (2019f). Fetal Bovine Serum (FBS) for Cell Culture. Retrieved June 13, 2019, from https://www.sigmaaldrich.com/life-science/cell-culture/cell-culture-products.html?TablePage=9628642

Sigma-Aldrich. (2019g). L Glutamine in Cell Culture. Retrieved June 13, 2019, from https://www.sigmaaldrich.com/life-science/cell-culture/learning-center/media-expert/glutamine.html

Sigma-Aldrich. (2019h). Penicillin-Streptomycin. Retrieved June 17, 2019, from https://www.sigmaaldrich.com/catalog/product/sigma/p4333?lang=en&region=GB

Starokozhko, V., Hemmingsen, M., Larsen, L., Mohanty, S., Merema, M., Pimentel, R. C., … Dufva, M. (2018). Differentiation of human-induced pluripotent stem cell under flow conditions to mature hepatocytes for liver tissue engineering. *Journal of Tissue Engineering and Regenerative Medicine*, *12*(5), 1273–1284. https://doi.org/10.1002/term.2659

STEMCELL Technologies. (2019). Resazurin (Sodium Salt). Retrieved August 10, 2019, from https://www.stemcell.com/resazurin-sodium-salt.html

Sudhakar, C. K., Upadhyay, N., Jain, A., Verma, A., Narayana Charyulu, R., & Jain, S. (2015). *Hydrogels-Promising Candidates for Tissue Engineering*. *Nanotechnology Applications for Tissue Engineering*. Elsevier Inc. https://doi.org/10.1016/B978-0-323-32889-0.00005-4

Thermo Fisher Scientific. (2019a). Calcein, AM, cell-permeant dye. Retrieved August 10, 2019, from https://www.stemcell.com/resazurin-sodium-salt.html

Thermo Fisher Scientific. (2019b). CellEvent Caspase-3/7 Green Detection Reagent. Retrieved August 10, 2019, from https://www.thermofisher.com/order/catalog/product/C10423

Thermo Fisher Scientific. (2019c). Dapi Protocol for Fluorescence Imaging. Retrieved June 25, 2019, from https://www.thermofisher.com/uk/en/home/references/protocols/cell-and-tissue-analysis/protocols/dapi-imaging-protocol.html

Thermo Fisher Scientific. (2019d). Ethidium Homodimer-1 (EthD-1). Retrieved August 10, 2019, from https://www.thermofisher.com/order/catalog/product/E1169?SID=srch-srp-E1169

Thermo Fisher Scientific. (2019e). Exosome Research Products. Retrieved August 25, 2019, from https://www.thermofisher.com/uk/en/home/life-science/cell-analysis/exosomes.html

Thermo Fisher Scientific. (2019f). Fixation Strategies and Formulations Used in IHC Staining. Retrieved June 25, 2019, from https://www.thermofisher.com/uk/en/home/life-science/protein-biology/protein-biology-learning-center/protein-biology-resource-library/pierce-protein-methods/fixation-strategies-formulations.html

Thermo Fisher Scientific. (2019g). L Glutamine. Retrieved June 13, 2019, from https://www.thermofisher.com/uk/en/home/life-science/cell-culture/mammalian-cell-culture/media-supplements/glutamine.html

Thermo Fisher Scientific. (2019h). Mr Frosty Freezing Container. Retrieved May 14, 2019, from https://www.thermofisher.com/order/catalog/product/5100-0001

Tibbitt, M. W., & Anseth, K. S. (2009). Hydrogels as extracellular matrix mimics for 3D cell culture. *Biotechnology and Bioengineering*, *103*(4), 655–663. https://doi.org/10.1002/bit.22361

Totti, S., Allenby, M. C., Dos Santos, S. B., Mantalaris, A., & Velliou, E. G. (2018). A 3D bioinspired highly porous polymeric scaffolding system for: In vitro simulation of pancreatic ductal adenocarcinoma. *RSC Advances*, *8*(37), 20928–20940. https://doi.org/10.1039/c8ra02633e

Totti, S., Vernardis, S. I., Meira, L., Pérez-Mancera, P. A., Costello, E., Greenhalf, W., … Velliou, E. G. (2017). Designing a bio-inspired biomimetic in vitro system for the optimization of ex vivo studies of pancreatic cancer. *Drug Discovery Today*, *22*(4), 690–701. https://doi.org/10.1016/j.drudis.2017.01.012

UKEssays. (2018). Effects os Static and Dynamic Culture Conditions. Retrieved April 8, 2019, from https://www.ukessays.com/essays/biology/effects-of-static-and-dynamic-culture-conditions-biology-essay.php

Ulukaya, E., Colakogullari, M., & Wood, E. J. (2004). Interference by anti-cancer chemotherapeutic agents in the MTT-tumor chemosensitivity assay. *Chemotherapy*, *50*(1), 43–50. https://doi.org/10.1159/000077285

Velliou, E. (2018). Research could lead to better understanding of pancreatic cancer.

Venkatasubramanian, P. N. (2012). Imaging the pancreatic ECM. In P. J. Grippo & H. G. Munshi (Eds.), *Pancreatic Cancer and Tumor Microenvironment*. Retrieved from https://www.ncbi.nlm.nih.gov/books/NBK98936/#ch2.ECM_composition

Wan, X., Li, Z., Ye, H., & Cui, Z. (2016). Three-dimensional perfused tumour spheroid model for anti-cancer drug screening. *Biotechnology Letters*, *38*(8), 1389–1395. https://doi.org/10.1007/s10529-016-2035-1

Wang, X., Zhang, X., Fu, Z., & Yin, H. (2013). A bioengineered metastatic pancreatic tumor model for mechanistic investigation of chemotherapeutic drugs. *Journal of Biotechnology*, *166*(4), 166–173. https://doi.org/10.1016/j.jbiotec.2013.05.008

Wang, Y., Lu, Y., Gong, J., & Yao, Y. (2019). Electrospun nanofiber regulates assembly of keratin and vimentin intermediate filaments of PANC-1 pancreatic carcinoma cells. *Materials Science and Engineering C*, *96*(March 2018), 616–624. https://doi.org/10.1016/j.msec.2018.11.072

Ware., M. ., Keshishian., V., Law., J. ., Ho., J. ., Favela., C. ., Rees., P., … Godin., B. (2016). Generation of an in vitro 3D PDAC stroma rich spheroid model. *Biomaterials*, *108*, 129–142. https://doi.org/http://dx.doi.org/10.1016/j.biomaterials.2016.08.041

Warren, S. M., Sailon, A. M., Allori, A. C., Davidson, E. H., Reformat, D. D., & Allen, R. J. (2009). A novel flow-perfusion bioreactor supports 3D dynamic cell culture. *Journal of Biomedicine and Biotechnology*, *2009*. https://doi.org/10.1155/2009/873816

Wettersten, H. I., Ganti, S., & Weiss, R. H. (2014). *Metabolomic profiling of tumor-bearing mice*. *Methods in Enzymology* (1st ed., Vol. 543). Elsevier Inc. https://doi.org/10.1016/B978-0-

12-801329-8.00014-3

Whatcott, C. J., Posner, R. G., Von Hoff, D. D., & Han, H. (2012). Desmoplasia and chemoresistance in pancreatic cancer. In P. J. Grippo & H. G. Munshi (Eds.), *Pancreatic Cancer and Tumor Microenvironment*. Retrieved from https://www.ncbi.nlm.nih.gov/books/NBK98939/

Wong, C. W., Han, H. W., Tien, Y. W., & Hsu, S. hui. (2019). Biomaterial substrate-derived compact cellular spheroids mimicking the behavior of pancreatic cancer and microenvironment. *Biomaterials*, *213*(1), 119202. https://doi.org/10.1016/j.biomaterials.2019.05.013

Yamada, K. M., & Cukierman, E. (2007). Modeling Tissue Morphogenesis and Cancer in 3D. *Cell*, *130*(4), 601–610. https://doi.org/10.1016/j.cell.2007.08.006

Yang, K., Yang, J., & Yi, J. (2018). Nucleolar Stress: hallmarks, sensing mechanism and diseases. *Cell Stress*, *2*(6), 125–140. https://doi.org/10.15698/cst2018.06.139

Zhou, Y., Sun, B., Li, W., Zhou, J., Gao, F., Wang, X., … Sun, Z. (2019). Pancreatic Stellate Cells: A Rising Translational Physiology Star as a Potential Stem Cell Type for Beta Cell Neogenesis. Retrieved April 26, 2019, from https://www.frontiersin.org/articles/10.3389/fphys.2019.00218/full

6 Appendix

6.1 Appendix A

6.1.1 Lab Compounds' Definition

6.1.1.1 Dulbecco's Modified Eagle Medium (DMEM)

DMEM is the most broadly suitable medium for a wide range of adherent cell phenotypes (Sigma-Aldrich, 2019). Many composition modifications of Eagle's medium have been developed since the original formulation appeared in the literature. The Dulbecco's modification contains a four-fold higher concentration of amino acids and vitamins as well as additional supplementary components regarding the first one (Sigma-Aldrich, 2019).

6.1.1.2 Fetal Buvine Serum (FBS)

FBS is the most widely used growth supplement for cell culture media due to its high content of embryonic growth promoting factors. It has been shown that when used at appropriate concentrations, FBS satisfies specific metabolic requirements for the cell culture (Sigma-Aldrich, 2019).

6.1.1.3 L-glutamine

L-glutamine is an unstable essential amino acid required in cell culture media formulations. Glutamine supports the growth of cells that have high energy demands and synthesize large amounts of proteins and nucleic acids. (Sigma-Aldrich, 2019) L-glutamine is supplied in both liquid and powdered forms (Thermo Fisher Scientific, 2019).

6.1.1.4 Penicillin-Streptomycin Solution (Pen Strep)

The Penicillin-Streptomycin Solution is the most commonly used antibiotic solution when culturing mammalian cells. It is required to supplement cell culture media to control any bacterial contamination. With the presence of this antibiotic, the sterile conditions are maintained during cell culture (Sigma-Aldrich, 2019).

6.1.1.5 Phosphate Buffered Saline Solution (PBS)

PBS is a buffer that consists in a salty solution containing sodium chloride, sodium phosphate and potassium chloride and potassium phosphate. The solution's buffer helps to maintain a constant pH and its osmolarity and ion concentrations usually match the ones in the human body. This is why PBS is so commonly used in biological research (Online, 2016).

6.1.1.6 Trypsin-EDTA Solution

Trypsin is a member of serine protease family that act as a proteolytic enzyme used to detach cells from an adherent substrate. It is necessary to have into account the long-term incubation with high trypsin concentration since it might damage cells by striping their cell surface proteins. Trypsin can be employed with various constituents and concentrations, EDTA (disodium ethylenediaminetetraacetic acid), for example, is one of them. It works by chelating the divalent cations (Ca^{2+}, Mg^{2+}), weakening this way the cell-cell and cell-matrix interactions that are determined by adhesion molecules in the presence of calcium (Sigma-Aldrich, 2019).

6.1.1.7 Trypan Blue Solution

Trypan Blue is a stain used to quantify live cells by labelling only the dead ones. This happens due to the fact the stain cannot penetrate the intact cell membrane of live cells. In the dead cells however, the situation is different since the trypan can pass through the membrane layer entering consequently in the cell's cytoplasm. This is why under light microscopy only dead cells have a blue colour (Fang et al., 2012).

6.1.1.8 Dimethyl Sulfoxide (DMSO)

Dimethyl Sulfoxide is a highly polar organic reagent with the formula $(CH_3)_2SO$, that has exceptional solvent properties for organic and inorganic chemicals (Sigma-Aldrich, 2019). This reagent also super cools easily and melts slowly at room temperature (Sigma-Aldrich, 2019).

6.2 Appendix B

6.2.1 Lab Equipments' Definition

6.2.1.1 Water Bath

The Water Bath is a laboratory device used to heat samples in the lab. This heating unit consists in a stainless-steel chamber that holds the water and samples and a control interface. Different types of these kind of devices range from Circulating Water Baths that keep a more even temperature or Shaking Water Baths that keep the samples in motion while they are being heated. The Water Baths are usually working at 36˚C (Labcompare, 2019).

6.2.1.2 Biological Safety Cabinet

The Laminar Flow Cabinet is a containment device that act as a primary barrier to protect the material within the hood from several contamination sources, the laboratory worker and the laboratory environment from exposure to infectious or other hazardous materials. Summing up, the biological safety cabinets provide a clean and safe environment for both the worker and the specimen in study. There are different types of laminar flow cabinets and the ones usually used for cell culture laboratories are the called Vertical Biosafety Cabinets (Class II) (ScienceDirect, 2012).

6.2.1.3 CO$_2$ Incubator

A CO$_2$ Incubator is an equipment designed to allow the development and survival of cell cultures. The mechanism beyond this effect consists in creating an atmosphere that matches the cell culture requirements concerning the temperature, the humidity and the CO$_2$ concentration. The interior of the CO$_2$ incubator is completely sealed off from the environment to ensure the atmosphere inside cannot be affected by external factors and that the samples grow in a safety way. The CO$_2$ incubators are usually working at 37˚C, with a 95% relative humidity and a 5 vol.% of CO$_2$ in the fields of immunology and tumour biology (Binder, 2015).

6.2.1.4 Phase-Contrast Microscope

The Phase Contrast Microscope has a contrast enhancing optical technique that produces high-contrast images of transparent specimens such as living cells in culture, microorganisms, cellular organelles such as the nuclei, thin tissue slices, fibers etc. One of the major advantages of the phase contrast microscopy is that living cells can be examined in their natural state without previously being killed, fixed or stained. As a result the ongoing biological processes can be observed and live recorded (MicroscopyU, n.d.).

6.2.1.5 Microplate Reader

The Microplate Reader is an instrument that can measure absorbance, fluorescence and luminescence. It can quantify protein, gene expression and various metabolic processes such as reactive oxygen species and calcium flux. Multiwell plates are integral to the microplate reader and allow for many experiments to be performed at once (JoVE Science Education Databse, 2019).

6.2.1.6 Confocal Microscope

The Confocal Microscope uses fluorescence optics that instead of illuminating the whole sample at once, focus onto a defined spot at a specific depth within the sample. This leads to the emission of fluorescent light at the exact chosen point. In addition, 3D objects can be visualized by scanning several optical planes and stacking them using a deconvolution software (z-stack). It is also possible to analyse multicolour immunofluorescence stainings using confocal microscopes that include several lasers and emission/excitation filters (ibidi, 2019).

6.3 Appendix C

The figure below shows phase-contrast microscopy images of the PANC-1 cells in the surface of the PU scaffolds, 24 hours after seeding.
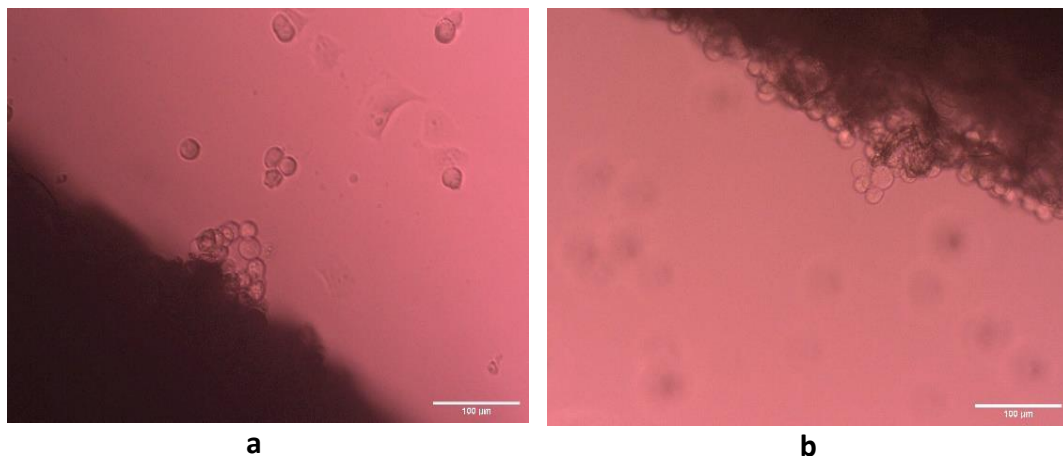

| a | b |

Figure 6.1: (a-b) Phase-contrast microscopy images of the PANC-1 cell line in the PU scaffolds' surface
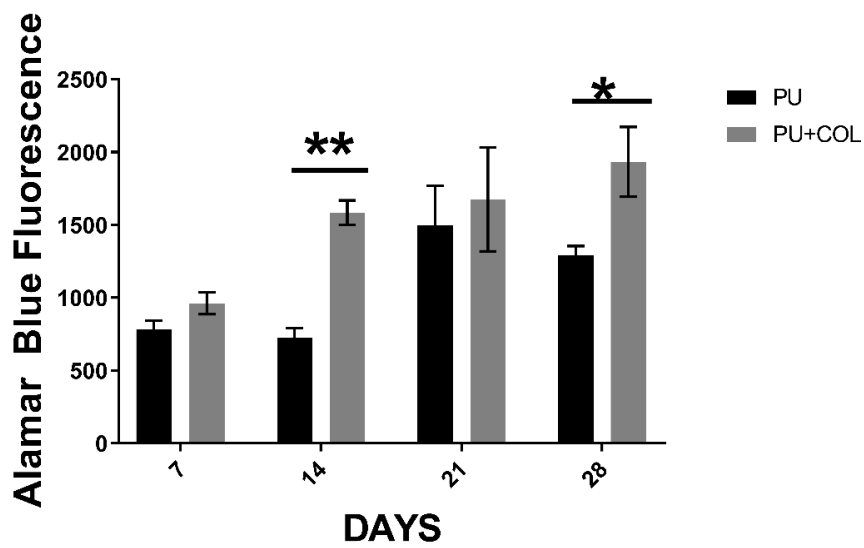
6.4 Appendix D

Figure 6.2: Growth of PANC-1 cancer cell lines in coated and uncoated PU scaffolds for 28 days in static culture. Data are presented as mean ± SEM (N=2, N=4). Statistical differences for the cell growth are marked by asterisks (*p<0.05; **p<0.0018). N = number of independent experiments; n = number of replicas.